MUSA
ON THE INTERACTION BETWEEN MUD AND SAND

Results of flume laboratory experiments

Results of Phase 1C + 1D with combined waves and currents

October, 2022; Results of flume laboratory experiments: Phase 1C and 1D with combined waves and currents

TKI MUSA project

Author(s)

Márcio Boechat Albernaz, MSc

Leo C. van Rijn, Em. Prof

Doke C. Schoonhoven, MSc

Luitze M. Perk, MSc

MUSA Laboratory experiments Phase 1C + 1D

TKI MUSA project

Client	MUSA consortium
Contact	Luitze Perk
Reference	
Keywords	Sand, mud, laboratory experiments, field measurements

Document control	
Version	Final version 2, with minor compared to the earlier version
Date	10-02-2023
Project nr.	11204950
Document ID	
Pages	116
Status	Final

Doc. version	Author	Reviewer	Approver	Publish
CONCEPT1	Márcio Boechat Albernaz, MSc Leo C. van Rijn, Em Prof Doke C. Schoonhoven, MSc Luitze M. Perk, MSc	B. Grasmeijer		
Final	Márcio Boechat Albernaz, MSc Leo C. van Rijn, Em Prof Doke C. Schoonhoven, MSc Luitze M. Perk, MSc	B. Grasmeijer		

About the MUSA project

Estuaries and tidal basins form the transition zones between land and sea. They contain important habitats for flora and fauna and are extensively used by people, like for navigation. For ecological and navigational purposes, it is important to understand and predict the evolution of channels and shoals, including sedimentation rates and the composition of the bed sediments. The bed material of large estuaries and tidal basins largely consists of mixtures of mud and sand, with predominantly sandy channels and mainly muddy intertidal areas. The interaction between sand and mud, in combination with currents and waves, leads to complex dynamics in these areas, with migrating channels and shoals.

Much is known about the behaviour of the individual sediment fractions, but the knowledge and understanding of sand-mud interaction remains limited, as do the available tools and models to accurately predict the bed evolution and sediment transport rates in sand-mud areas. Existing models, like the ones by Van Ledden (2003), Soulsby & Clarke (2005) or Van Rijn (2007) have only limitedly been verified with observations due to a lack of good quality observational data. Also, none of the available approaches cover the complete spectrum of sand-mud interaction, which includes settling, erosion processes induced by the combination of waves and currents, and the bed shear stress. Therefore, in practice sand and mud fractions are often treated separately. This decoupled approach limits the predictive capacity of numerical models, and therefore the impact of human intervention such as deepening of channels and port construction on maintenance dredging volumes and other morphological changes.

In the MUSA-research project, a consortium of contractors, consultants and research organizations join forces to increase the understanding of sand-mud dynamics by means of fieldwork campaigns and laboratory experiments, and to implement this knowledge in engineering tools and advanced models for the prediction of mud and sand transport and associated morphology in tidal conditions with both currents and waves.

Summary

The overall goal of MUSA is to improve the engineering tools predicting the amount of erosion and deposition of mud-sand mixtures. The investigation and prediction of the erosion and deposition behaviour focused on the interrelation of sediment fluxes related to:

- sediment composition of the bed;
- bulk density of the top layer of the bed;
- critical bed-shear stress for erosion;
- erosion rate of the bed surface;
- settling velocity in low and high concentration flows.

Most of these parameters are strongly interrelated, however clear relationships that can be broadly applied in engineering tools are not well known.

Herein we present the results derived from Phase 1C and 1D of the MUSA-project. Phase 1C focused on the characterization of critical shear stress for erosion of mud-sandy mixtures under combinations of waves and currents. Phase 1D aimed to assess the erodibility, sediment concentrations and sediment transport of mud-sand mixtures under combinations of waves and currents. .

Specifically, we focused on the behaviour of mud-sand beds with percentages of fines (<63 μm) varying in the range of 10% to 50% in conditions with currents alone, waves alone and combined currents and waves. In particular, the percentage of fines at which the bed sediment shows a dominant cohesive behaviour is of interest.

The results show that the critical bed-shear stress is not much influenced by cohesive effects if the percentage of fines (< 63 μm) is smaller than about 10%, while for p_{fines} > 15%, the critical bed-shear stress increases for increasing mud content. However, our flume experiments indicate that the development of bed ripple and near-bed sand transport may already be affected for lower percentage of fines, e.g. 5%. Most likely, the percentage of the clay-dominated fraction (<8 μm) with stronger cohesive properties is the key element in the change of the bed dynamics. Van Ledden (2003) and Van Ledden et al. (2004) have re-analyzed laboratory data and found that this transition between non-cohesive and cohesive behaviour may occur at a clay content of 5% to 10% which implies a percentage of fines of about 30% when assuming a clay/silt ratio of 0.5.

When the bed-shear stress due to combined currents and waves at the mud-sand bed surface with p_{fines}< 30% gradually increases to beyond the critical bed-shear stress, the mud particles at the surface are eroded. The suppression of sandy ripple development already occurs for p_{fines} of about 10% but increases proportional with the percentage of fines (10% to 30%) resulting in a strong reduction (up to factor of 10) of the near-bed sand concentrations and transport. When the bed-shear stress is sufficiently high, the mud is eroded from between the sand crests and almost immediately suspended in the water column (almost uniform mud concentration profiles).

Contents

2 Introduction to the lab and field measurements

2.1 Background

The main goal of MUSA is to improve the engineering tools predicting the amount of erosion and deposition of sand-mud mixtures. Basic parameters involved are:

- sediment composition of the bed;
- bulk density of the top layer of the bed;
- critical bed-shear stress for erosion;
- erosion rate of the bed surface;
- settling velocity in low and high concentration flows.

Most of these parameters are strongly interrelated, but proper relationships are not well known.

Based on a literature analysis performed at the start of the MUSA project, relevant knowledge gaps have been identified (Van Rijn et al., 2020 – Report 1204950_TKI-MUSA_01A_FINAL). Based on these knowledge gaps research questions have been defined.

2.2 Research questions

The main research questions of this MUSA project are grouped in 3 main subjects; (1) erosion, (2) deposition and (3) sediment density and are described below:

Main research questions related to erosion:

1. What is the effect of varying percentages of clay, silt and sand and degree of consolidation on the erodibility?
2. What is the role of bed irregularities (gravel, shells) on the erodibility?
3. How are the critical stresses and erosion rates of the sand and mud fractions related to bulk sediment properties (bed density) and basic hydrodynamic parameters?
4. What is the effect of the easily erodible upper fluffy layer (as found in field conditions)?

Main research questions related to deposition:

5. What is the influence of the settling velocity and sediment concentration distribution on the deposition flux close to the bed, and how can this be related to hydrodynamic forcing and sediment properties?
6. What is the role of sand on mud floc size, shape, density, and the resulting settling rates?
7. How to obtain an accurate settling velocity distribution using settling tube and video-camera results? And, related to this, what is the effect of sample transfer to the laboratory on floc size and settling velocity?

Main research questions related to sediment density:

8. What is the best method to measure the density of the upper 50 cm of the bed, with a focus on the transition layer between water and seabed?
9. What is the dry bed density of the upper 50 cm of mud-sand beds in tidal conditions and how does this relate to other sediment properties (e.g. composition, compaction, mud/clay content and minerology)?
10. What is a simple method for extraction and analysis of samples in shallow and in deep water?

2.3 Approach

In tidal systems the bed generally consists of a mixture of sand, silt, clay and organic materials. The sand, silt and clay mixture generally behaves as a mixture with cohesive properties when the clay-silt fraction (<63 μm) is larger than about 0.3 and as a non-cohesive mixture when the mud fraction is smaller than about 0.3.

True cohesion is a soil property mainly depending on electrochemical bonds between the particles, often enhanced by organic materials in the soil. Cohesive effects in mud-sand mixtures become important in

the case that the sand particles are fully surrounded (coated) by very fine cohesive particles. A mixture of sand-mud particles forms a network structure, if the particles are in contact with each other. Van Rijn (2020) has shown that a minimum percentage of 10% (by volume) of cohesive clay-type particles (≤ 8 μm m) is required for complete coating of the sand particles (63 to 200 μm) in agreement with a critical percentage of fines (<63 μm) of 30%.

Based on this, the basic research questions for this study are formulated, as follows:

- what is the effect of mud-type sediments on the behaviour of the near-bed sediment dynamics for percentages of fines < 63 μm varying in the range of 5% to 50%?;
- what is the (critical) bed-shear stress for surface erosion for increasing percentage fines (5% to 50%)?;
- what is the effect of varying percentage of fines on the bed features (suppression of ripples)?
- what is the effect of varying percentage of fines on near-bed sediment concentrations and transport (sand, fines)?

To answer the above research questions an extensive Measurement Plan has been prepared (Perk and Van Rijn, 2020). The proposed experiments and field measurements are divided in 2 main phases; (1) Laboratory experiments and (2) Field measurements. Each phase comprises a number of sub-phases in which focus is given on a certain type of experiments and measurements. The experiments foreseen for Phase 1 and Phase 2 are listed below.

Phase 1: Laboratory experiments

- 1A: Erosion of remoulded bed samples of mud and sand under currents
- 1B: Erosion of placed-bed and deposited-bed samples of mud-sand in currents.
- 1C: Erosion of remoulded bed samples of mud and sand in waves
- 1D: Erosion of placed-bed samples of mud and sand in combined currents and waves
- 1E: Settling velocity and floc size in laboratory (HR Wallingford)
- 1F: Spare: experiments to fill in knowledge gaps identified during the project

Phase 2: Field measurements

- 2A: Settling velocities and floc size in tidal channel with mud-sand bed (Holwerd); spring 2022
- 2B: Erosion of mud-sand beds in tidal channels (Field measurements spring 2022)
- 2C: Erosion of mud-sand beds in tidal channels (Field measurements autumn 2022)

This report addresses the combined results of Phase 1C and 1D.

This report is a living document and is continuously updated each time more results from the experiments performed under the various phases become available and will be finalized at the end of the MUSA-Project.

2.4 Outline

This report describes the method and results of the experiments performed within Phase 1C and 1D of the MUSA project.

Chapters 3.1 to 3.3 characterizes the flume, instrumentation and the sediment samples; Chapter 3.4 describes the methodology of laboratory physical experiments, Chapter 4 presents the results and analyses, and conclusions are drawn in Chapter 5. Extensive and detailed results of the individual experiments are available in the Appendix section.

3 Methods and procedures

3.1 Current-wave flume

The wave-current experiments were performed in the laboratory flume of WaterProof. The flume has 13 m of length, width of 0.4 m and depth of 0.6 m (see Figure 3.2.1). The flume bed has sand attached to the bottom plates to create a bed roughness in the order of 0.5 mm. For the mud-sand experiments, the sediment samples were placed near the centre of the flume, between the flume plates, with a sediment layer in the order of 5-7cm that is aligned with the adjacent flume plates. The water flow is (re)circulated by a centrifugal pump with electronic control. The maximum flow velocity is of the order of 1 m/s at a water depth of about 0.3 m. The mechanical wave maker at the upstream end of the flume can produce regular waves up to about 0.15 m (wave period of 1 s) at a water depth of 0.3 m. Here, waves can be generated together with currents, in the same direction. An adjustable wave damping ramp is placed at the downstream end of the flume to control the water level and to prevent wave reflection as much as possible.

3.2 Instrumentation

During the experiments we measured flow and sediment properties, including: water level, wave height/period, profile of flow velocity, pore water pressure and profiles of sediment concentration. The instruments used are presented in Figure 3.2.2

- Vectrino ADV Nortek (25 Hz) for measuring flow velocities, including wave orbital velocities;
- wave gages (30 Hz) for measuring instantaneous water level elevations, including waves;
- OBS3+ optical sensor (1 Hz) for measuring instantaneous mud concentrations;
- ASTM acoustic sand transport meter (1 Hz) for measuring instantaneous sand velocities and sand concentrations;
- Pump sampler with intake tubes for collection of water-sediment samples; the water samples were poured over a sieve of 63 μm for separation of the sand particles; small subsamples were taken from the muddy water (collected in a perspex cylinder beneath the sieve; Figure 3.2.3) without sand particles;
- pore water pressure sensors installed in the sediment bed.

For profiling over the water column and over the bed forms, the Vectrino ADV, the ASTM and pump sampler were mounted to a carriage. This set of equipment can (1) be adjusted vertically over controlled distances from the bed and (2) slowly move forward and backward (horizontally) over a distance of about 0.5 m for space-averaging of the data (used when bed ripples were present). The horizontal movement was operated by an electronic controlled stepped engine. The horizontal carriage velocity was set as such the flow velocity data was not affected by the carriage movement. Velocity and water samples were collected at determined distances above the mean bed surface level (Figure 3.2.4). The water column was sampled from ca. 2 cm of the average bed (or near the ripple crest) up to the wave trough as shown in Figure 3.2.4. The detailed sampling program is depicted in Section 3.

Table 3.2.1 shows measured peak orbital velocities (U_{max}) near the bed based on Vectrino-measurements.

Table 3.2.1 Wave characteristics; water depth=0.25 m and U_{mean} = 0.

Water depth H (m)	Wave height H (m)	Wave period T (s)	Peak orbital velocity Umax (m/s)
0.25	0.05	2.2	0.19
0.25	0.06	2.0	0.20
0.25	0.07	1.75	0.205
0.25	0.08	1.5	0.215
0.25	0.09	1.38	0.225
0.25	0.10	1.26	0.235
0.25	0.11	1.13	0.24
0.25	0.12	1	0.25

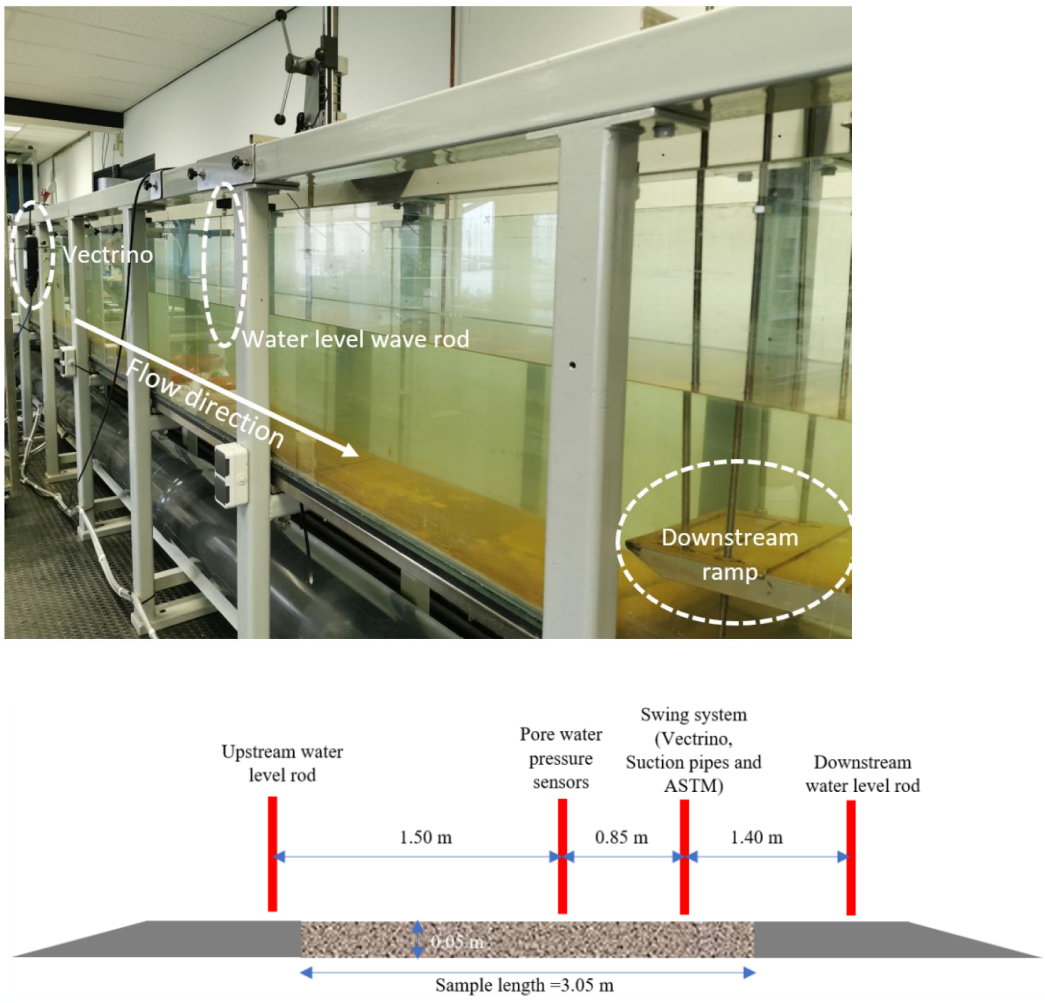

Figure 3.2.1 Current-wave flume of WaterProof, Lelystad, NL

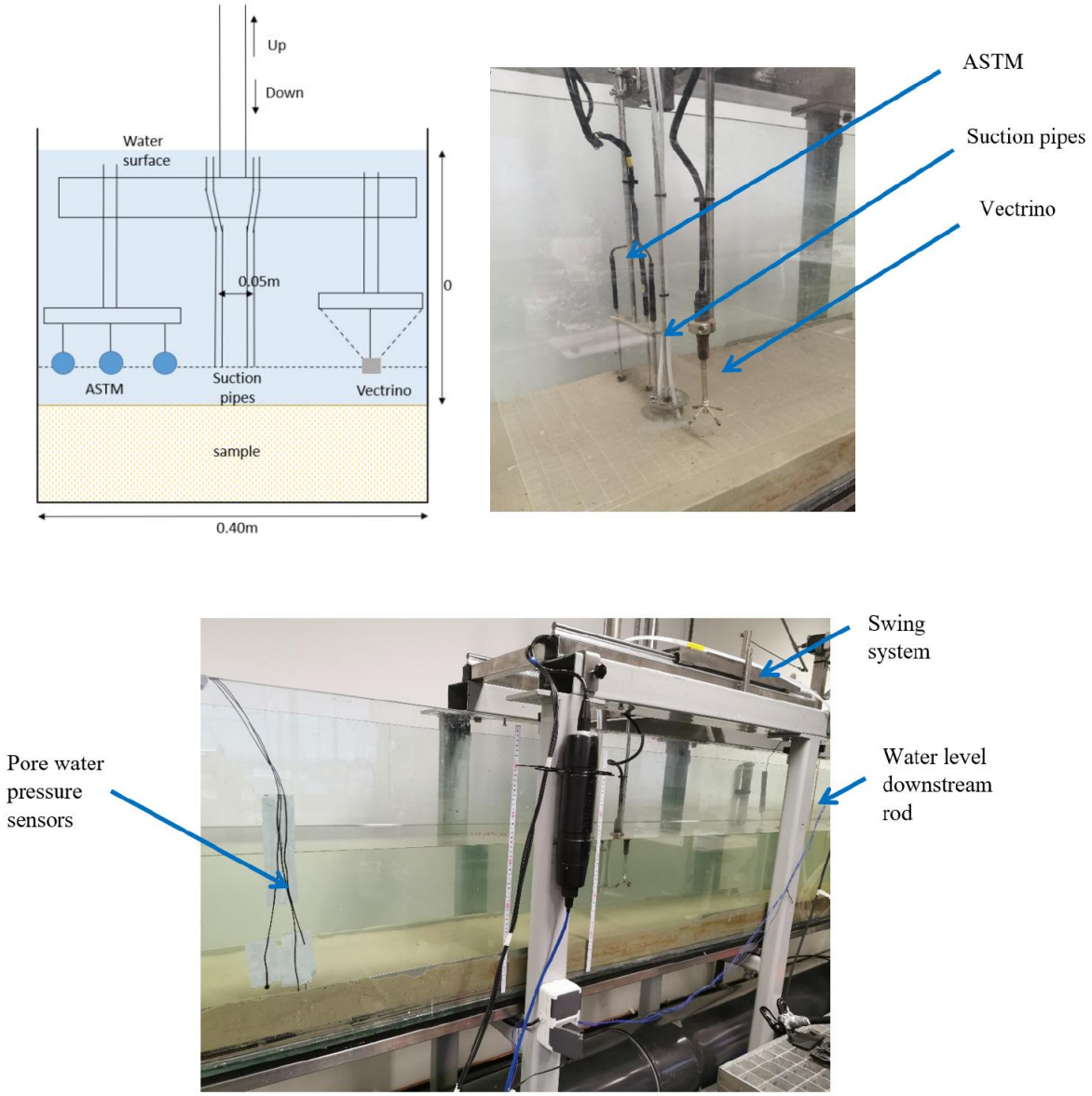

Figure 3.2.2 Instrumentation installed on the current-wave flume

Figure 3.2.3 Sediment collection stack.

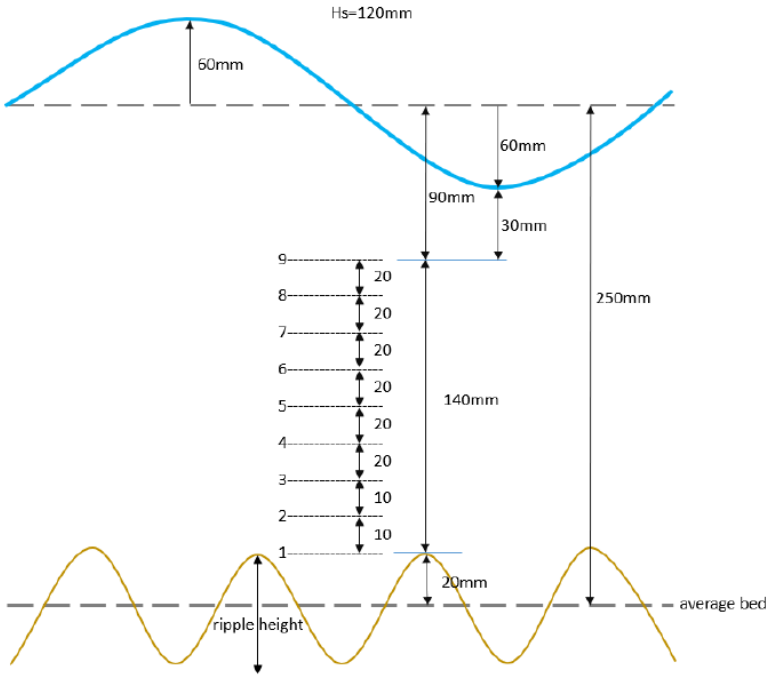

Figure 3.2.4 Scheme of measurement positions over the water column in a hypothetical situation with bed ripples under waves.

3.3 Sediments

Based on the insights gained during the Phase1A-B (see MUSA Report Phase 1AB, Boechat Albernaz *et al*., 2022), the sediments were selected to cover especially the transition between high and low cohesion induced by the percentage of mud. This transition should occur when the mud percentage is higher than 30% (Van Ledden, 2003,2004). In order to reach specific mixtures targets, here we artificially mixed sand and mud samples.

The sediment mixtures used in the flume consisted of combinations among:

- pure (commercial) fine sand (d_{10}=0.05mm, d_{50}=0.13 mm and d_{90}=0.22 mm);
- mud-sand samples from the Western Scheldt (NL) near the village of Bath, NL (BA4, BA-PU, BA-APP);
- mud-sand samples from Noordpolderzijl, NL (NPZ);
- mud-sand sample from Bengal Bay (BB-TP).

Table 3.3.1 presents the characteristics of the samples involved. The artificial mixed samples used were combinations of the commercial fine sand (d_{50}=0.13 mm) with the dark grey-black mud from the small harbour of Noordpolderzijl (NPZ) collected in October 2021 and in April 2022. The Bengal sediment was used without mixture (experiment H) as it contained a higher percentage of low cohesive silt.

Table 3.3.1 Original sediment characteristics

Sample	Wet/dry density (kg/m^3)	Percentage fines <63 µm
Pure sand (d_{50}=130µm)	2000/1600	0
NPZ-harbour mud 1 (October 2021)	1480/780	65%
NPZ-harbour mud 2 (April 2022)	1345/550	85%
Western Scheldt BA-4 (August 2021)	1850/1400	5%
Western Scheldt BA-APP (August 2021)	1790/1200	25%
Western Scheldt BA-PU (August 2021)	1400/670	70%
Bengal Bay (BB-TP) – Sample H	1750/1205	90%

For the flume experiments, apart from the samples described in Table 3.3.1, Table 3.3.2 describes the further mixtures and codes applied during the Phase 1D experiments.

Table 3.3.2 Sample characteristics used in the flume experiments of Phase 1D long bed experiments.

Experiment	Sample composition	Type of sediment bed	Dry density	P_{fines} (%)
A	Sand 130	pure sand (d_{50}=0.13 mm)	1600	0
I	NPZ + sand 130	remoulded artificial	1205	18
J	NPZ + sand 130	remoulded artificial	1260	13
K	NPZ + sand 130	remoulded artificial	1150	30
H	Bengal Bay (BBTP)	remoulded natural (silty sample)	1205	90

3.4 Experiments

The sediment bed mixtures were used in flume experiments under combinations of waves and currents. The long wave-current flume was used for waves-only and combined waves and currents while currents only experiments were performed in the small flume (see Phase 1-AB experiments). The small flume results with currents only were used to compare especially the critical bed shear stress.

This report encloses the results of the phase 1C and 1D experiments, both under combinations of waves and currents. The experiments of Phase 1C were performed to determine the critical bed-shear stress for erosion. The Phase 1D experiments aimed for quantifying the suspended sand and mud concentrations. Table 3.4.1 presents the experiments and sediment characteristics of the experiments. The experiment descriptions including photographs are presented in the Appendix.

The samples were prepared as follows:

- sediment is mixed thoroughly;
- wet density and percentage of fines< 63 μm is determined from small subsample;
- sediment is placed in the flume compartment and the sediment surface is smoothed at the same level as the adjacent flume floor;
- consolidation period of 20 to 40 hours;

The flume experiments followed the sequence described below:

- gradual filling of the flume with fresh water (water depth ≅ 0.25 m);
- generation of current (in steps) with increasing velocities until movement of bed surface particles and initiation of ripples and scour/erosion marks;
- generation of waves (in steps) with increasing wave heights (note that wave period decreases) and orbital velocities until the movement of bed surface particles;
- generation of mud-sand suspension (concentrations) by increasing wave height (up to 0.12 m); and mean current velocities (up to 0.75 m/s in long-bed test only);
- measurement of parameters; observation of bed features (ripple height/length); collection of small bed surface samples at end of test (after draining of flume).

Before each condition, the flume was run (warm up) for approximately 15 minutes to build up an equilibrium condition. The entire measurements cycle for one hydrodynamic condition took about 45-60 minutes while sampling over each vertical position for c.a. 3-5minutes.

Measured parameters are:

- flow velocities, water level and wave height;
- concentrations of sand (> 63 μm) and fines (< 63) – for Phase 1D only;
- sediment parameters (wet/dry density, percentage fines< 63 μm, ripple height and length; erosion volume)

Table 3.4.1 Summary of experiments with mud-sand bed mixtures performed during Phase 1C and D. c=current, w=waves; wc=wave-currents; dd=dry density

Dates	Type of bed	Forcing	Samples
August September 2021 (Phase 1C)	c-flume: short bed (0.15 m) wc-flume: short bed (0.5 m)	current current; waves	remoulded natural mud-sand mixtures from Westerschelde estuary -sandy BA-4 ($p_{fines<63um}$=5%; dd=1400 kg/m^3) -muddy BA-PU ($p_{fines<63um}$=70%; dd=670 kg/m^3) -sandy-muddy BA-APP ($p_{fines<63um}$=25%; dd=1200 kg/m^3)
October 2021 (Phase 1C)	wc-flume: short bed (0.5 m)	current; waves	undisturbed field samples from Westerschelde estuary -sandy BA-4 ($p_{fines<63um}$=5%; dd=1400 kg/m^3) -muddy BA-PU ($p_{fines<63um}$=70%; dd=670 kg/m^3) -sandy-muddy BA-APP ($p_{fines<63um}$=25%; dd=1200 kg/m^3)
January-May 2022 (Phase 1D)	tray experiments (0.2 m)	oscillating flow	1. remoulded artificial mixtures of NPZ-mud and fine sand (0.13 mm) $p_{fines<63\ um}$=25% and 40%; dd=1220 to 970 kg/m^3
January-May 2022 (Phase 1D)	wc flume short bed (0.5 m)	waves	1. remoulded artificial mixtures of NPZ-mud and fine sand (0.13 mm) $p_{fines<63\ um}$=8% to 22%; dd=1390 to 1200 kg/m^3 2. remoulded natural mixtures of silty mud from Bengal Bay $p_{fines<63\ um}$=90%; dd=1220 to 1030 (diluted) kg/m^3
January-May 2022 (Phase 1D)	wc flume long bed (3 m)	currents; waves	1. pure sand (d_{50}=0.13 mm; p_{fines}=0%) 2. remoulded artificial mixtures of NPZ-mud and fine sand (0.13 mm) $p_{fines<63\ um}$=13% to 30%; dd=1260 to 1150 kg/m^3 3. remoulded natural mixtures of silty mud from Bengal Bay $p_{fines<63\ um}$=90%; dd=1205 kg/m^3

4 Analysis of flume experiments

4.1 Introduction

Our analyses focused on the behaviour of mud-sand bed mixtures with mud up to 30% which represents the transition between non-cohesive to cohesive. The Phase 1C experiments, explored the beginning of motion and the assessment of the critical shear stress under waves and currents.

Earlier research (e.g Van Rijn 2017, 2019) on sand-mud has shown the existence of two typical critical conditions regarding the initiation of motion:

- initiation of particle movement of sand particles by rolling and sliding at relatively low bed-shear stresses and
- initiation of small-scale scour/erosion marks (grooves, craters) at muddy cohesive spots at higher bed-shear stresses.

In addition, a critical analysis of the bed shear stress formulations of Soulsby (1995) and Van Rijn (1993) is carried out based on the results of Phase 1C experiments.

The experiments of Phase 1D aimed to quantify the sediment suspension of sand and mud under combinations of waves and currents.

4.2 Bed-shear stress formulations

4.2.1 Definitions

The bed shear stress is a key variable to link the flow conditions with the bed erosion and sediment concentrations. However, bed shear stress can be hardly measured and in fact the bed stress used in models and transport estimates is based on empirical equations. Especially under combined waves and currents, there are uncertainties and large variations between estimates of available methods. Flow velocities and bed shear stress vary through the wave cycle. This is different from the fairly constant behaviour in the case of currents only. The relation between bed shear stress and sediment transport under wave-current conditions can be represented by:

- mean bed-shear stress (τ_m) over the wave cycle in the direction of the current;
- maximum bed-shear stress (τ_{max}) at the peak of the wave cycle.

The mean bed shear stress is commonly used to compute the combined wave-current shear stress (Figure 4.2.1) and the mixing of sediment over the water column. The maximum bed shear stress (τ_{max}) is used mainly to determine the stirring of sediment at the bed.

Soulsby (1995) gives an explicit equation for the mean bed-shear stress (τ_m). When neglecting the wave current interaction and the angle between the waves and the current, it reads as follows:

$$\tau_m = \tau_c [1+1.2(\tau_{w,max}/(\tau_c + \tau_{w,max}))^{3.2}] \quad \text{for rough-beds} \qquad \text{Equation 1}$$

with:

τ_c= bed-shear stress for current alone,

$\tau_{w,max}$= maximum bed-shear stress for waves alone (at the peak of wave cycle).

Equation 1 gives the mean bed-shear stress in the direction of the current and is based on data fitting between measured data and computed results from detailed mathematical models for the wave-current boundary layer. Equation 1 is available for example in the Delft3D-model to account for the effects of the waves on the current-induced friction.

The τ_{max}-parameter is given by vector addition on the τ_m.

The maximum shear stress takes into account the angle between the current and the waves as follows:

$$\tau_{max} = [(\tau_m + \tau_{w,max} |\cos\phi|)^2 + (\tau_{w,max}|\sin\phi|)^2]^{0.5}$$ Equation 2

For waves normal to the current: $\phi=90^o$ and $\tau_{max} = [\tau_m^2 + \tau_{w,max}^2]^{0.5}$

For Waves following the current: $\phi=0^o$ and $\tau_{max} = \tau_m + \tau_{w,max}$

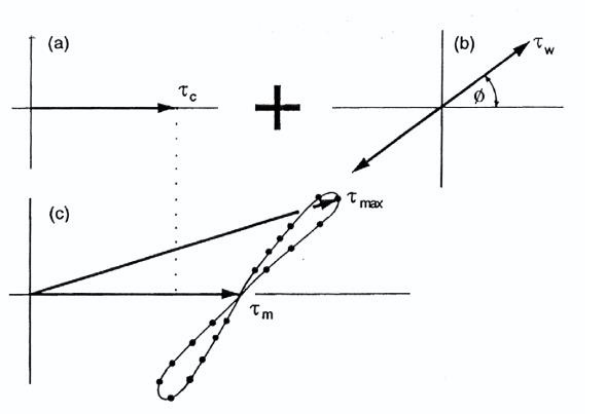

Figure 4.2.1 Vectorial sum of bed shear stress for currents and waves

Van Rijn (1993) proposes a different approach that mainly takes into account the mean bed shear stress over the wave period. The proposed formulation reads as follows:

$$\tau_{cw,s} = 0.125\ \rho\ f_{cw}\ u_c^2$$

$$\tau_{cw} = \alpha_r\ \tau_c + \tau_{w,mean}$$ Equation 3

with:

$\tau_c = 0.125\ \rho\ f_c\ u_c^2$ as the current-related bed-shear stress;
$\tau_{cw,s}$ =time-averaged bed-shear stress in the direction of the depth-averaged current vector (u_c);
τ_{cw}= time-averaged bed-shear stress acting on the sediment particles due to combined currents and waves;
$\tau_{w,mean} = \alpha_w\ \rho\ f_w\ U_{max}^2$=time-averaged bed-shear stress over wave cycle for waves alone;
In case of $\alpha_w = 0.25$, $\tau_{w,mean} = 0.5\ \tau_{w,max}$
$\tau_{w,max} = 0.5\ \rho\ f_w\ U_{max}^2$= maximum bed-shear stress of wave cycle due to waves alone;
U_{max}= peak orbital velocity;
u_c= depth-averaged current velocity;
h=water depth;
ρ=fluid density;
α_r = wave-current interaction factor reducing the current-related bed shear stress ($0<\alpha_r<1$);
$f_c = 0.24\ [\log(12h/k_s)]^{-2}$= current-related friction factor without wave effect;
$f_{cw} = 0.24\ [\log(12h/k_a)]^{-2}$= current-related friction factor including wave effect;
$f_w = \exp(-6+5.2(A_w/k_{s,w})^{-0.19})$=wave-related friction factor;
k_s= equivalent bed roughness for rough bed (plane bed $1d_{90} \cong 2d_{50}$);
k_a= apparent roughness height based on bed roughness, wave parameters and angle between waves and currents;
$A_{w,max} = [T/(2\pi)]U_{max}$ =peak orbital excursion,
T= peak wave period;
ρ_w = fluid density;
α_c = coefficient= 0.125;
α_w = coefficient $\cong$ 0.25 (Van Rijn 1993).

The term $\tau_{cw,s}$ in Equation 3 account for the effects of the waves on the friction for the current, while the τ_{cw} should be used as the bed-shear stress (for all ϕ-values) acting on the sediment particles.

Table 4.2.1 presents example computations for 5 hypothetical cases (input data as the current-related bed shear stress=0.5 N/m^2 and 5 values of the wave-related bed shear stress between 1 and 0.1 N/m^2) comparing bed stress values between Soulsby and Van Rijn. It is assumed that the wave-current interaction factor $\alpha_r \cong 1$ for following waves (current and waves in the same direction). It is important to note that the τ_{max}-parameter of Soulsby, representing the maximum shear stress, is consistently higher than the time-averaged τ_{cw}-parameter of Van Rijn.

Table 4.2.1 Bed-shear stress acting on sediment particles. BSS= Bed shear stress (N/m^2)

Case	Angle between current and waves ϕ	BSS for current alone τ_c	Maximum BSS for waves alone $\tau_{w,max}$	Soulsby		Van Rijn τ_{cw} (N/m^2) [τ_c + 0.5 $\tau_{w,max}$]
				τ_m (N/m^2)	τ_{max} (N/m^2)	
1	0	0.5	1.0	0.66	1.66	0.5+0.5=1.0
2	0	0.5	0.75	0.62	1.37	0.5+0.375=0.875
3	0	0.5	0.5	0.57	1.07	0.5+0.25=0.75
4	0	0.5	0.25	0.52	0.77	0.5+0.125=0.625
5	0	0.5	0.1	0.50	0.6	0.5+0.05=0.55

During the Phase 1C we further investigated the differences between the shear stress formulations and we performed a further calibration/validation of the α_w coefficient included in the Van Rijn formula (see Section 4.2.2).

Table 4.2.2 presents bed-shear stress values for the range of experimental conditions as used in the long wave-current flume (MUSA experiments).

Table 4.2.2 Bed-shear stresses for range of experimental conditions in long wave-current flume (bed roughness k_s=0.5 mm; α_r=1))

Water depth h (m)	Depth-averaged current velocity u_c (m/s)	Peak orbital velocity $U_{w,max}$ (m/s)	Wave Height Hs (m)	Angle between current and waves (°)	Mean (time-averaged) bed shear stress (N/m²) based on method Van Rijn		
					current c (N/m²)	waves w (N/m²)	current and waves cw (N/m²)
0.25	0	0.15	0.06	0	0	0.13	0.13
0.25	0	0.20	0.08	0	0	0.22	0.22
0.25	0	0.25	0.12	0	0	0.38	0.38
0.25	0.2	0.15	0.06	0	0.1	0.13	0.23
0.25	0.2	0.20	0.08	0	0.1	0.22	0.32
0.25	0.2	0.25	0.12	0	0.1	0.38	0.48
0.25	0.35	0.15	0.06	0	0.25	0.13	0.38
0.25	0.35	0.20	0.08	0	0.25	0.22	0.47
0.25	0.35	0.25	0.12	0	0.25	0.38	0.63
0.25	0.75	0.15	0.06	0	0.75	0.13	1.23
0.25	0.75	0.20	0.08	0	0.75	0.22	1.32
0.25	0.75	0.25	0.12	0	0.75	0.38	1.48

4.2.2 Calibration

The value of the α_w-coefficient used in the bed shear stress of Van Rijn can be verified by using the critical bed-shear stress of the Shields curve for initiation of movement of (sand) grains. Van Rijn (1993) used Equation 3 with α_w= 0.25, α_r=1 and k_s=1.5 d_{90} to compute the critical bed-shear stress for experimental data from the international literature. Figure 4.2.2 shows the data points in a plot of the Shields' curve which represents a critical stage when ca 10% of the bed surface particles are in motion. The vertical error bars express the influence of the wave period and the bed roughness. The variation between the results of different studies is mainly caused by the definition problem of initiation of movement. The data points are scattered around the Shields' curve, which means that Equation 3 can be used with sufficient accuracy to compute the critical bed-shear stress.

Here, we calibrated the α_w-coefficient by using the Shield's curve as a reference for the initiation of motion of 2 sandy samples with different grain sizes (d_{50}=0.27 mm and 0.61 mm). The experiments were performed with a short bed (0.5 m long) in the long flume under combinations of waves and currents. The results are provided in Table 4.2.3.

The instantaneous near bed velocity at z=0.02 m above the flume bottom was measured with the vectrino ADV-sensor. The time series of the velocity signal was used to derive the mean flow velocity ($u_{c,z=0.02}$) and the maximum orbital velocity ($u_{z=0.02}=u_{c,z=0.02}+ u_{w,max}$). The depth-averaged current velocity (u_c) was obtained by multiplying the near bed mean velocity ($u_{c,z=0.02}$) by a factor 1.1 based on early measurements during the pilot tests in the long flume.

During the experiment, the wave height (regular waves) was increased gradually until clear movement of the sand surface particles just before initiation of ripples was observed. At this mobility condition, the bed-shear stress due to current and waves is equal to the critical bed-shear stress derived from the Shields' curve. Therefore, using Equation 3 and k_s=1 to 2 d_{90} (plane bed conditions), the α_w-coefficient can be isolated and computed backwards. The α_w-coefficient from the MUSA experiments varied between 0.17 and 0.37 while the mean value was equal to α_w= 0.31. This verification is rather similar and within the range of the previously found 0.25 value from Van Rijn (1993).

The computed bed-shear stress according the Van Rijn-method and the Soulsby-method are also given in Table 4.2.3 (last 4 columns). The τ_{max}-values of Soulsby are much higher (factor 2) than the τ_{cw}-values of Van Rijn. In this comparison, the Van Rijn values are reasonably close to the critical bed-shear stress values of the Shields' curve (second column).

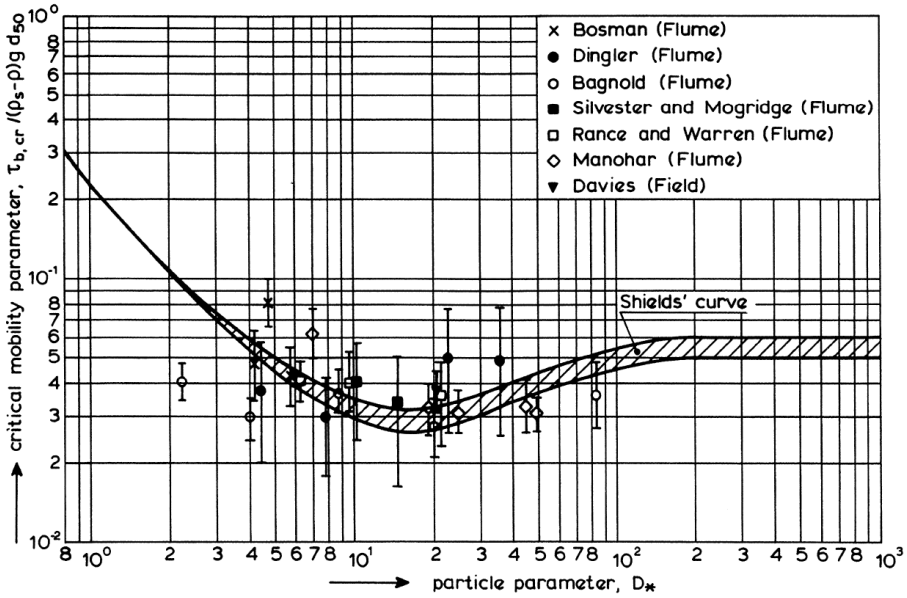

Figure 4.2.2 Shields' curve for combined currents and waves (Van Rijn 1993)

Table 4.2.3 Measured and computed data of wave-current conditions at initiation of motion of sand; (10% to 30% of bed is moving)

Sand	Critical bed-shear stress based on Shields Curve $\tau_{b,cr}$ (N/m^2)	Water depth *h* (m)	Angle between wave and current direction (°)	Depth-averaged current velocity u_c (m/s)	Critical Wave height and period H; T; U_{max} (m), (s), (m/s)	Computed α_w (-)	Bed shear stress Van Rijn method α_w=0.25	Bed-shear stress Soulsby-method τ_m τ_{max} (N/m^2) (N/m^2)	
d_{50}=0.27 mm k_s=0.5 mm	0.18	0.285	0	0	0.075; 1.7; 0.16	0.31	0.15	0	0.3
	0.18	0.285	0	0.1	0.065; 1.9; 0.14	0.35	0.14	0.04	0.27
	0.18	0.285	0	0.18	0.052; 2.3; 0.115	0.37	0.14	0.09	0.25
d_{50}=0.6 mm k_s=1 mm	0.30	0.285	0	0	0.105; 1.4; 0.25	0.17	0.44	0	0.87
	0.30	0.285	0	0.1	0.068; 1.6; 0.15	0.37	0.21	0.05	0.42

4.3 Critical bed shear stress

4.3.1 Experimental results and analyses

The results of the current-related and wave-related critical bed-shear stress for the experiments with mud-sand beds (Phase 1C and 1D) are summarized in Table 4.3.1. Test results from earlier studies (2017; 2019) are also presented to enrich the analyses.

The most important variables explored in the experiments are:

- length of bed: short beds (length <0.5 m); long beds (length=3 m);
- type of bed mixtures and combinations of percentages of mud and dry density:
  -remoulded natural (rn); mud-sand samples from field sites, thoroughly mixed;
  -remoulded artificial (ra); artificial mixtures of mud and sand; thoroughly mixed;
  -undisturbed field samples (uf); samples from field sites and placed in flume; top layer (biomat/film) with marks of benthic fauna creating additional roughness and turbulence;
- type of hydrodynamic conditions: currents (c), waves (w), combined currents and waves (cw);
  -current velocity and wave height are increased in small steps to generate erosion and transport (maximum current=0.75 m/s; maximum wave height=0.12 m, water depth=0.25 m);
  -combined cw-conditions, a steady current is set and the wave height is increased in steps (maximum wave height is limited to about 0.06 m at strong following current of 0.75 m/s due to wave stretching).

The most important characteristics of the experiments with remoulded artificial mixtures (Phase 1D) of mud-sand are:

- development of relatively low (~10 to 20 mm), symmetrical isolated ripple-type sand spots and mud spots between the ripple crests (see Figure 4.3.1);
- sandy ripples become more asymmetrical and migrate over the muddy spots at more energetic wc-conditions;
- mud is entrained and eroded from the muddy spots between the sandy ripple crests at stronger wc-conditions;

The aforementioned developments were clear and consistent for most artificial mixtures of mud and sand, but less clear for the natural silty mud from Bengal Bay. The BB sample was rather stable (no erosion observed for most wc-conditions). On the high energetic wc-conditions, nearly flat ripples (< 1 mm height) developed under nearly breaking waves.

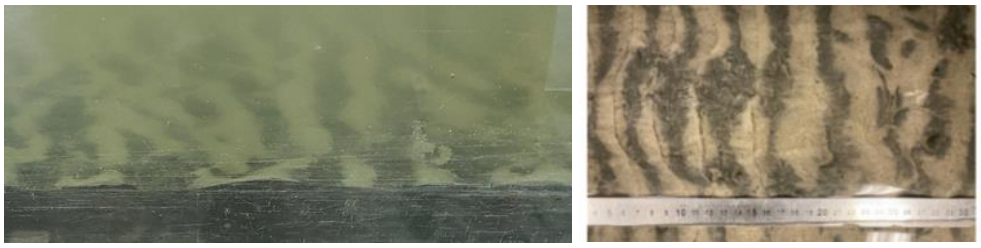

Figure 4.3.1 Alternating spots of sandy ripples (lighter-coloured) and muddy (darker) troughs between sand crests

The most important characteristics of the tests with undisturbed field samples (Phase 1C) are:

- presence of a top layer of biota (e.g. biomat/film) with fluffy mud, benthic fauna, structures, tubes, holes and bulges. These features affected the erodibility by creating bonding effects, and also by altering the bed roughness and turbulence;
- retarded incipient erosion due to the presence of cohesive/adhesive top layer;
- no development of bed forms even for the BA-4 sample with higher sand content.

The undisturbed field samples showed the presence of many tube worms being a variety of marine worms and tubes with diameter of order 0.5-1 mm partly sticking out of the bed (Figure 4.3.2). The tubes are made of a strong but flexible material coated with a layer of detritus, mud and sand. The biota showed contrasting effects during the flume experiments. The biofilms and secretions act on stabilizing and holding the bed (and sediment grains/flocs) attached to the bed. On the other hand, tubes and structures helped to increase roughness and turbulence once part of the top layer started to erode. Therefore, the benthic biota acted for both stabilizing and destabilizing the bed in our experiments. Most of the bulges remained stable during the experiments till the end of the test; tubes were moving forward and backward in the oscillating water motion. Mud erosion was gradually from the areas between the bulges.

Figure 4.3.2 BA-4 sample after wave-current experiment from Phase 1C. (left) Large scour marks without bedforms; (right) abundant presence of tubes and benthic structures within the sediment.

Types of erosion:

Under combined waves and current, the sand-mud mixtures commonly present multiple stages of incipient erosion. Here, two types of critical bed-shear stress (at increasing strength) are distinguished for the purpose of analyses: i) erosion of individual fine and sand particles and ii) erosion of cohesive mud-sand surface in the form of scour marks (craters, grooves, ripples).

Particle erosion is the (lowest) flow stage at which individual sand particles and/or fine mud particles or flocs are eroded from the sediment surface based on visual observations. The critical shear stress for particle erosion of mud and sand is assumed to be similar. In reality, loose and fluffy mud particles are usually washed away first, before sand particles start sliding or rolling. Later, under more energetic condition, the stronger cohesive mud is eroded.

Surface erosion is herein defined as the flow stage at the initiation of ripples, grooves or small craters at the sediment surface. Therefore, surface erosion occurs at higher mobility stages in comparison with the particle erosion. Often, these small-scale bed features are generated at initial disturbances. In the case of artificial mud-sand mixtures, sandy spots were sorted into isolated sandy ripples. Here, mud erosion mostly occurred from the muddy troughs (darker grey/black spots) between the sand ripple crests (Figure 4.3.1). Mud erosion from the muddy trough spots was defined as the stage of surface erosion for artificial mud-sand mixtures (last 2 columns of Table 4.3.1).

Computation of bed shear stress:

As introduced in Section 4.2, two methods have been used to compute the critical wave-related bed-shear stress: method of Van Rijn (VR-method) which computes the time-averaged bed shear stress over the wave cycle ($\tau_{w,cr}$) and the method of Soulsby (S-method) which calculates the maximum bed-shear stress over the wave cycle ($\tau_{w,max,cr}$).

The wave-related critical shear stress ($\tau_{w,cr}$-value) of the VR-method is commonly higher than the current-related critical bed shear stress ($\tau_{c,cr}$-value); compare columns 6 and 7 of Table 4.3.1. The critical shear stress ($\tau_{w,max,cr}$-value) of the S-method is consistently higher (up to a factor 2) than the current-related critical bed shear stress ($\tau_{c,cr}$-value). Due to the overestimation of the critical bed shear stress of erosion from the Soulsby-method, we mainly focused our analyses on the bed shear stress derived from the Van Rijn method.

Critical bed-shear stress

The experimental results on the critical bed shear stress (based on the VR-method) of the long bed experiments are shown in Figure 4.3.3, Figure 4.3.4 and Figure 4.3.5. Both particle and surface erosion are discussed, as well as the effects of current and/or waves.

Figure 4.3.4 shows the critical bed-shear stress of particle erosion (dashed line) and surface erosion (solid line) for the data of the long bed experiments of MUSA. The key results are:

- particle erosion: the τ_{crit}-values of fines are slightly lower than that of sand particles; the τ_{crit}-values based on the VR-method in conditions with waves alone are roughly 20% to 40% higher than those of currents alone;
- surface erosion: the τ_{crit}-values in experiments with waves alone are similar to the experiments with currents only; the τ_{crit}-values of the fines are to some extent higher than the conditions at which small sand ripple start to form, because the fines are lying in the trough of the ripples requiring higher erosion stresses.

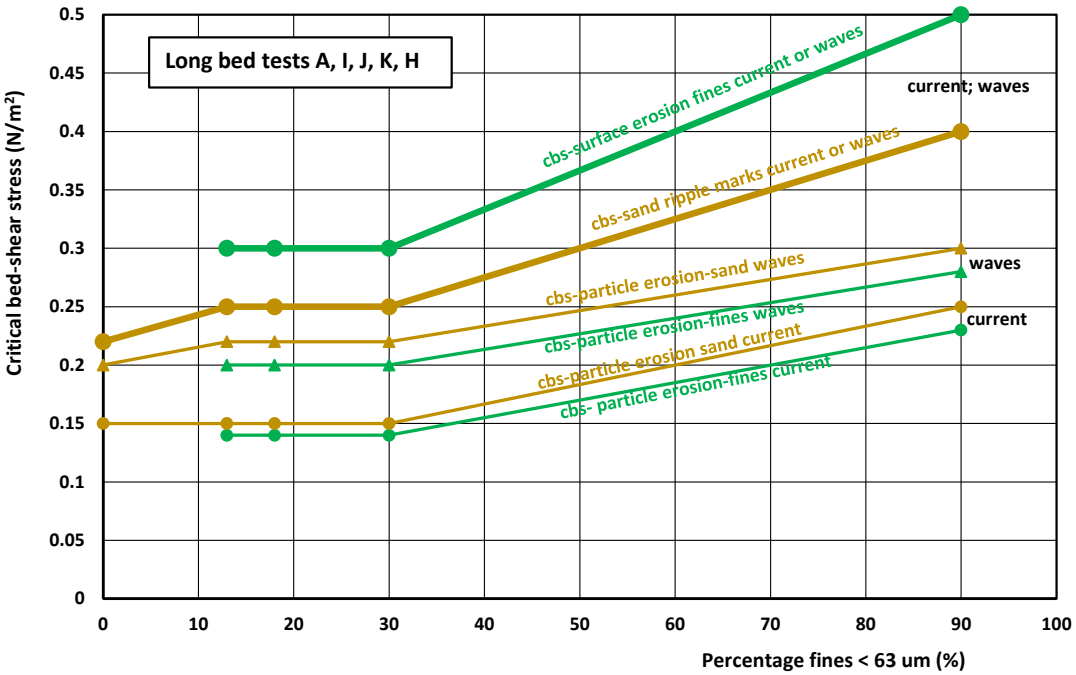

Figure 4.3.3 Critical bed-shear stress for erosion of sand (yellow) and fines < 63 μm (green); long bed data (cbs=critical bed-shear stress)

Figure 4.3.4 shows the τ_{crit}-values for particle erosion and surface erosion of fines of all MUSA-data with long and short beds. The τ_{crit}-values of particle and surface erosion is the average value of the results with currents and waves (average of columns 6/7 and 7/8 of Table 4.3.1, as the values in both columns are in the same range). The critical bed shear stress values of long bed tests are significantly smaller than those of the short bed tests. This can also be seen in Figure 4.3.5 which shows all available data including earlier data of Noordpolderzijl (NPZ; HTS) and Holwerd. It is important to note that the bed preparation of the early (Phase 1A/B) experiments with short beds in the small flume with current only conditions were different than the long flume experiments (Phase 1C/D). For the small flume, the samples had the top layer of sediments (in practice about 1-2 cm) removed before the experiment in order to perfectly level the flume and sediment bed after the resting period. For the large flume, the sediment beds did not have the top layer removed. Therefore, we expected a certain level of extra compaction and resistance to erosion on the scrapped samples derived from the short (current only) experiments.

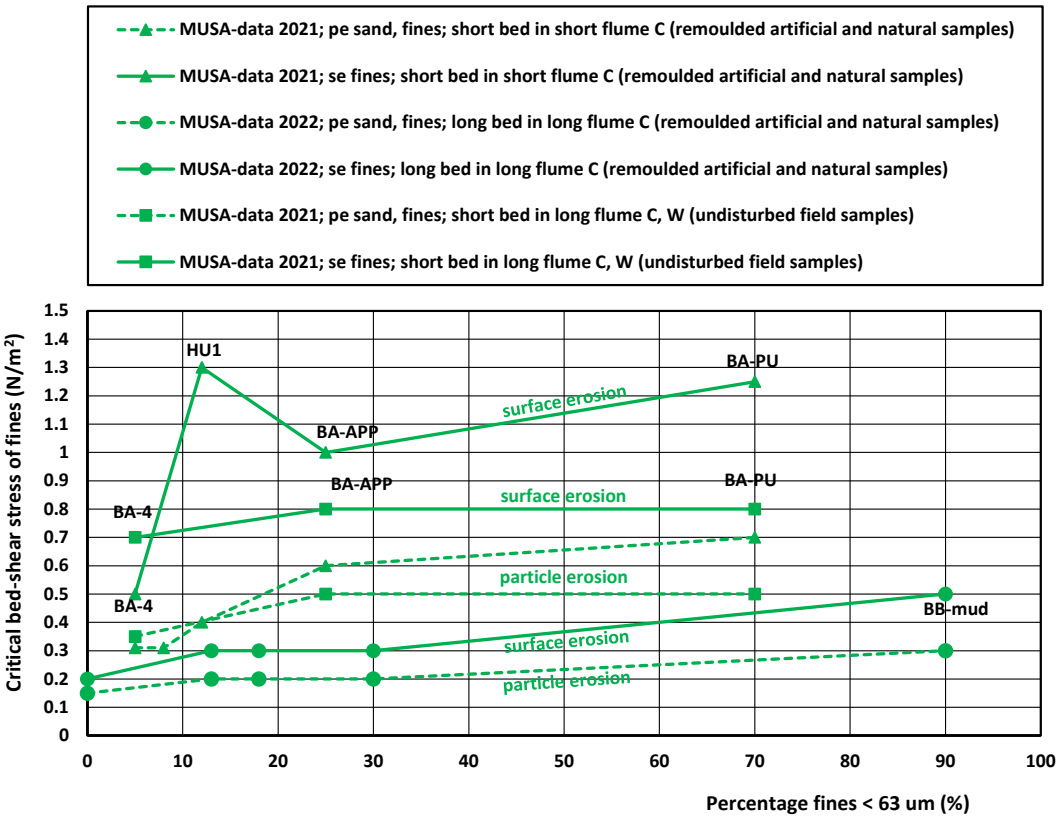

Figure 4.3.4 Critical bed-shear stress for particle and surface erosion of fines; all MUSA-data

4.3.2 Comparison with literature data

Here we compared our results of critical shear stress with data from the literature.

De Smit et al. (2021) used a mobile flow oscillatory flume (so called OSCAR) to measure the critical wave-generated shear stress on sediment samples directly taken from the field which also included the effects of biota on the critical shear stress. The performance of the OSCAR-flume was further studied by conducting erodibility measurements on a range of artificial sand-mud mixtures and field samples.

The critical bed-shear stress values (τ_{crit}) of the artificial mud-sand mixtures of De Smit et al. (2021) are in the range of 0.4 to 1.6 N/m^2 for p_{fines} between 4% and 21% (Table 4.3.1) which is in the same range as those of the present study (see Figure 4.3.3) .

The τ_{crit} -values for the undisturbed field samples show low values for p_{fines} =7% and higher values for p_{fines} in the range of 25% to 55%. The τ_{crit} -value of their field sample 4 is comparable to that of pure sand, despite the presence of more cohesive muddy sediments (p_{fines}=7%). This is an indication that the effect of cohesivity is counteracted by the effect of macrobenthos in their experiment. Comparison of the τ_{crit} -values of field samples 2 and 3 with almost the same p_{fines}=25% shows a much higher τ_{crit} -value for sample 2 with almost no benthos. Overall, it seems that the presence of benthos leads to lower τ_{crit} -values due to loosening (bioturbation) of the top layer of sediments. Within the MUSA experiments we observed that benthic structures usually lead to higher critical shear stress for erosion due to binding effects (biostabilization).

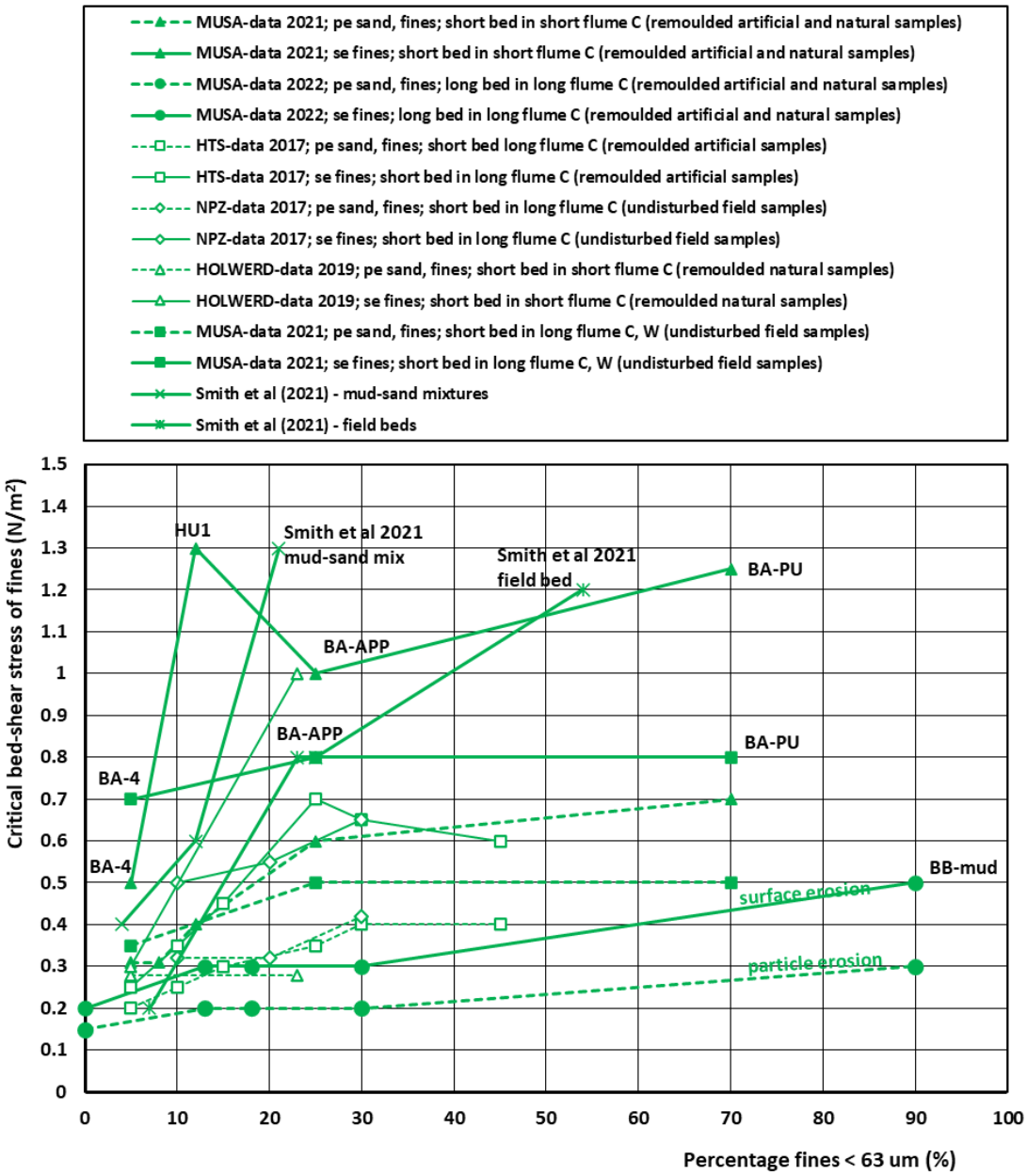

Figure 4.3.5 Critical bed-shear stress for particle and surface erosion of fines; MUSA data and earlier data from Noordpolderzijl and Holwerd

Yao et al. (2022) studied the erosion threshold of silt-sand mixtures (silt dominated; percentage of clay smaller than< 8 μm < 3%) by carrying out series of erosion experiments for different bed compositions. The results suggest that there exists a critical silt content ($p_{silt\ 8\text{-}63um}$) of about 35%, separating two domains. For p_{silt}<35%, the critical bed shear stress follows the values of the Shields' curve with $\tau_{cr}\cong$0.1 N/m^2. For p_{silt}>35%, the erosion threshold of a mixed bed is increased abruptly and remains constant at about $\tau_{cr}\cong$0.2 N/m^2 with further increase of silt content. For the silt-dominated matrix, a stable silt-skeleton can be formed by the attraction forces to resist erosion, whereas the attraction forces are too weak to form a stable silt-skeleton when silt content is small. These values of silt-sand erosion can be compared with the results of the silty BB-sample of Table 4.3.1 (Experiment H). The critical bed-shear stress values of the silty BB-samples are in the range of 0.2 to 0.5 N/m^2 (τ_{cr}=0.2 to 0.5 N/m^2), when considering particle erosion, and are larger than those of Yao et al. (2022) for silty sediments. This difference is most likely due to a higher fraction of clay in the BB-samples that adds clay cohesion to the sample matrix.

4.3.3 Summary of results

The overall results regarding the critical bed shear stress are:

- the long bed tests with artificial mixtures of mud and fine sand show that the critical bed shear stress for particle erosion (fines < 63 μm and sand 63-130 μm) is in the range of 0.15 to 0.22 N/m^2 for mud content between 0% and 30%; the τ_{crit}-value of fines is slightly lower than that of fine sand particles; the critical shear stress for surface erosion of fines is about constant at a value of 0.3 N/m^2 for p_{fines} < 30% when the mud is eroded from the sand ripple troughs;
- the short bed experiments with undisturbed field samples of mud-sand show that the critical bed-shear stress for particle erosion is in the range of 0.35 to 0.5 N/m^2 for p_{fines} between 0% and 30%; the τ_{crit}-value of fines is slightly lower than that of fine sand particles; the critical shear stress for surface erosion of fines is about constant at a value of 0.75 N/m^2 for p_{fines} < 30%;
- the τ_{crit}-values of long bed tests are substantially smaller than those of short bed tests. This difference can be attributed to the scrapping of the top layer of the short bed samples, however it is also related to the larger spatial variability of the mud in the top layer of a long bed (percentage of fines, bed irregularities-roughness, bed density) and the interference of boundary conditions in the short bed tests, e.g. the tray/flume edge;
- the critical bed-shear stress for surface erosion of mud-sand mixtures is found to be somewhat smaller in conditions with current alone compared to combined waves and currents; which can be related to the method used to compute bed-shear stress due to combined current and waves. The (bed-shear stress according to Van Rijn-method yield lower values in comparison with the Soulsby-method. Alternatively, our results point out that either waves add other processes (pressure and flow acceleration) that change the erosion behaviour that are not accounted in the bed shear stress formulations, or that critical bed shear values are not an intrinsic sample characteristic but actually varies its value depending on the hydrodynamic conditions (waves and currents).
- The long bed tests are more consistent than the short beds. The critical bed shear stress is close to the Shields τ_{crit}, in line with van Ledden (2004), for Pmud <= 0.3.
- Short bed results need to be interpreted and used with care due to limitation in the sample preparation and boundary conditions.

The present results clearly show significant differences between the critical bed-shear stresses of short-bed and long-bed and between current-only and wave-current conditions with mud-sand mixtures. This raises the question whether the observed discrepancies derive from missing processes (bed shear stress cannot fully relate flow to erosion), the empirical bed shear stress equations fail in representing erosion over the whole range of mud-sand and wave-current conditions, or that experiments with short beds are not really suitable for determination of the critical bed-shear stress for erosion. Additional tests with long beds of natural mud-sand mixtures are highly recommended (BA-4; BA-APP; HU1). Long bed test with natural sandy muds are strongly recommended to assess whether the differences in critical bed shear stresses between short bed and long bed tests is caused by boundary/artificial effects, differences between empirical equations or natural processes.

Table 4.3.1 Critical conditions of mud-sand mixtures; short-bed and long-bed tests. fines=fraction < 63 μm; nm=not measured; VR=Van Rijn; remoulded artificial bed mixture= mixture of fine sand (0.13 mm) and mud from Noordpolderzijl NPZ (NL); Bed shear stress waves alone and combined waves-currents based on Van Rijn-method with α_{cw}=0.25.

Dates	Test	Mixture of mud and fine sand	Dry density (kg/m^3)	Bed roughness (mm)	Bed shear stress (N/m^2) for critical conditions			
					sand particle movement		surface erosion scour marks (ripples/grooves)	
					c	w; cw (VR)	c	w; cw (VR)
This study Jan-April 2022 (Long bed)	A (Sand 130)	p_{fines}=0%;pure sand (d_{50}=0.13 mm)	1600	0.5	0.15	0.22	0.2	0.25
	I (Sand 130+NPZ)	p_{fines}=18%; remoulded artificial b.m.	1205	0.5	0.15	0.22	0.3	0.3
	J (Sand 130+NPZ)	p_{fines}=13%; remoulded artificial b.m.	1260	0.5	0.15	0.22	0.3	0.3
	K (Sand 130+NPZ)	p_{fines}=30%; remoulded artificial b.m.	1150	0.5	0.15	0.22	0.3	0.3
	H (BBTP)	p_{fines}=90%; remoulded natural b.m.	1205	0.3	0.25	0.3	0.5	0.5
This study Aug-Sep 2021 (Short bed)	BA-4	p_{fines}=5%; remoulded natural b.m.	1400	0.5	0.3	0.35	0.5	0.5
	BA-APP	p_{fines}=25%; remoulded natural b.m.	1200	0.3	0.5	0.7	1.0	1.0
	BA-PU	p_{fines}=70%; remoulded natural b.m.	670	0.2	0.5	0.9	1.4	1.1
	B	p_{fines}=8%; remoulded artificial b.m.	1245	0.5	nm	0.3	nm	nm
	WS-HU1	p_{fines}=12%; remoulded natural b.m.	1000-1300	0.5	0.4	nm	1.3	nm
This study Oct 2021 (Short bed)	BA-4	p_{fines}=5%; undisturbed natural b.m.	800-1400	0.5-2		0.35		0.7
	BA-APP	p_{fines}=25%; undisturbed natural b.m.	1235	0.5-1		0.5		0.8
	BA-PU	p_{fines}=70%; undisturbed natural b.m.	650	0.5-2		0.5		0.8

Earlier research 2017 (Short bed) (VR 2018)	HTS-45	p_{fines}=45%; remoulded artificial b.m.	700	0.1	0.4	nm	0.6	nm
	HTS-30	p_{fines}=30%; remoulded artificial b.m.	1100	0.1	0.4	nm	0.65	nm
	HTS-25	p_{fines}=25%; remoulded artificial b.m.	1450	0.1	0.35	nm	0.7	nm
	HTS-15	p_{fines}=15%; remoulded artificial b.m.	1450	0.3	0.3	nm	0.45	nm
	HTS-10	p_{fines}=10%; remoulded artificial b.m.	1450	0.3	0.25	nm	0.35	nm
	HTS-5	p_{fines}= 5%; remoulded artificial b.m.	1450	0.3	0.2	nm	0.25	nm
Earlier res. 2017 (Short bed (VR2018)	NPZ-B7	p_{fines}=30%; natural field sample NPZ	1200	0.1	0.4	nm	0.65	nm
	NPZ-B9	p_{fines}=20%; natural field sample NPZ	1350	0.1	0.3	nm	0.55	nm
	NPZ-B15	p_{fines}=10%; natural field sample NPZ	1425	0.1	0.3	nm	0.5	nm
Earlier res. 2019 (Short bed (VR2019)	Hol-4km	p_{fines}=23%; remoulded natural b.m.	1050	0.3	0.5	nm	1.0	nm
	Hol-5km	p_{fines}=5%; remoulded natural b.m. Hol=Holwerd	1500	0.3	0.3	nm	0.3	nm
Smith et al (2021)	Mud-sand	p_{fines}=4%; d_{50} = 0.34 mm; remoulded artificial	na		0.4			
	Mud-sand	p_{fines}=12%; d_{50} = 0.33 mm; remoulded artificial	na		0.6			
	Mud-sand	p_{fines}=21%; d_{50} = 0.33 mm; remoulded artificial	na		1.3			
	Low benthos	p_{fines}=54%; d_{50} = 0.065 mm; field undisturbed	na		1.2±0.3			
	High benthos	p_{fines}=23%; d_{50} = 0.25 mm; field undisturbed	na		0.8±0.5			
	Low benthos	p_{fines}=7%; d_{50} = 0.25 mm; field undisturbed	na		0.2			
	No benthos	p_{fines}=25%; d_{50} = 0.15 mm; field undisturbed	na		1.8±0.1			

4.4 Mud and sand concentrations and transport

4.4.1 Introduction

Here, the experimental results from Phase 1D of high mobility test conditions with significant sediment concentrations and sediment transport are analysed. These Phase 1D-experiments were executed in the long wave-current flume over various sediment mobility conditions under combinations of waves and currents for assessing the sand-mud transport and concentrations on the water column. This series of experiments will provide insights into how the mud-sand mixtures influence erosion rates under waves and currents, and consequently the resulting sediment concentrations and mud-sand sediment transport.

Long-bed and short-bed experiments with artificially mixed and natural mud-sand were performed in a long wave-current flume, see Table 3.4.1. The short-bed tests were mostly pilot tests to assess the behaviour of various mud-sand bed mixtures as preparation for the more detailed and exhaustive long-bed experiments.

The first long-bed experiment consisted of pure sand (d_{50}=0.13 mm; p_{fines}=0%) to be used as a reference scenario to assess the effect of increasing percentages of fines on the sediment transport processes.

Based on the previous experiments and the short-bed tests, three long-bed experiments (i.e. I, J and K) were performed with remoulded artificial mixtures of natural mud from Noordpolderzijl (NPZ) and fine sand (0.13 mm). In addition, one experiment was performed with the remoulded natural silty-mud from Bengal Bay (Experiment H) without any further artificial mixture (Table 3.3.2).

During the experiments, we measured the flow velocities and the concentrations of sand (> 63 μm) and mud (< 63 μm) in the vertical profile; wave height, sediment pore pressure, ripple dimensions and the erosion volume. The sediment characteristics were determined for every sample such as the percentage of fines and wet/dry bulk densities.

Table 4.4.1 presents basic data of the bed mixtures, currents, waves and the bed ripple characteristics of the long-bed test.

Important characteristics of the remoulded artificial mixtures of mud-sand are summarized below:

- development of relatively low, symmetrical isolated ripple-type sand spots and mud spots between the ripple crests (see Figure 4.3.1);
- sandy ripples become more asymmetrical and migrate over the muddy spots at higher wc-conditions;
- mud is entrained and eroded from the muddy spots between the sandy ripple crests at higher wc-conditions;
- strong erosion of mud and sand and generation of very irregular bed with deeper scour marks at highest wc-conditions;
- sandy ripples at surface of mud-sand beds are much lower compared to the ripples on a pure sand bed for the same wc-conditions;
- mud cracks and craters developed at bed surface from which mud clouds were eroded producing a fluffy layer on top of surface (in some tests with mixture of fine sand and NPZ-mud).

Table 4.4.1 Basic data of long-bed tests (water depth=0.25 m). H= wave height; u_c=depth-averaged current velocity

Exp	Percentage fines $p_{fines<63\ um}$ (%)	Dry density (kg/m^3)	Wave height (m)	Ripple characteristics (height; length, mm)				
				u_c=0 m/s	u_c=0.1 m/s	u_c=0.2 m/s	u_c=0.35 m/s	u_c=0.75 m/s
A	0	1600	H=0.06					3-7; 80-100
			H=0.08	10-15; 40-60	7-10; 40-60	10-15; 50-70	10-15, 70-90	
			H=0.12	7-10; 40-60	7-10; 40-60	10-15; 60-80		
J	13	1260	H=0.06	1; 40				25; 150
			H=0.08	2; 40		5; 60	4; 60	
			H=0.12	6; 50		5; 60		
I	18	1205	H=0.06	1; 50				25; 150
			H=0.08	2; 70		3; 50	2; 50	
			H=0.12	4; 50		2; 50		
K	30	1150	H=0.06					10; 150
			H=0.08	2; 60			7; 70	
			H=0.12	3; 60		3; 60		
H	90	1205	H=0.06	2; 30				2; 70
			H=0.08	2; 40			2; 70	
			H=0.12	2; 40				

4.4.2 Long bed experiment with fine sand (Exp A)

Flume experiments with a long bed of commercial fine sand (d_{50}=0.13 mm) were performed to measure sand concentration profiles in conditions with waves alone and combined currents and waves which are used as reference values to evaluate the effect of mud fraction in the case of mixed beds under the same hydrodynamic conditions. The summary of the experimental results is given in Table 4.4.1. Figure 4.4.1 shows the measured sand concentration profiles for the pure sandy bed covered with small-scale ripples (ripple height in the range of 5 to 15 mm; ripple length in the range of 40 to 100 mm).

Figure 4.4.2 shows the measured depth-averaged sand concentrations as function of the current velocity for 2 wave heights H=0.08 and H=0.12 m.

The most important results derived from the sandy experiment are:

- near-bed sand concentrations are very sensitive to the bed forms such as ripples, see Figure 4.4.2. Small vortices are generated in the troughs between the ripple crests producing turbulence and relatively high sand concentrations;
- ripples are nearly symmetrical for waves alone; ripples are more asymmetrical for conditions with waves plus a current of 0.2 m/s (near the current-only beginning of motion);
- near-bed and depth-averaged sand concentrations are lowest for waves combined with weak current of 0.1 m/s (below the current-only beginning of motion) because the current generates slightly flatter and more asymmetrical ripples with weaker vortices in the ripple troughs; near-bed and depth-averaged sand concentrations are progressively high for waves combined with stronger current, in or cases, the 0.35 and 0.75 m/s flow velocity conditions;
- currents produce more turbulence-related mixing resulting in higher concentrations (more uniform) in the water column (see Figure 4.4.1).
- the effect of increasing wave height only affected the sediment concentration when the flow velocity was below the current-only beginning of motion (here 0.1 m/s), see Figure 4.4.1. Above and including the 0.2 m/s of flow velocity, the increase of wave condition did not alter the sediment concentrations.

The depth-integrated sand transport rates are given in Table 4.4.2. The sand transport rates are strongly related to the depth-averaged flow velocity. The effect of wave height is rather small, which is related to the decreasing ripple height for higher waves.

Table 4.4.2 Depth-integrated sand transport for Test A with pure sand bed

Experiment	Depth-averaged velocity (m/s)	Wave height (m)	Depth-integrated sand transport (kg/m/s)
A3	0.1	0.08	0.0035
A4	0.1	0.12	0.004
A5	0.2	0.08	0.03
A6	0.2	0.11	0.04
A7	0.35	0.08	0.1
A8	0.75	0.06	0.8

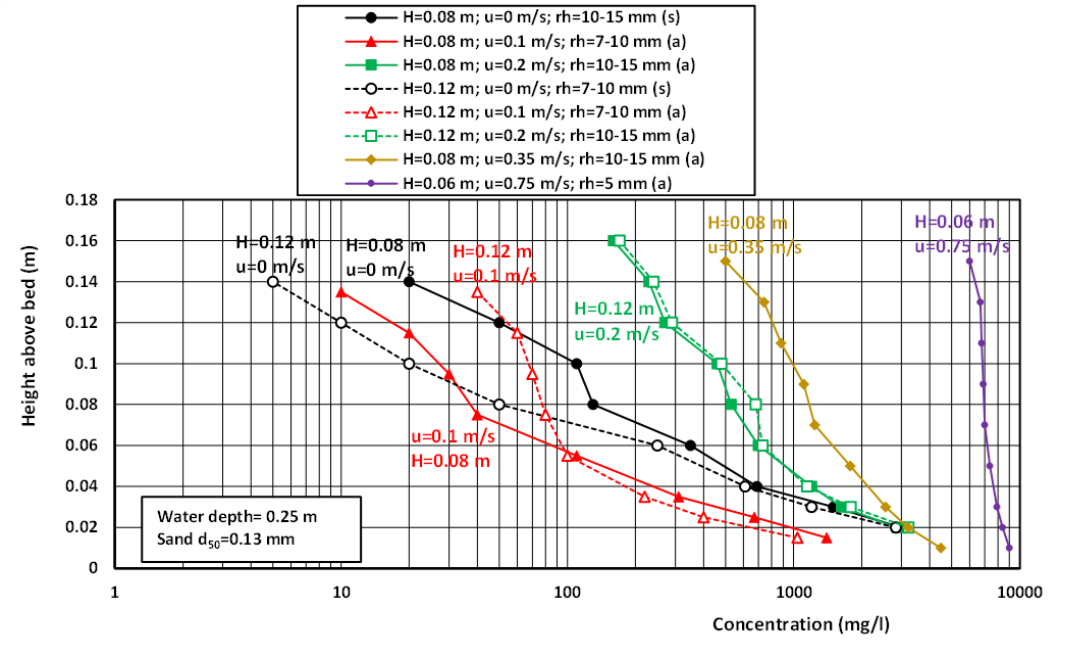

Figure 4.4.1 Sand concentration profiles; pure sand bed (d_{50}=0.13 m); rh=ripple height; s=symmetrical ripples; a=asymmetrical ripples

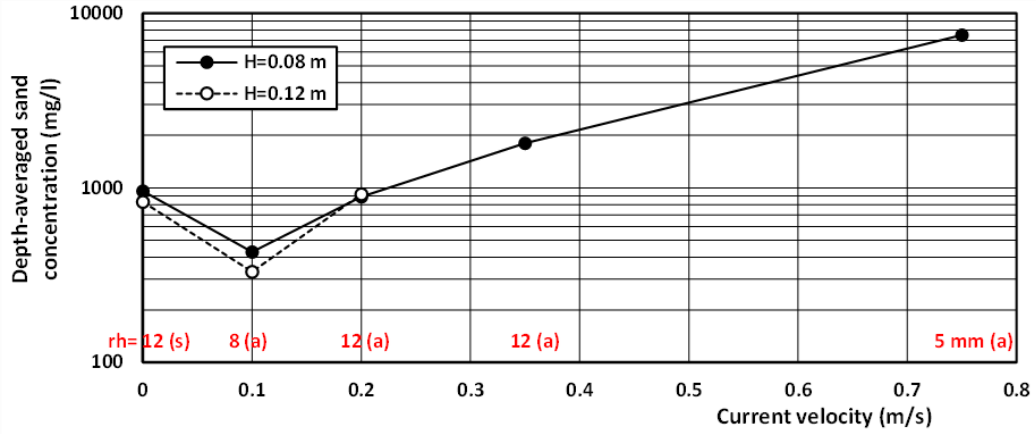

Figure 4.4.2 Depth-averaged sand concentration profiles; pure sand bed. d_{50}=0.13 mm; rh=ripple height; a=asymmetrical; s=symmetrical; H= wave height

4.4.3 Beds of mud and fine sand mixtures

The analysis results of the experiments are divided into waves-only and combined wave-currents.

The short-bed experiments (i.e. Experiments B-G) were pilot experiments with wave-currents to quickly assess the erodibility of the various bed mixtures. The outcome of the wave-current short bed tests was used to further choose and prepare bed mixtures for the long-bed experiments while limited analyses were performed based on these experiments.

Waves only scenarios

The detailed experimental program and results are shown in Table 4.4.3.

The sediment bed mixtures used have a wet density near 1750 kg/m^3 and dry density equal to about 1200 kg/m^3, representing higher values in comparison with pure mud dry densities that average 500-600 kg/m^3.

Figure 4.4.3 shows the sand and mud concentration profiles for long-bed Test I, J and H with waves alone (H=0.12 m). The most important results are, as follows:

- the sand concentrations in the near-bed zone of Tests J and I with p_{fines}=13% and 18% are roughly a factor 2 to 3 lower than those for a pure sand bed;
- the sand concentrations in the near-bed zone of Test K with p_{fines}=30% are a factor of 100 lower than those for a pure sand bed;
- the sand concentrations of Test H with a pure mud-silt bed with p_{fines}=90% are rather low < 10 mg/l;
- the mud concentrations (< 200 mg/l) are more uniformly distributed over the depth (much lower settling velocities).
- Mud concentration decreases when increasing the mud content from 0 to 30%. This suggest that, assuming a rather similar τ_{crit} for mud, the erosion rate (M) decreases when increasing the mud percentage.

Figure 4.4.4 shows the depth-averaged sand and mud concentrations as function of the percentage of fines < 63 μm in the bed mixture of mud and sand and waves alone (H=0.12 m). The depth-averaged sand concentrations are higher for the pure sand bed (d_{50}=0.13 mm) in Exp A. The depth-averaged sand concentrations for a bed mixture with p_{fines} <30% are roughly a factor 3 to 50 lower than for a bed of pure fine sand. The sand concentrations are extremely low for a pure mud-silt bed (BB-bed mixture of Test H; p_{fines}=90%). Figure 4.4.5 shows a similar plot for a lower wave height of H=0.08 m.

Table 4.4.3 Data summary of mud-sand experiments in conditions with waves only (water depth=0.25 m)

Exp	Description	Consolidation period (hours)	Wet and dry bulk density (kg/m^3)	Ripple height (mm)	Mud p_{fines} (%)	Depth-averaged concentration (mg/l)			
						H=0.08 m (T=1.5 s)		H=0.012 m (T=1 s)	
						C_{sand}	C_{fines}	C_{sand}	C_{fines}
A	Long bed; pure sand d_{50}=0.13 mm	0	2000/1600	<10	0	960	<10	830	<10
B	Short bed; fine sand NPZ-mud	24 (1 day)	1775/1245	<3	8	20	<10	80	30
D	Short bed; fine sand and BB-mud	24(1day)	1730/1170	<15	13	300	<50	400	50
J	Long bed; fine sand and NPZ-mud	24 (1 day)	1800/1285	<2	13	20	<5	200	150
C	Short bed; fine sand and NPZ-mud, same as J	2 (slurry)	1760/1220	<3	17	20	<5	350	20
CC	Short bed; fine sand and NPZ-mud, same as C	96 (4 day)	1865/1390	<1	17	20	<5	50	10
E	Short bed; same as CC + 5% water	48 (2 days)	1790/1270	<1	17	10	<5	20	5
I	Long bed; fine sand and NPZ-mud	24 (1 day)	1750/1205	<2	18	5	<5	200	100
F	Short bed; fine sand BB-mud	24 (1 day)	1840/1350	<10	22	50	<5	300	50
K	Long bed: fine sand and NPZ-mud	24 (1 day)	1715/1150	<3	30	5	<5	20	50
G2	Short bed; only BB-mud	24 (1 day)	1630/1010	<1	90	<5	<5	<10	<50
H	Long bed; only BB-mud	24 (1 day)	1750/1205	<3	90	<5	<5	<10	<50

The depth-averaged mud concentrations remain rather low with maximum values in the range of 50 to 150 mg/l for the waves-only scenarios.

Figure 4.4.6 shows the effect of dry density on the sand concentration profiles compared to the sand concentrations for a pure fine sand bed. The density of the mud-sand mixture was also varied by using different consolidation times (2 hours, 2 days and 4 days). Extra water (5%) was added to the mud-sand mixture of Test E (short bed) to decrease the initial bed density. The sand concentrations decrease for increasing bed density and are extremely low < 100 mg/l for the highest bed density in Test CC. The sand particles were easily eroded from the relatively mobile slurry into sand ripples in Test C (consolidation=2 hours) resulting in near-bed sand concentrations which are factor of 3 lower than for a pure sand bed.

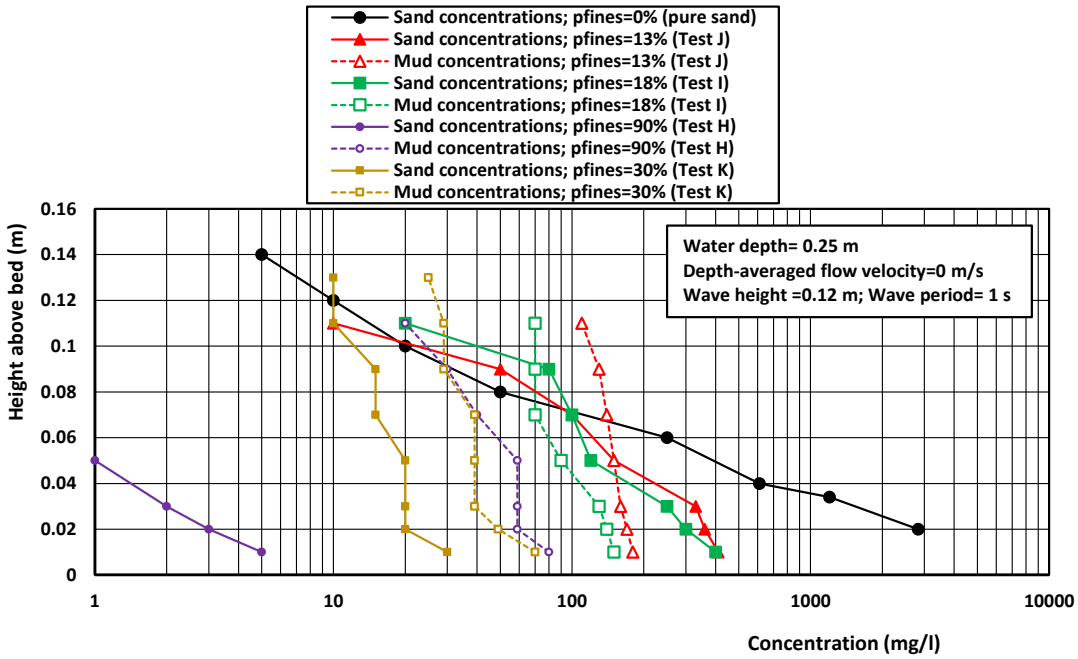

Figure 4.4.3 Sand and mud concentration profiles for mud-sand beds; waves alone (H=0.12 m)

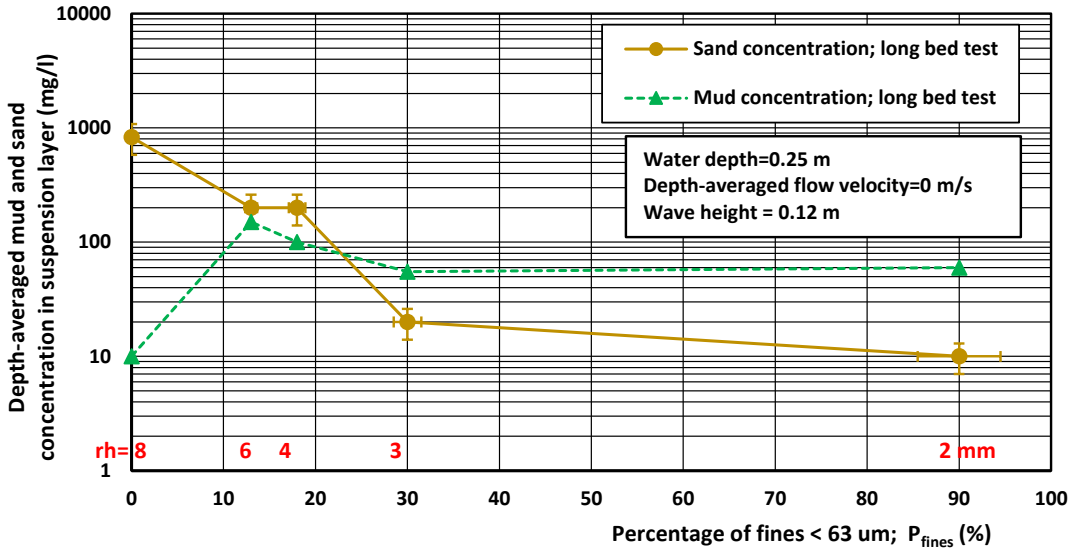

Figure 4.4.4 Depth-averaged sand and mud concentrations as function of percentage of fines <63 μm; waves alone (H=0.12 m; water depth=0.25 m). Rh = Ripple height in millimetres.

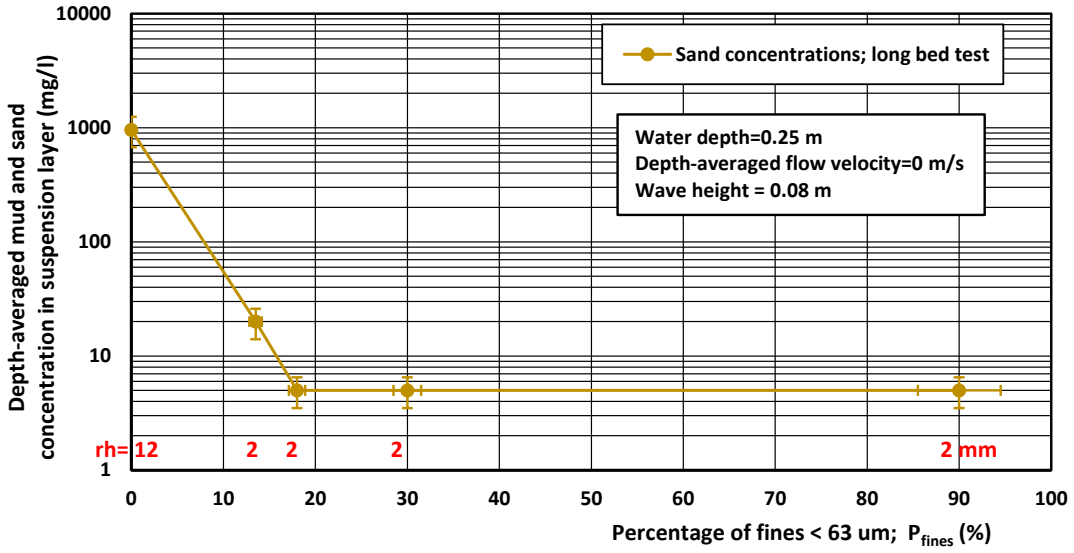

Figure 4.4.5 Depth-averaged sand and mud concentrations as function of percentage of fines <63 μm; waves alone (H=0.08 m). Rh = Ripple height in millimetres.

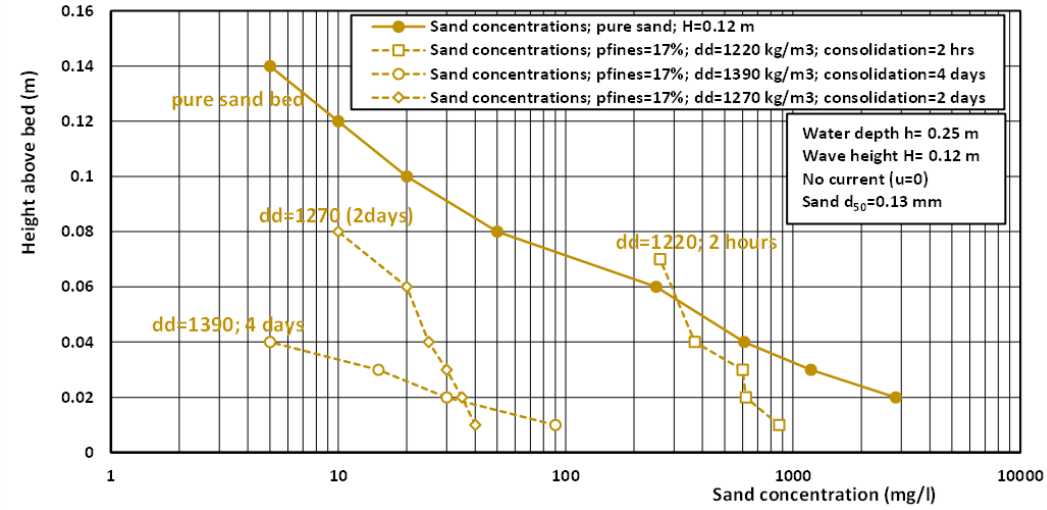

Figure 4.4.6 Effect of dry density (consolidation time) on sand concentration profiles; short bed tests with waves alone: Experiments A, C (2 hours), CC (4 days) and E (2 days)

Combined currents and waves

Data from the long-bed experiments (Experiments A, I, J and H) are used to study the effect of the percentage of fines < 63 μm on the sand and mud concentrations. The hydrodynamic conditions are, follows (water depth=0.25 m):

- current velocity u_c=0.2 m/s; H=0.12 m (T=1 s);
- current velocity u_c=0.35 m/s; H=0.08 m (T=1.2 s);
- current velocity u_c=0.75 m/s; H=0.06 m (T=1 s).

The results are shown from Figure 4.4.7 to Figure 4.4.11.

The key findings are:

- sand concentrations in the near bed zone are substantially reduced for increasing percentage of fines (reduction up to factor of 10 for p_{fines} > 10% and currents <0.35 m/s and factor 4 for higher current of 0.75 m/s);
- mud concentrations are rather uniform over the water column.

During wave-current experiments with mud percentages higher than 30%, the gradual increase in cw-shear stress resulted in the erosion of mud particles at the surface. The mud particles derived specifically in between the sand particles and small-scale isolated barchan-type sand ripples slowly grew with darker grey/black spots (troughs) between the sand crests. The sand ripples remained relatively flat (ripple suppression) while the sand was not fully available and partly bonded by cohesive effects within the muddy matrix. The ripples had a symmetrical shape when waves were dominant, but became more asymmetrical for increasing current strength. The suppression of ripple development already occurred for p_{fines} of about 10% but increased strongly for increasing percentage of fines (10% to 30%) resulting in a strong reduction (up to factor of 10) of the near-bed sand concentrations and transport. When the bed-shear stress was sufficiently high, the mud was eroded from the muddy troughs and almost immediately suspended in the water column (almost uniform mud concentration profiles).

It is noted that the present results were observed for the artificial mixtures of mud and fine sand (0.13 mm). Additional experiments with natural mixtures of mud and sand are required to confirm the present results. Suitable natural mixtures of mud and sand can be found at the sites BA-APP ($p_{fines}\cong25\%$) and HU ($p_{fines}\cong12\%$) along the banks of the Westerschelde.

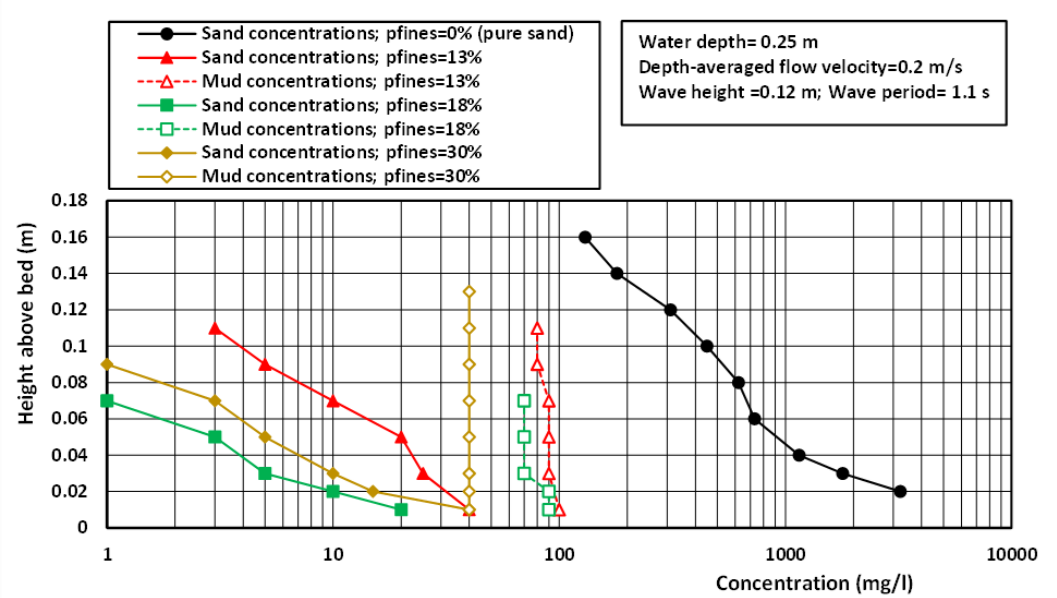

Figure 4.4.7 Sand and mud concentration profiles for mud-sand beds; current plus waves (u_c=0.2 m/s; H=0.12 m; water depth=0.25 m)

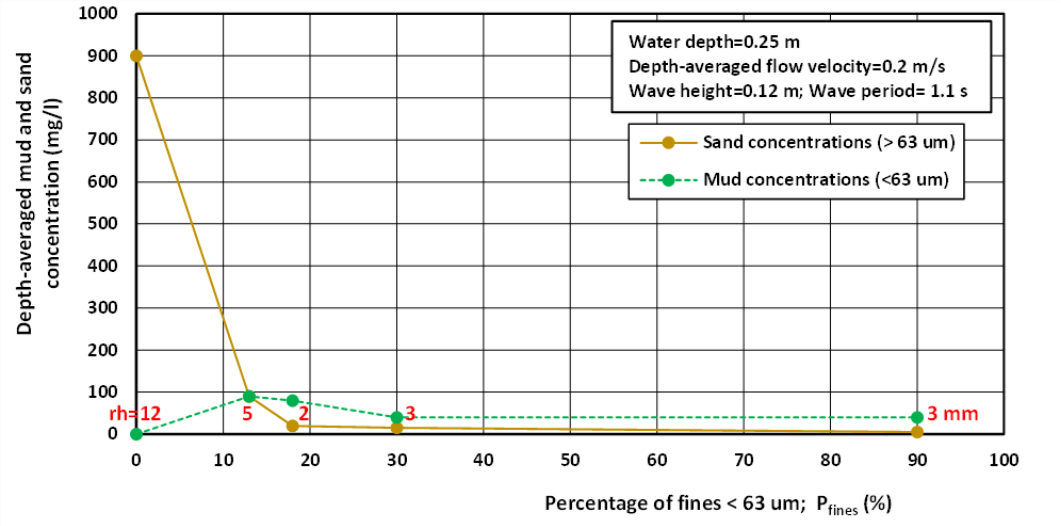

Figure 4.4.8 Depth-averaged sand and mud concentration as function of percentage of fines < 63 μm; current u_c=0.2 m/s; wave height H=0.12 m; water depth h=0.25 m; rh = ripple height

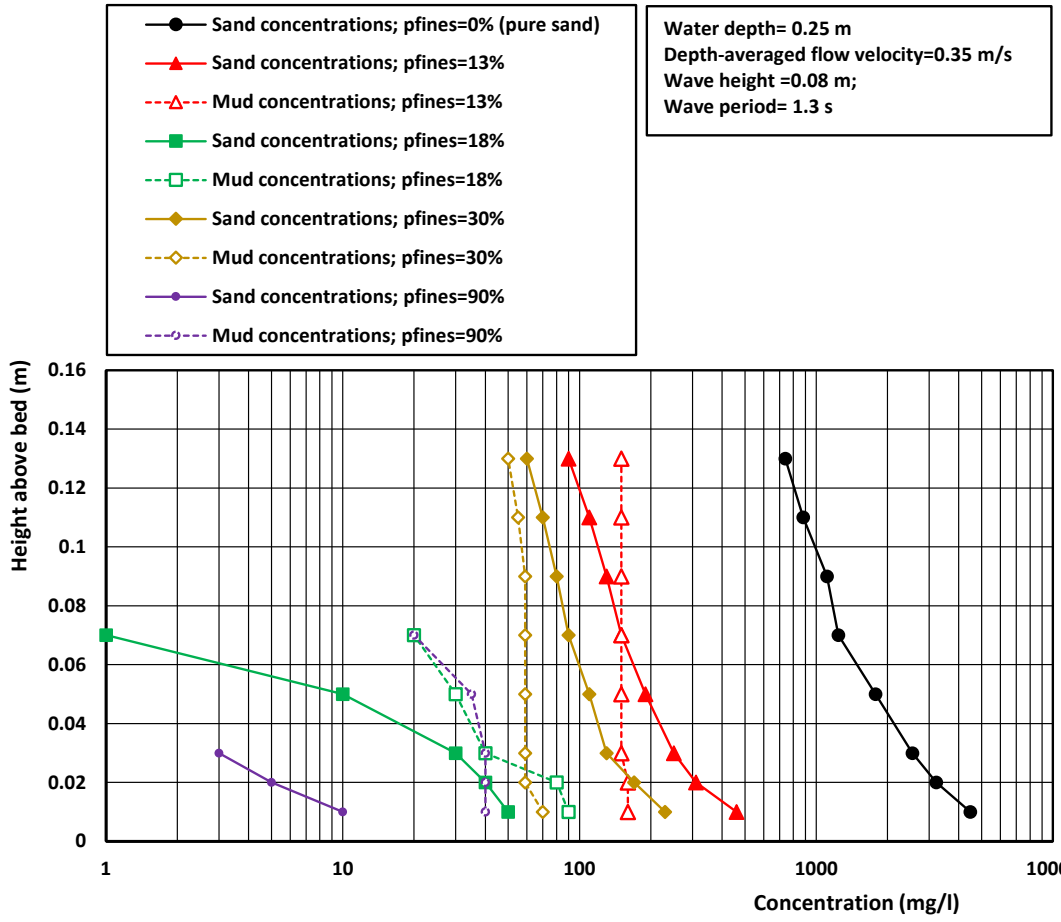

Figure 4.4.9 Sand and mud concentration profiles for mud-sand beds; current plus waves (u_c=0.35 m/s; H=0.08 m; water depth=0.25 m)

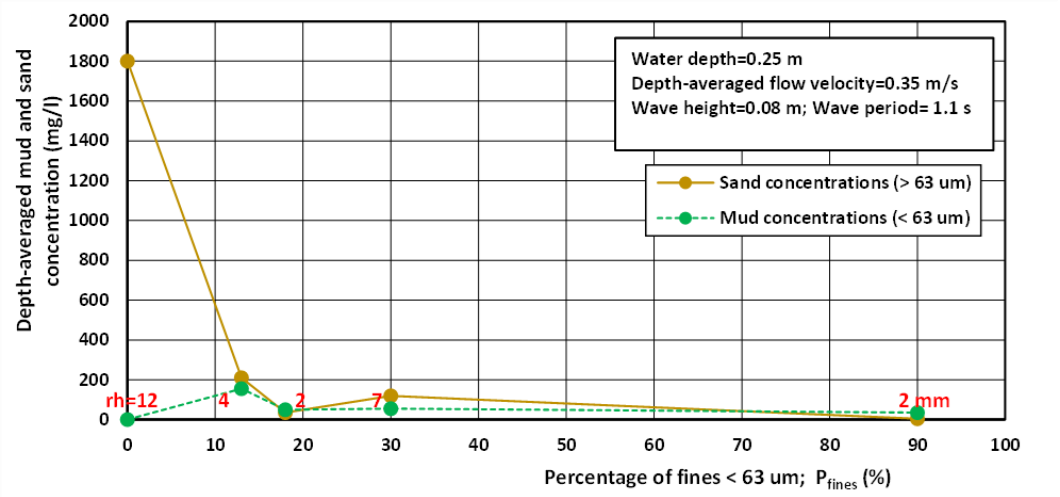

Figure 4.4.10 Depth-averaged sand and mud concentration as function of percentage of fines < 63 μm; current u_c=0.35 m/s; wave height H=0.08 m; water depth h=0.25 m; rh = ripple height

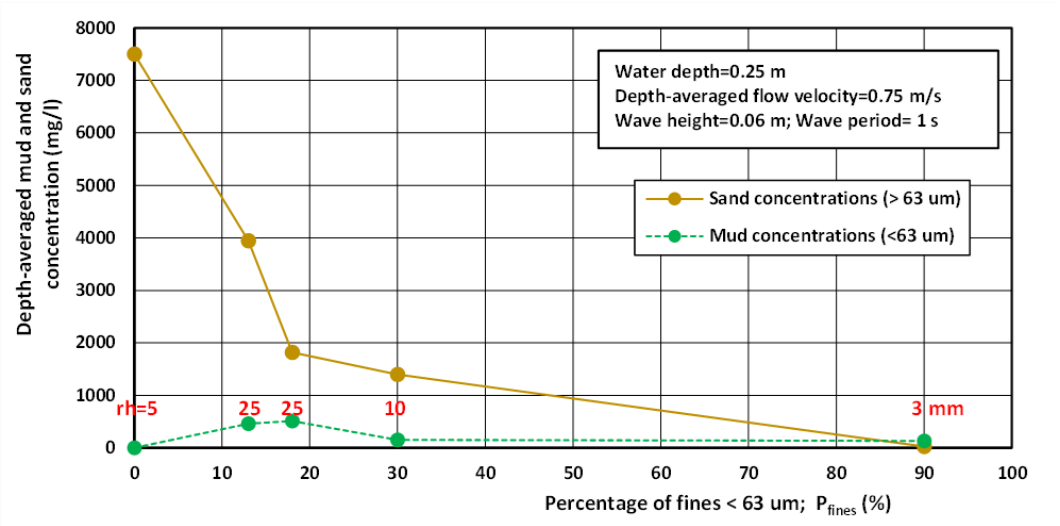

Figure 4.4.11 Depth-averaged sand and mud concentration as function of percentage of fines < 63 μm; current u_c=0.75 m/s; wave height H=0.06 m; water depth h=0.25 m; rh = ripple height

Erosion rates

A simplified compilation of the erosion rates of mud-sand mixtures based on earlier results is given in Figure 4.4.12 (Van Rijn 2019). For clarity, the measured values have been omitted as they are represented by the curves. The erosion rate increases for increasing bed-shear stress ($E \sim \tau_b^2$) and decreases strongly for increasing the bed dry density (400, 600, 700, 800 and > 1000 kg/m^3). The erosion rate of fine cohesionless sand of 63 μm measured in a high-velocity pipeline circuit is also shown (Van Rijn et al. 2018). Strong damping of turbulence at high bed-shear stress conditions was observed for cohesionless fine sand resulting in a less steep increase of the erosion rate of fine sand. The erosion rate of mixtures of clay-silt-sand is smaller than that of fine (cohesionless) sand. The cohesive effects of the very fine clay fraction reduces the erosion rate of cohesive mixtures.

The erosion results from the MUSA-long-bed tests with currents of 0.75 m/s (A, J, I and K) can be used to estimate the erosion rate from the volume of eroded sediment, see Table 4.4.4. The results are of the correct order of magnitude compared to other data, see Figure 4.4.12. Those erosion rates will be further studied during the future detailed analyses within the MUSA project.

Table 4.4.4 Mass erosion rates for Test A, J, I and K (u_c=0.75 m/s; H=0.06 m)

Test	Percentage of fines $p_{fines<63\ um}$ (%)	Dry density (kg/m³)	Mass erosion rate (g/m²/s)	Bed-shear stress (N/m²)
A (pure sand)	0		50±0.20	1.35 ±0.2
J	13		15±5	1.35 ±0.2
I	18		10±2	1.35 ±0.2
K	30		5±2	1.35 ±0.2

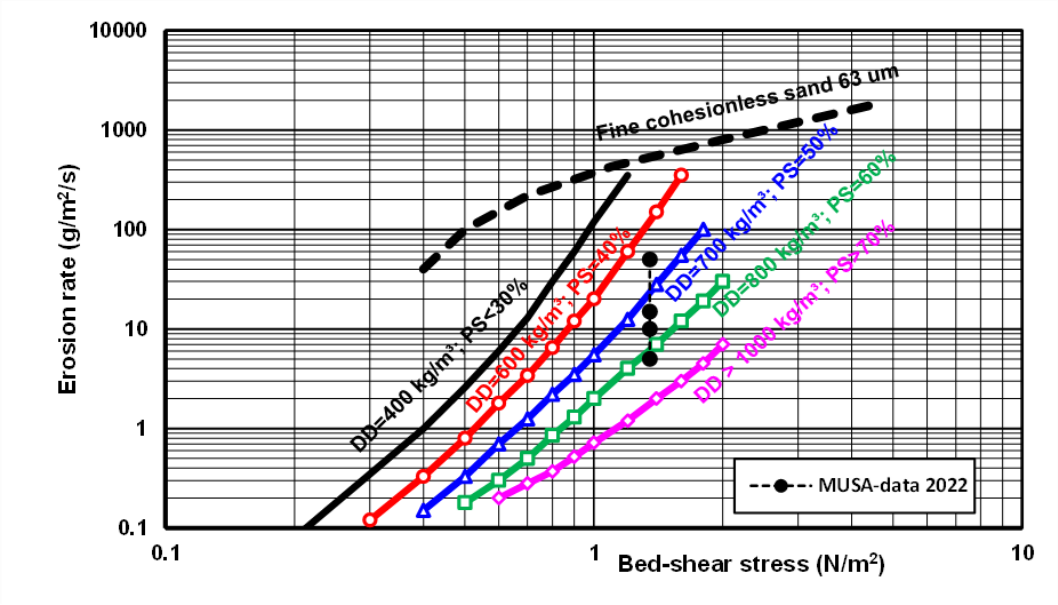

Figure 4.4.12 Erosion rates of mud-sand mixtures (DD=dry density; PS= percentage of sand)

5 Conclusions

This study focusses on the erosional behaviour of mud-sand beds with percentages of fines (<63 μm) varying in the range of 10% to 30% when we expect large variations in the cohesion behaviour. Experiments were executed in the wave-current flume of WaterProof in conditions with currents alone, waves alone and combined currents and waves.

5.1 Critical bed-shear stress

The critical bed-shear stress values of the Van Rijn-method (Van Rijn, 1993) are close to the Shields curve. Those of the Soulsby-method (Soulsby, 1995) are much higher (up to factor 2). This difference between formulations highlights a relevant mismatch in the empirical equations of bed shear stress under combined wave-current conditions. The critical bed-shear stress for surface erosion of mud-sand mixtures is found to be somewhat smaller in conditions with current alone compared to combined waves and currents; this discrepancy can be related to the method used to compute bed-shear stress due to combined current and waves. Alternatively, our results point out that either waves add other processes (pressure and flow acceleration) that change the erosion behaviour that are not accounted in the bed shear stress formulations, or that critical bed shear values are not an intrinsic sample characteristic but actually varies its value depending on the hydrodynamic conditions (waves and currents).

The results derived from the flume experiments show that the critical bed-shear stress is not strongly influenced by cohesive effects if the percentage of fines (< 63 μm) is smaller than about 10%, while for p_{fines} > 15%, the critical bed-shear stress increases for increasing mud content. The results also indicate that the bed ripple development and near-bed sand transport may already be affected for a much lower percentage of fines (5%). Most likely, the percentage of the clay-dominated fraction (<8 μm) with cohesive properties is the key element in the change of the bed dynamics. Earlier research shows that the transition between non-cohesive and cohesive behaviour may occur at a clay content of 5% to 10% which implies a percentage of fines of about 30% assuming a clay/silt ratio near 0.5.

Here we observed significant differences between the critical bed-shear stresses of short-bed and long-bed and between current-only and wave-current conditions with mud-sand mixtures. This raises the question whether the observed discrepancies derive from missing processes (bed shear stress cannot fully relate flow to erosion), the empirical bed shear stress equations fail in representing erosion over the whole range of mud-sand and wave-current conditions, or that experiments with short beds are not really suitable for determination of the critical bed-shear stress for erosion.

5.2 Erosion of mud and sand

Flume experiments with currents and waves over a pure fine sand bed show the generation of small-scale sand ripples and strong ripple-induced vortex motions resulting in relatively high sand concentrations in the boundary layer close to the bed. The near-bed sediment dynamics of a fine sand bed may change drastically when low amounts (e.g. <15%) of cohesive sediments (mud) is added to the sand bed. Bed properties, such as the bulk density, change when increasing the mud percentage in the sediment mixture. Also, the mixtures lead a variation of muddy and sandy spots and overall suppression of the bed ripples and therefore to lower sand concentrations and transport.

Sand concentrations in the near bed zone are substantially reduced for increasing percentage of fines (reduction up to factor of 10 for p_{fines} > 10% and currents <0.35 m/s and factor 4 for higher current of 0.75 m/s). Mud concentrations are rather uniform over the water depth.

When the bed-shear stress due to combined currents and waves at the mud-sand bed surface with p_{fines}< 30% gradually increases to beyond the critical bed-shear stress, the mud particles at the surface are washed out from between the sand particles and small-scale isolated barchan-type sand ripples are slowly build up with darker grey/black spots (troughs) between the sand crests. The sand ripples remain relatively flat (ripple suppression) as sand is not fully available and partly bonded by cohesive effects. They have a symmetrical shape when waves are dominant but become more asymmetrical for increasing

current strength. The suppression of ripple development already occurs for p_{fines} of about 10% but increases strongly for increasing percentage of fines (10% to 30%) resulting in a strong reduction (up to factor of 10) of the near-bed sand concentrations and transport. When the bed-shear stress is sufficiently high, the mud is eroded from between the sand crests and almost immediately suspended in the water column (almost uniform mud concentration profiles).

Mud concentration decreases when increasing the mud content from 0 to 30%. This suggest that, assuming a rather similar critical shear stress for a range of mud content, the erosion rate (M) decreases when increasing the mud percentage.

5.3 Erosion rates

A simplified compilation of the erosion rates of mud-sand mixtures based on earlier results is given in Figure 4.4.12 (Van Rijn 2019). The erosion rate increases for increasing bed-shear stress ($E \sim \tau_b^2$) and decreases strongly for increasing the bed dry density (400, 600, 700, 800 and > 1000 kg/m³). The erosion rate of fine cohesionless sand of 63 μm measured in a high-velocity pipeline circuit is also shown (Van Rijn et al. 2018). Strong damping of turbulence at high bed-shear stress conditions was observed for cohesionless fine sand resulting in a less steep increase of the erosion rate of fine sand. The erosion rate of mixtures of clay-silt-sand is smaller than that of fine (cohesionless) sand. The cohesive effects of the very fine clay fraction reduces the erosion rate of cohesive mixtures.

The erosion results from the MUSA long-bed experiments with currents of 0.75 m/s are of the correct order of magnitude compared to other data. Those erosion rates should be further investigated in future projects.

6 Recommendations

- Additional tests with long beds of natural mud-sand mixtures are highly recommended (e.g. BA-4; BA-APP; HU1). Long bed test with natural sandy muds are strongly recommended to assess whether the differences in critical bed shear stresses between short bed and long bed tests is caused by boundary/artificial effects, differences between empirical equations or natural processes.
- Further data analyses on the long bed experiments to assess if increasing the mud content between 0 and 30% affects the erosion rate. The current results suggest that increasing P_{fines} in this range reduces the mud concentration in the water column.

7 References

Boechat Albernaz, M., Van Rijn, L., Schoonhoven, D., Perk, L., 2022 TKI MUSA: Results of laboratory experiments Phase 1A and 1B; 1A - Sediment analysis & erosion of remoulded beds under currents; 1B- Erosion of placed-bed and deposited-beds under currents. Technical Report

De Smit, J.C., Kleinhans, M.G., Gerkema, T. and Bouma, T.J., 2021. Quantifying natural sediment erodibility using a mobile oscillatory flow channel. Estuarine, Coastal and Shelf Science, Vol. 262. Doi: 10.1016/j.ecss.2021.107574

Perk, L., Van Rijn, L., 2020 TKI MUSA: Measurement plan *Technical report*

Soulsby, R.L. and Clarke, S. 2005. Bed shear stress under combined waves and currents on smooth and rough beds. Report TR 137, HR Wallingford, UK

Soulsby R.L., 1995. Bed shear stress due to combined waves and currents. In: Advances in coastal morphodynamics edited by Stive et al., Delft Hydraulics, Delft, NL.

Van Ledden, M., Van Kesteren, W.G.M. and Winterwerp, J.C., 2004. A conceptual framework for the erosion behaviour of sand-mud mixtures. Continental Shelf Research 24, 1-11.

Van ledden, M., 2003. Sand-mud segragation in estuaries and tidal basins. Doctoral Thesis, Delft University of Technology, Delft, The Netherlands

Van Rijn, L.C., 1993. Principles of sediment transport in rivers, estuaries and coastal seas. Aquapublications, NL

Van Rijn, L.C., 2018. Erodibility of mud-sand mixtures. Report, www.leovanrijn-sediment.com

Van Rijn, L.C., 2019. Erodibility of mud-sand mixtures. Journal of Hydraulic Engineering. Doi.org/10.1061/(ASCE)HY.1943-7900.0001677

Van Rijn, L.C., 2019. Analysis of laboratory and field measurements Holwerd Channel 2019. Report, www.leovanrijn-sediment.com

Van Rijn, L. C., R. Bisschop, and C. Van Rhee. 2019. Modified Sediment pick-up function. J. Hydraul. Eng. 145 (1): 06018017. https://doi.org/10.1061/(ASCE)HY.1943-7900.0001549

Yao, P., Su, M., Van Rijn, L.C., Stive, M. Wang, Z. and Chen, Y., 2022. Erosion behavior of sand-silt mixtures. In preparation

Appendix A

Short-bed tests in small current flume (September 2021)

Objective: determine critical bed shear stress for sand and fines particles of remoulded natural mud-sand mixtures due to current.

Three mud-sand samples have been tested in the short current flume.

The sample sites are along the north bank of the Western Scheldt Estuary near the village of Bath, as follows:

- BA-4 sample; wet density=1870 kg/m^3 (dry density= 1400 kg/m^3); percentage of fines < 63 um=5%;
- BA-APP sample; wet density=1750 kg/m^3 (dry density= 1200 kg/m^3); percentage of fines < 63 um=25%;
- BA-PU sample; wet density=1420 kg/m^3 (dry density= 670 kg/m^3); percentage of fines < 63 um=70%.

Table A. 1 presents the descriptions of the tests in short current flume.

Figure A. 1 to Figure A. 3 show the bed before and during the tests.

Table A. 1: Critical conditions of remoulded samples BA-4, BA-APP and BA-PU in short current flume (September 2021). w,d = wet density; d,d = dry density.

Sample	**Water depth (m)**	**Depth-averaged current velocity (m/s)**	**Bed shear stress (N/m^2)**	**Description**
BA-4 w.d.=1870 kg/m^3 d.d.= 1400 kg/m^3 $p_{fines<63\ \mu m}$=5% bed roughness=0.5 mm (C=65 m$^{0.5}$/s)	0.13	0.25	0.16	occasional particle movement (5%)
		0.30	0.23	frequent particle movement (30%)
		0.35	0.31	general particle movement (100%)
		0.40	0.40	initiation of ripples
		0.50	0.63	growing and migrating ripples
		0.55	0.75	initiation of suspension
BA-APP w.d.=1750 kg/m^3 d.d.= 1200 kg/m^3 $p_{fines<63\ \mu m}$=25%	0.13	0.30	0.2	occasional particle movement (5%)
		0.35	0.27	more particle movement (10%)
		0.55	0.67	frequent particle movement (30%)
		0.70	1.0	initiation of grooves

bed roughness=0.3 mm (C=67 $m^{0.5}/s$)		1.0	2.2	growing grooves
		1.05	2.4	local mass erosion (E=2.5 $g/m^2/s$)
BA-PU w.d.=1420 kg/m^3 d.d.= 670 kg/m^3 $p_{fines<63\ \mu m}$=70% bed roughness=0.2 mm (C=70 $m^{0.5}/s$)	0.13	0.30	0.2	few loose particles moving
		0.60	0.7	initiation of scour marks upstream edge
		0.90	1.4	initiation of grooves
		1.0	2.0	growing grooves in middle
		1.1	2.4	local mass erosion (E<1 $g/m^2/s$)

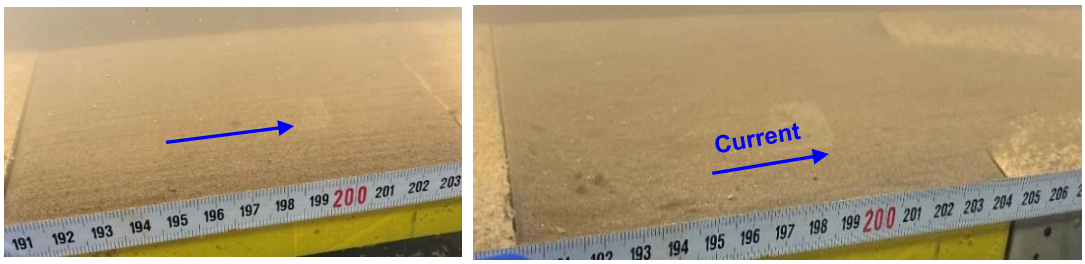

Figure A. 1: Sediment bed before (left) and during (right) Test BA-4.

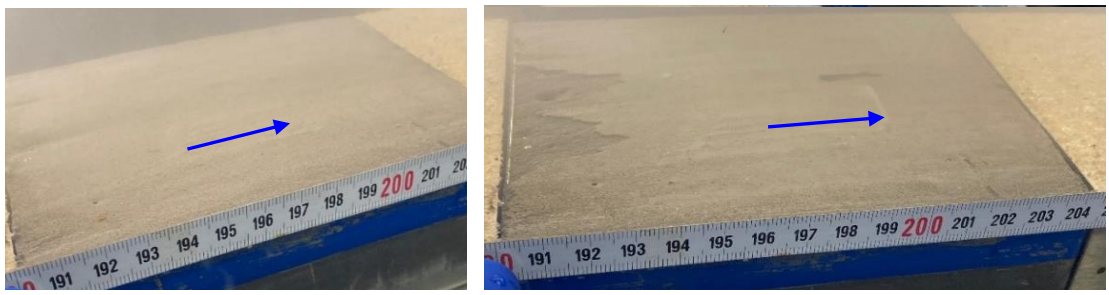

Figure A. 2: Sediment bed before (left) and during (right; u=0.95 m/s) Test BA-APP.

Figure A. 3: Sediment bed before (left) and during (right; u=1.1 m/s) Test BA-PU.

Appendix B

Short-bed tests in wave-current flume (August-September 2021)

Objective: determine critical bed shear stress for sand and fines particles of remoulded and undisturbed natural mud-sand mixtures due to currents and waves.

Three mud-sand samples have been tested in the long wave-current flume.

The sample sites are along the north bank of the Western Scheldt Estuary near the village of Bath, as follows:

- BA-4 sample; wet density=1870 kg/m^3 (dry density= 1400 kg/m^3); percentage of fines < 63 um=5%;
- BA-APP sample; wet density=1750 kg/m^3 (dry density= 1200 kg/m^3); percentage of fines < 63 um=25%;
- BA-PU sample; wet density=1420 kg/m^3 (dry density= 670 kg/m^3); percentage of fines < 63 um=70%.

Sample preparation of remoulded mixtures before testing is, as follows:

- sediment in the base container is mixed thoroughly;
- wet density is determined from small subsample;
- sediment is placed in the test compartment and the mud surface is smoothed at the same level as the adjacent flume floor;
- glass flume walls and adjacent bed are cleaned;
- consolidation time of 1 day before start of test.

Sample preparation of undisturbed mixtures before testing is, as follows:

- sediment sample (0.4x0.5 m^2; about 0.07 m thick) from field site is transferred to laboratory and placed in the test compartment of the flume;
- wet density is determined from small subsample;
- glass flume walls and adjacent bed are cleaned;
- consolidation time of 1 day before start of test.

The test procedure is, as follows:

- remoulded sandy sample BA-4;
  - current velocity of 0.07 m/s and increase wave height in steps until particle movement is observed;
  - current velocity of 0.15 m/s and increase wave height in steps until particle movement is observed;
- remoulded muddy sand sample BA-APP; increase current velocity in steps between 0.1 and 0.6 m/s; vary wave height between 0 and 0.15 m until a combination of current and waves is found which produces particle movement;
- remoulded muddy sample BA-PU; increase current velocity in steps between 0.1 and 0.6 m/s; vary wave height between 0 and 0.15 m until a combination of current and waves is found which produces particle movement (maximum wave height at stronger current is limited to about 25% of water depth);
- undisturbed samples: increase current velocity in steps between 0.1 and 0.6 m/s; vary wave height between 0 and 0.15 m until a combination of current and waves is found which produces particle movement (maximum wave height at stronger current is limited to about 25% of water depth);
- measure current velocity signal using Nortek-vectrino velocity sensor; measure wave height
- estimate bed roughness height and observe particle movement (percentage of bed with moving particles) and or ripple dynamics (initiation of ripples; ripple height and length).

Remoulded sample BA-4 (u_c=0.1 m/s)

Table B. 1 presents the descriptions of the tests in long wave-current flume for Test BA-4 (u_c=0.1 m/s).

Figure B. 1 shows the measured velocity as function of time for Test Ba-4 (u_c=0.1 m/s).

Figure B. 2 shows the computed bed-shear stress values as function of time for Test BA-4 (u_c=0.1 m/s).

Figure B. 3 shows the development of ripples for Test BA-4 (u_c=0.1 m/s)

Table B. 1: Critical conditions of remoulded sample BA-4 (um=0.1 m/s) in long wave-current flume (September 2021). d,d = dry density; c = current; w = waves; cw = current and waves; VR = Method van Rijn; S = method Soulsby.

Sample	**Depth-averaged current velocity (m/s)**	**Wave height (m) and wave period (s)**	**Maximum orbital velocity (ms/)**	**Bed shear stress (N/m^2)**			**Description**
				c	**w (VR)**	**cw (VR; S)**	
BA-4 w.d.=1870 kg/m^3 d.d.= 1400 kg/m^3 $p_{fines<63\ \mu m}$=5% water depth=0.28 m bed roughness= 0.5 mm (C=70 m$^{0.5}$/s)	0.1	0.064 1.9	0.2	0.03	0.27	0.3 0.59	initiation of particle movement in center
	0.11	0.075 1.6	0.21	0.03	0.32	0.35 0.69	general particle movement (100%)
	0.12	0.099 1.3	0.26	0.035	0.47	0.51 1.02	initiation of ripples
	0.14	0.115 1.2	0.26	0.05	0.52	0.58 1.17	initiation of suspension
	0.14	0.111 1.1	0.25	0.05	0.52	0.58 1.16	suspended sand transport and growing ripples

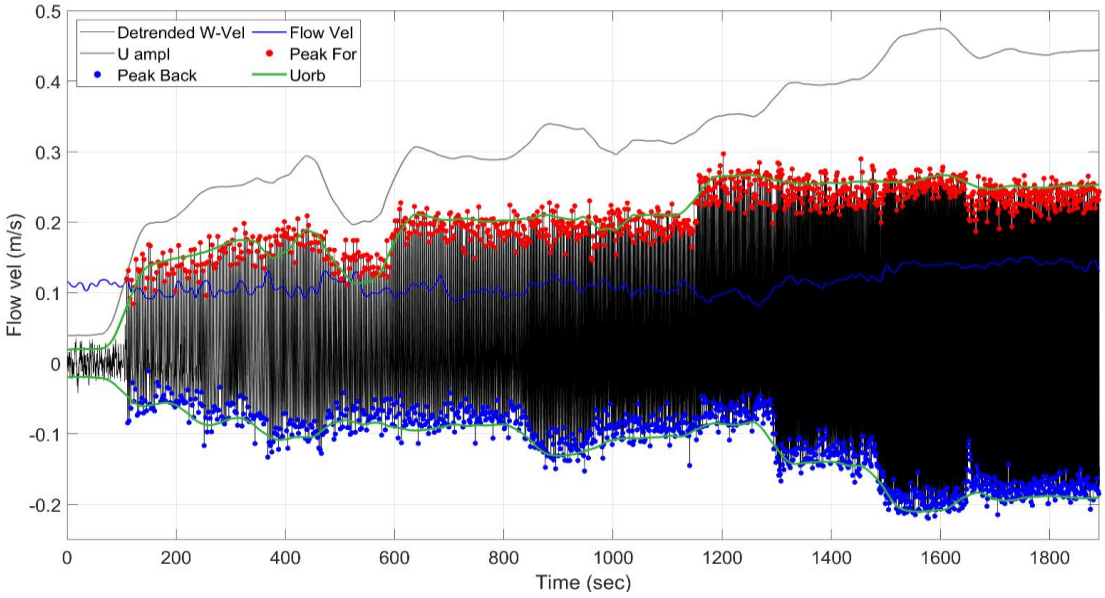

Figure B. 1: Measured velocity signal as function of time; remoulded sample BA-4 (um=0.1 m/s). Detrende W-vel = orbital velocity minus time-averaged velocity; Flow vel = time-averaged flow velocity; U amp = maximum velocity; Peak Back = maximum backward orbital velocity; Peak For = maximum forward orbital velocity; Uorb = smoothed peak orbital velocity.

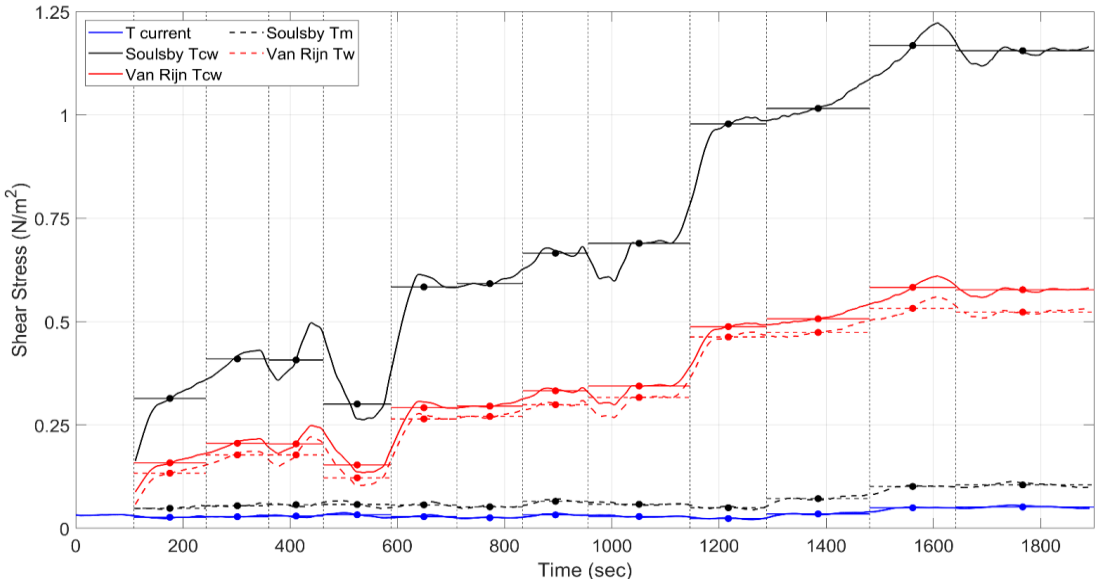

Figure B. 2: Computed bed-shear stress as function of time; remoulded sample BA-4 (um=0.1 m/s). T current = current-related bed-shear stress; Soulsby Tcw = maximum bed-shear stress current+waves according to method of Soulsby; Van Rijn Tcw = time-averaged bed-shear stress current+waves according to method of Soulsby; Van Rijn Tcw = time-averaged bed-shear stress current+waves according to method of Van Rijn; Soulsby Tm = time-averaged bed-shear current+waves according to method of Soulsby; Van Rijn Tw = time-averaged bed-shear stress waves according to method of Van Rijn.

Figure B. 3: Initiation of ripples (left) and growing ripples (right) for Test BA-4 (um=0.1 m/s).

Remoulded sample BA-4 (u_c=0.27 m/s)

Table B. 2 presents the descriptions of the tests in long wave-current flume for Test BA-4 (u_m=0.27 m/s).

Figure B. 4 shows the measured velocity as function of time for Test Ba-4 (u_m=0.27 m/s).

Figure B. 5 shows the computed bed-shear stress values as function of time for Test BA-4 (u_m=0.27 m/s).

Figure B. 6 shows the development of ripples for Test BA-4 (u_m=0.27 m/s)

Table B. 2: Critical conditions of remoulded sample BA-4 (um=0.27 m/s) in long wave-current flume (September 2021). d.d.= dry density; c=current; w=waves; cw=current and waves; VR= Method van Rijn; S= method of Soulsby.

Sample	**Depth-averaged current velocity (m/s)**	**Wave height (m) and wave period (s)**	**Maximum orbital velocity (ms/)**	**Bed shear stress (N/m^2)**			**Description**
				c	**w (VR)**	**cw (VR; S)**	
BA-4 w.d.=1870 kg/m^3 d.d.= 1400 kg/m^3 $p_{fines<63\ \mu m}$=5% water depth=0.29 m bed roughness= 0.5 mm (C=70 m$^{0.5}$/s)	0.29	0.035 2.8	0.095	0.22	0.08	0.3 0.39	general particle movement (100%)
	0.29	0.035 2.8	0.117	0.22	0.11	0.33 0.47	initiation of ripples
	0.27	0.051 2.1	0.164	0.19	0.19	0.39 0.64	growing ripples
	0.27	0.055 1.9	0.138	0.19	0.16	0.35 0.56	initiation of suspension
	0.26	0.082 1.4	0.197	0.18	0.3	0.48 0.88	suspended sand transport and growing ripples

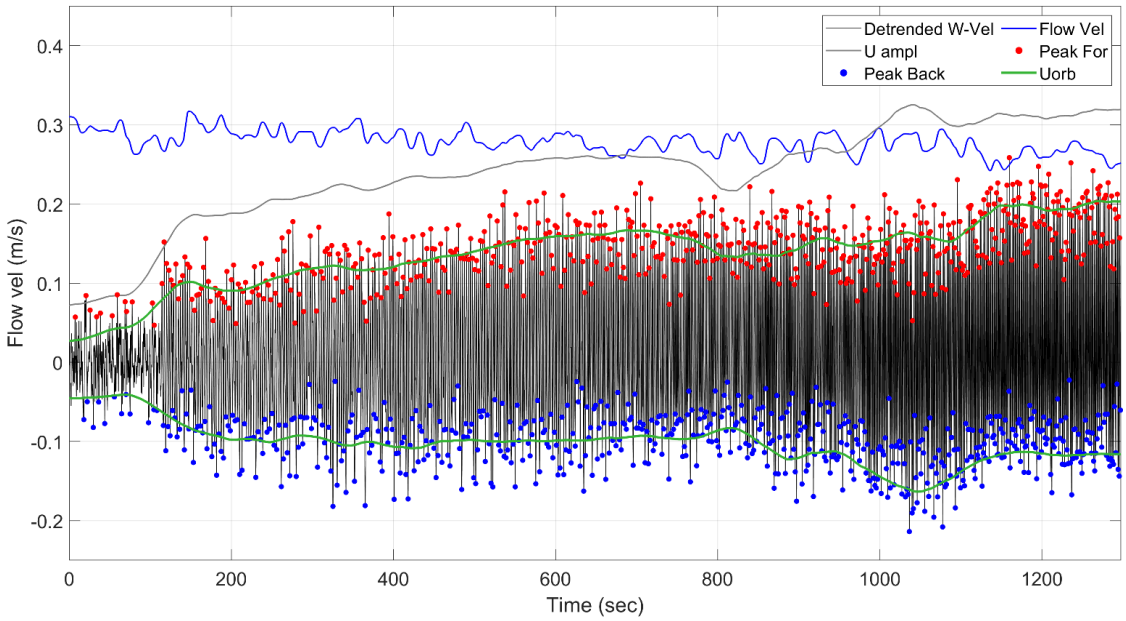

Figure B. 4: Measured velocity signal as function of time; remoulded sample BA-4 (u=0.27 m/s). Detrended W-vel = orbital velocity minus time-averaged velocity; Flow vel=time-averaged flow velocity; U amp = maximum velocity; Peak Back = maximum backward orbital velo velocity; Peak For = maximum forward orbital velocity; Uorb = smoothed peak orbital velocity.

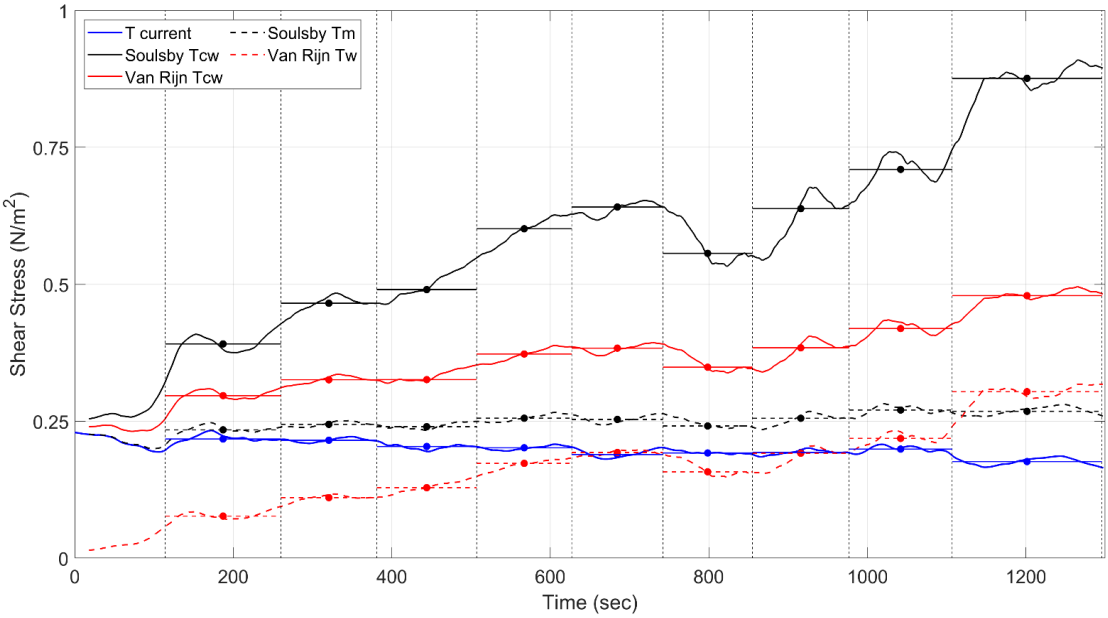

Figure B. 5: Computed bed-shear stress as function of time; remoulded sample BA-4 (um=0.27 m/s). T current = current-related bed-shear stress; Soulsby Tcw = maximum bed-shear stress current+waves according to method of Soulsby; Van Rijn Tcw = time-averaged bed-shear stress current+waves according to method of Soulsby; Van Rijn Tcw = time-averaged bed-shear stress current+waves according to method of Van Rijn; Soulsby Tm = time-averaged bed-shear current+waves according to method of Soulsby; Van Rijn Tw = time-averaged bed-shear stress waves according to method of Van Rijn.

Figure B. 6: Initiation of ripples (left) and growing ripples (right) for test BA-4 (um=0.27 m/s)

Remoulded sample BA-APP

Table B. 3 presents the descriptions of the tests in long wave-current flume for Test BA-APP.

Figure B. 7 shows the measured velocity as function of time for Test BA-APP.

Figure B. 8 shows the computed bed-shear stress values as function of time for Test BA-APP.

Figure B. 9 shows the development of surface erosion for Test BA-APP.

Table B. 3: Critical conditions of remoulded sample BA-APP in long wave-current flume (September 2021). d.d.= dry density; c=current; w=waves; cw=current and waves; VR= Method van Rijn; S= method of Soulsby.

Sample	**Depth-averaged current velocity (m/s)**	**Wave height (m) and wave period (s)**	**Maximum orbital velocity (ms/)**	**Bed shear stress (N/m^2)**			**Description**
				c	**w (VR)**	**cw (VR; S)**	
BA-APP w.d.=1750 kg/m^3 d.d.= 1200 kg/m^3 $p_{fines<63\ \mu m}$=25% water depth=0.31 m bed roughness=0.3 mm (C=70 $m^{0.5}$/s)	0.52	0.029 2.8	0.14	0.6	0.13	0.74 0.89	initiation of sand particles
	0.52	0.04 2.1	0.18	0.6	0.18	0.78 0.99	initiation of growing grooves
	0.55	0.044 1.74	0.18	0.68	0.19	0.87 1.09	growing grooves
	0.57	0.075 1.1	0.2	0.72	0.27	1.0 1.32	growing grooves

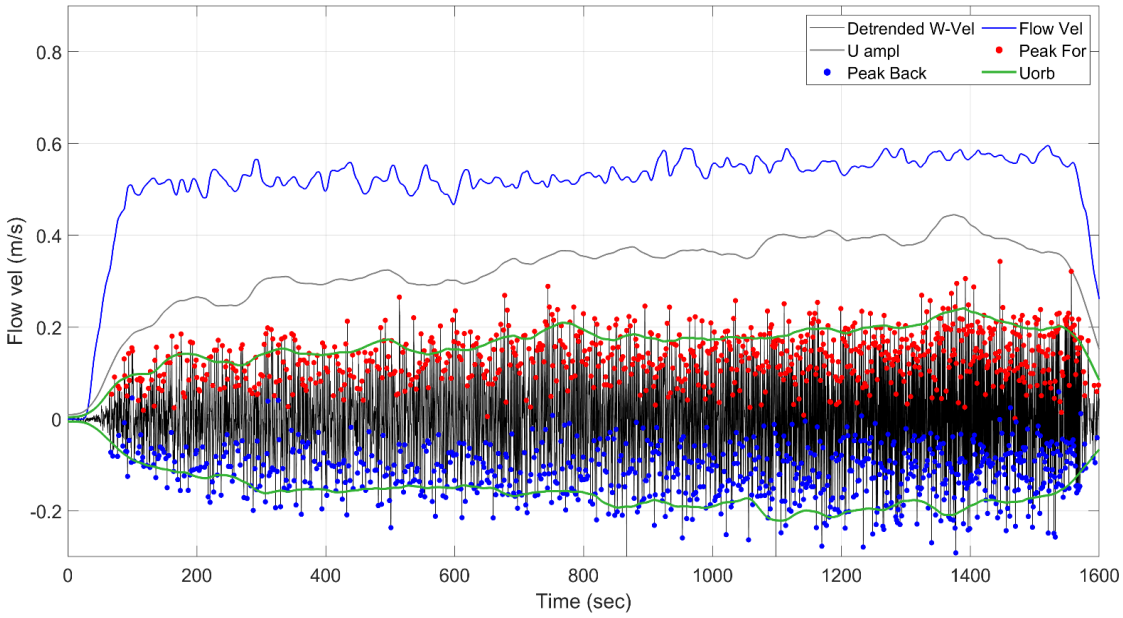

Figure B. 7: Measured velocity signal as function of time; remoulded sample BA-APP. Detrended W-vel = orbital velocity minus time-averaged velocity; Flow vel=time-averaged flow velocity; U amp = maximum velocity; Peak Back = maximum backward orbital velo velocity; Peak For = maximum forward orbital velocity; Uorb = smoothed peak orbital velocity.

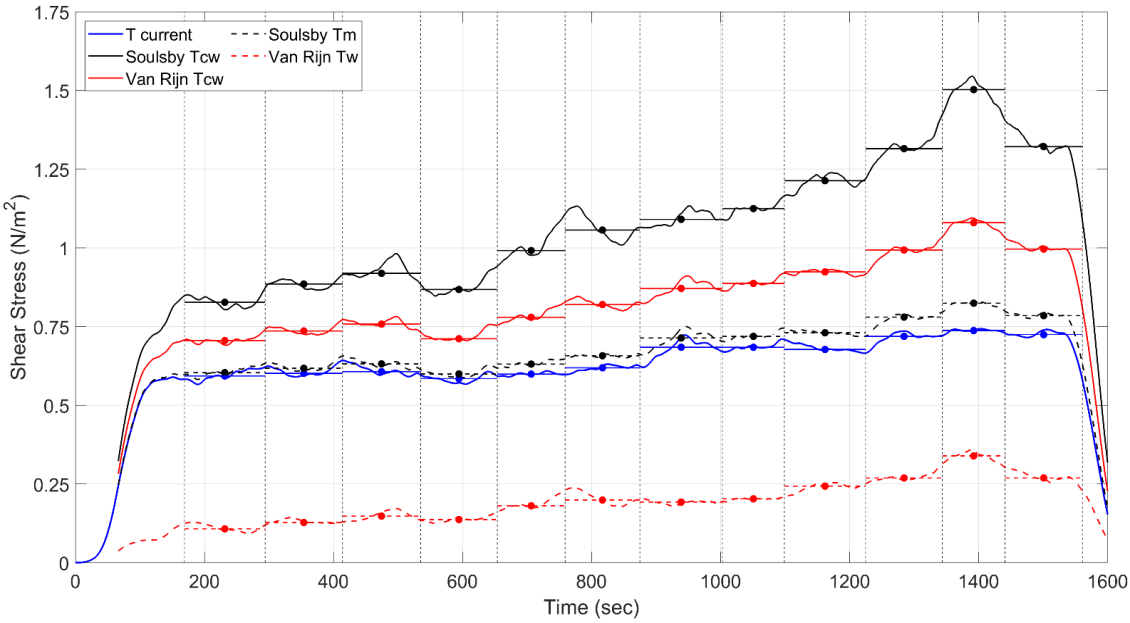

Figure B. 8: Computed bed-shear stress as function of time; remoulded sample BA-APP. T current = current-related bed-shear stress; Soulsby Tcw = maximum bed-shear stress current+waves according to method of Soulsby; Van Rijn Tcw = time-averaged bed-shear stress current+waves according to method of Soulsby; Van Rijn Tcw = time-averaged bed-shear stress current+waves according to method of Van Rijn; Soulsby Tm = time-averaged bed-shear current+waves according to method of Soulsby; Van Rijn Tw = time-averaged bed-shear stress waves according to method of Van Rijn.

Figure B. 9: Development of surface erosion for Test BA-APP.

Remoulded sample BA-PU

Table B. 4 presents the descriptions of the tests in long wave-current flume for Test BA-PU.

Figure B. 10 shows the measured velocity as function of time for Test BA-PU.

Figure B. 11 shows the computed bed-shear stress values as function of time for Test BA-PU.

Figure B. 12 shows the development of surface erosion for Test BA-PU.

Table B. 4: Critical conditions of remoulded sample BA-PU in long wave-current flume (September 2021). d.d.= dry density; c=current; w=waves; cw=current and waves; VR= Method van Rijn; S= method of Soulsby.

Sample	**Depth-averaged current velocity (m/s)**	**Wave height (m) and wave period (s)**	**Maximum orbital velocity (ms/)**	**Bed shear stress (N/m^2)**			**Description**
				c	**w (VR)**	**cw (VR; S)**	
BA-PU w.d.=1420 kg/m^3 d.d.= 670 kg/m^3 $p_{fines<63\ \mu m}$=70% water depth=0.31 m bed roughness=0.5 mm (C=70 $m^{0.5}$/s)	0.53	0.035 2.5	0.17	0.72	0.2	0.92 1.14	initiation of grooves
	0.56	0.042 2.0	0.15	0.8	0.19	1.02 1.23	growing grooves
	0.56	0.048 1.65	0.16	0.8	0.23	1.02 1.29	more growing grooves
	0.54	0.074 1.2	0.22	0.74	0.39	1.11 1.63	growing grooves

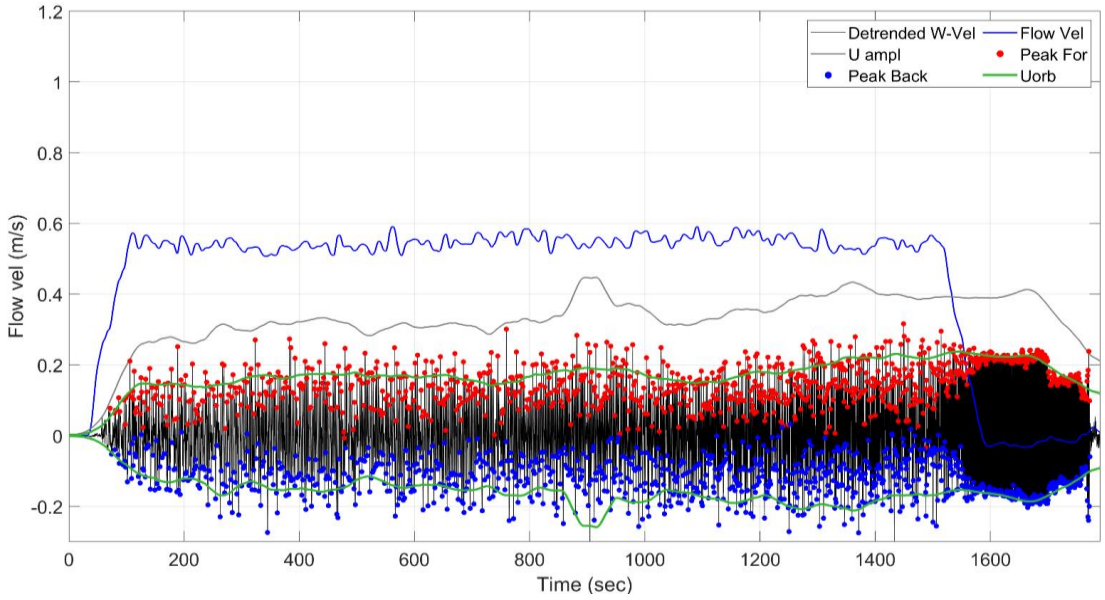

Figure B. 10: Measured velocity signal as function of time; remoulded sample BA-PU. Detrende W-vel = orbital velocity minus time-averaged velocity; Flow vel = time-averaged flow velocity; U amp = maximum velocity; Peak Back = maximum backward orbital velocity; Peak For = maximum forward orbital velocity; Uorb = smoothed peak orbital velocity.

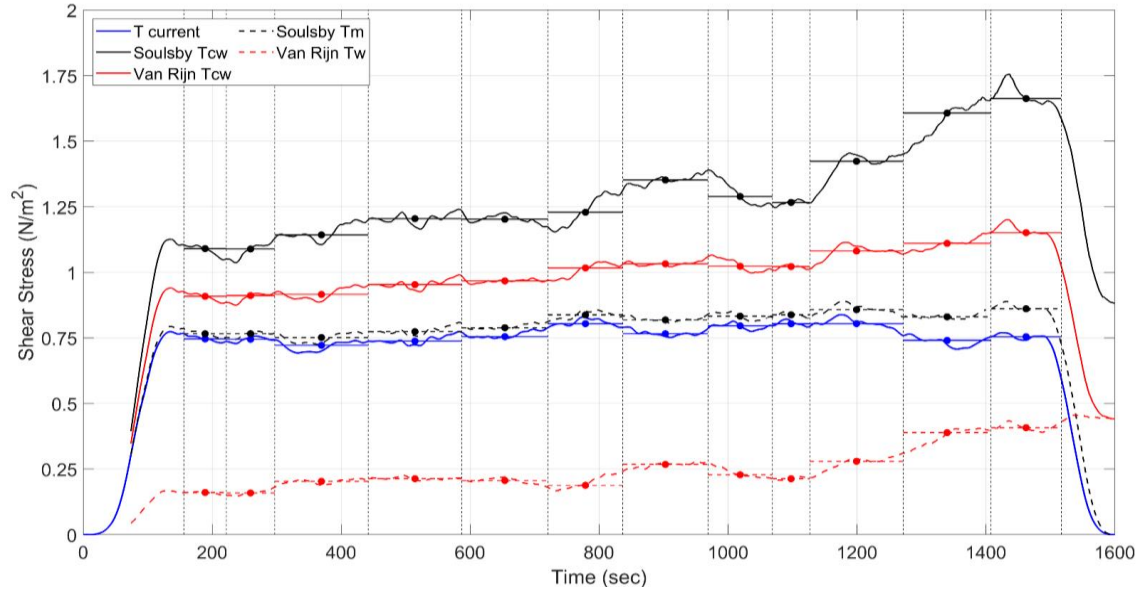

Figure B. 11: Computed bed-shear stress as function of time; remoulded sample BA-PU. T current = current-related bed-shear stress; Soulsby Tcw = maximum bed-shear stress current+waves according to method of Soulsby; Van Rijn Tcw = time-averaged bed-shear stress current+waves according to method of Soulsby; Van Rijn Tcw = time-averaged bed-shear stress current+waves according to method of Van Rijn; Soulsby Tm = time-averaged bed-shear current+waves according to method of Soulsby; Van Rijn Tw = time-averaged bed-shear stress waves according to method of Van Rijn.

Figure B. 12: Development of surface erosion for Test BA-PU.

Undisturbed natural sample BA-APP

Table B. 5 presents the descriptions of the tests in long wave-current flume for Test BA-APP.

Figure B. 13 shows the measured velocity as function of time for Test BA-APP.

Figure B. 14 shows the computed bed-shear stress values as function of time for Test BA-APP.

Figure B. 15 shows the development of surface erosion for Test BA-APP. The bed surface shows many marks (bulges) of benthic fauna creating additional roughness and local turbulence. Bulges remain stable.

Table B. 5: Critical conditions of undisturbed sample BA-APP in long wave-current flume (October 2021). d.d.= dry density; c=current; w=waves; cw=current and waves; VR= Method van Rijn; S= method of Soulsby.

Sample	**Depth-averaged current velocity (m/s)**	**Wave height (m) and wave period (s)**	**Maximum orbital velocity (ms/)**	**Bed shear stress (N/m^2)**			**Description**
				c	**w (VR)**	**cw (VR; S)**	
BA-APP w.d.=1770 kg/m^3 d.d.= 1235 kg/m^3 d.d top=990 kg/m^3 $p_{fines<63\ \mu m}$=25% water depth=0.283 m bed roughness=0.5-1 mm (C=65 $m^{0.5}$/s)	0.25	0.07; 1.3	0.17	0.15	0.18	0.33; 0.56	initiation of particle erosion
	0.43	0.04; 1.9	0.16	0.43	0.15	0.58; 0.76	first signs of erosion around benthic fauna
	0.44	0.07; 1.1	0.20	0.45	0.25	0.70; 1.03	very slowly developing erosion
	0.52	0.08; 1.0	0.21	0.62	0.28	0.90; 1.26	erosion of chunks; water very turbid
	0.64	0.06; 1.0	0.20	0.94	0.27	1.0; 1.56	ongoing erosion; water very turbid

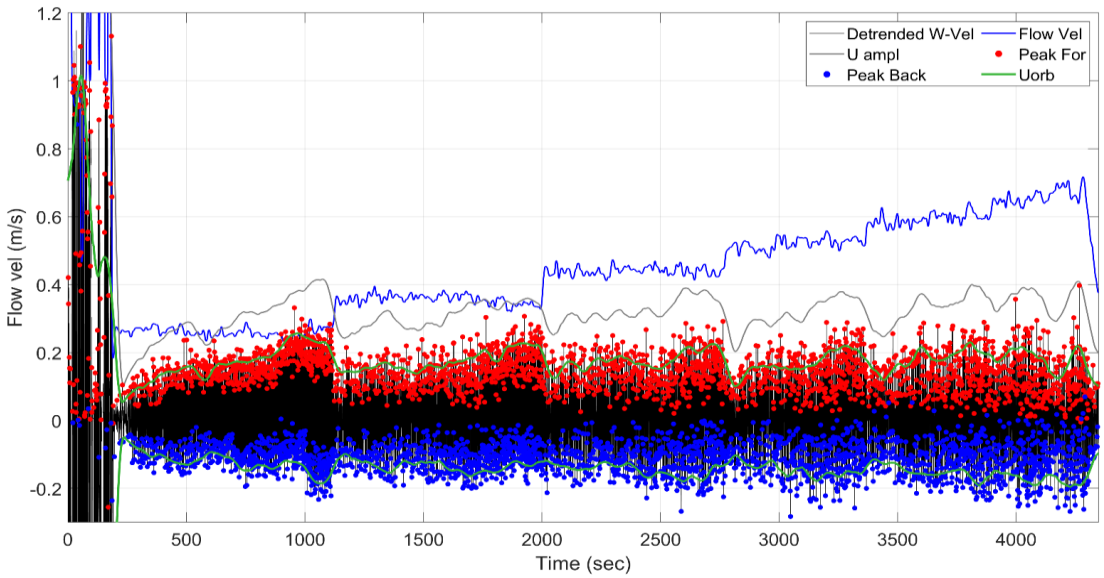

Figure B. 13: Measured velocity signal as function of time; sample BA-APP. Detrende W-vel = orbital velocity minus time-averaged velocity; Flow vel = time-averaged flow velocity; U amp = maximum velocity; Peak Back = maximum backward orbital velocity; Peak For = maximum forward orbital velocity; Uorb = smoothed peak orbital velocity.

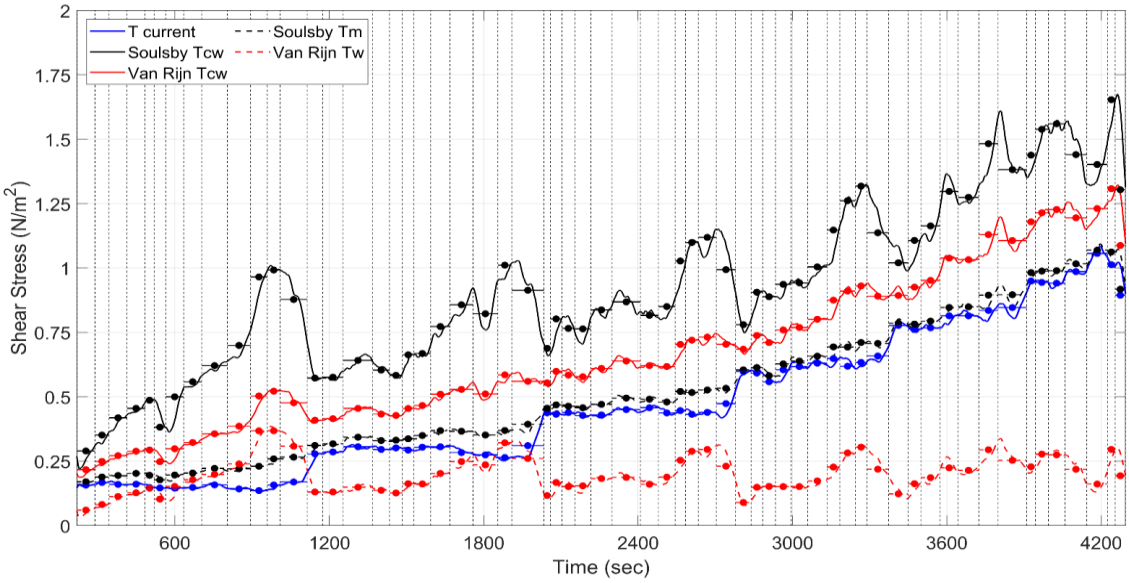

Figure B. 14: Computed bed-shear stress as function of time; undisturbed sample BA-APP. T current = current-related bed-shear stress; Soulsby Tcw = maximum bed-shear stress current+waves according to method of Soulsby; Van Rijn Tcw = time-averaged bed-shear stress current+waves according to method of Soulsby; Van Rijn Tcw = time-averaged bed-shear stress current+waves according to method of Van Rijn; Soulsby Tm = time-averaged bed-shear current+waves according to method of Soulsby; Van Rijn Tw = time-averaged bed-shear stress waves according to method of Van Rijn.

Figure B. 15: Bed surface before test (upper) and at end (lower) of test; undisturbed sample BA-APP.

Undisturbed natural sample BA-4

Table B. 6 presents the descriptions of the tests in long wave-current flume for Test BA-4 with muddy sand.

The top layer (upper 10 mm) consisted of a biomat/film of sediments, benthic fauna, tubes and holes with dry density of about 800 kg/m^3.

Figure B. 16 shows the measured velocity as function of time for Test BA-4.

Figure B. 18 shows the computed bed-shear stress values as function of time for Test BA-4.

Figure B. 17 shows the development of surface erosion for Test BA-4. The bed surface shows many marks of benthic fauna (biomat/film of 10 mm deep) creating additional roughness and local turbulence.

Table B. 6: Critical conditions of undisturbed sample BA-4 in long wave-current flume (October 2021). d.d.= dry density; c=current; w=waves; cw=current and waves; VR= Method van Rijn; S= method of Soulsby.

Sample	**Depth-averaged current velocity (m/s)**	**Wave height (m) and wave period (s)**	**Maximum orbital velocity (ms/)**	**Bed shear stress (N/m^2)**			**Description**
				c	**w (VR)**	**cw (VR; S)**	
BA-4 w.d.=1500 kg/m^3 d.d.= 800 kg/m^3 $p_{fines<63\ \mu m}$=5% water depth=0.27 m bed roughness=0.5-2 mm (C=60-65 m$^{0.5}$/s)	0.15	0.06; 1.4	0.2	0.06	0.26	0.32; 0.67	exposed sand is moving;
	0.25	0.09; 1.3	0.23	0.14	0.44	0.58; 1.15	initiation of erosion of biomat/film
	0.35	0.09; 1.2	0.22	0.32	0.37	0.69; 1.19	growing scour marks
	0.45	0.06; 1.1	0.18	0.53	0.27	0.8; 1.13	scour marks up to 10 mm deep Erosion volum≅0.5 liter (in 1 hour) Erosion rate=1 g/m^2/s

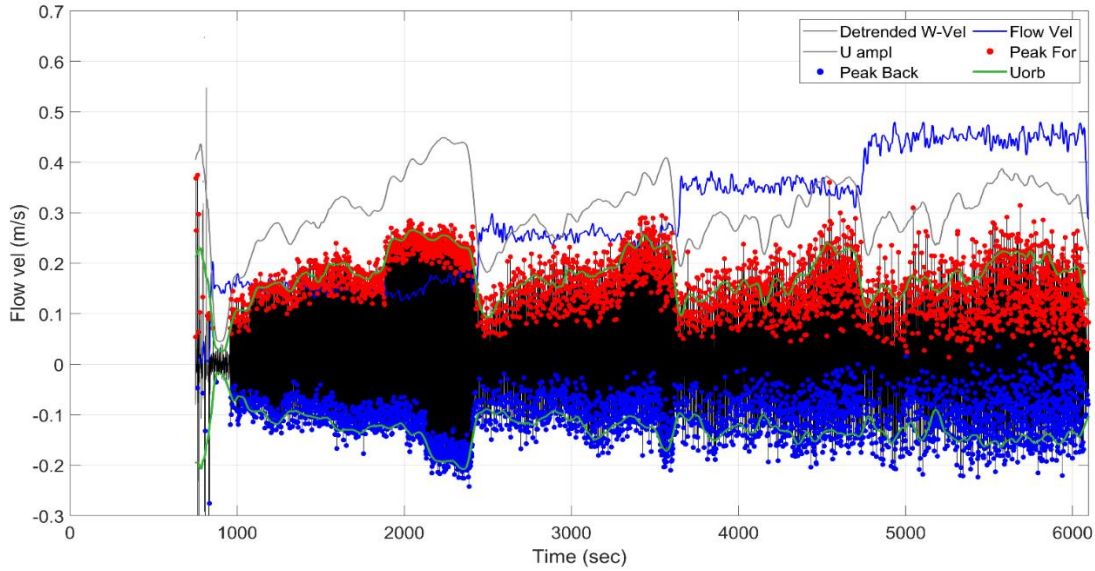

Figure B. 16: Measured velocity signal as function of time; undisturbed sample BA-4. Detrende W-vel = orbital velocity minus time-averaged velocity; Flow vel = time-averaged flow velocity; U amp = maximum velocity; Peak Back = maximum backward orbital velocity; Peak For = maximum forward orbital velocity; Uorb = smoothed peak orbital velocity.

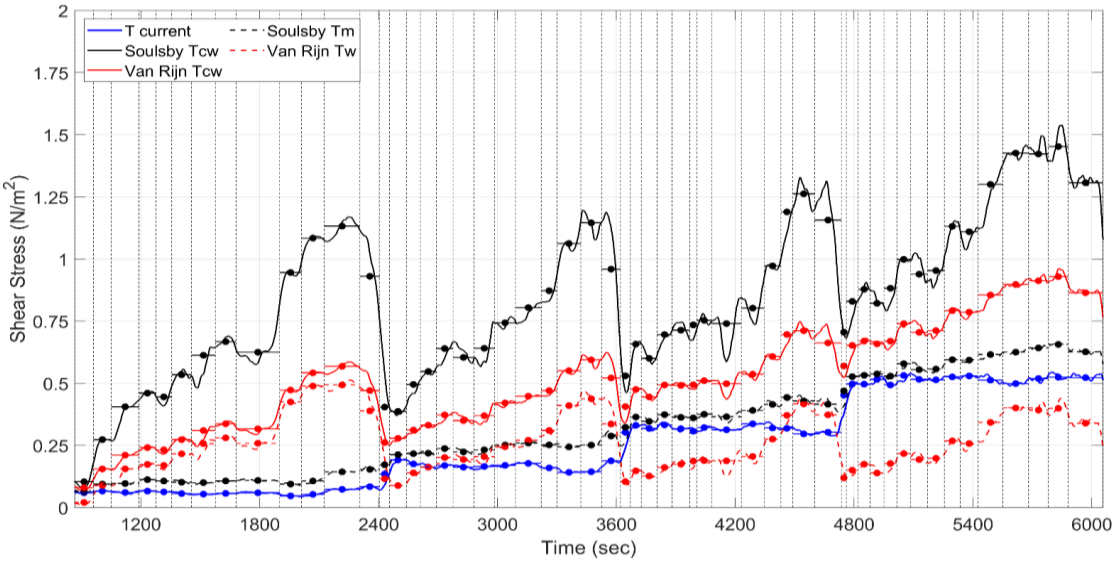

Figure B. 18: Computed bed-shear stress as function of time; undisturbed sample BA-APP. Detrende W-vel = orbital velocity minus time-averaged velocity; Flow vel = time-averaged flow velocity; U amp = maximum velocity; Peak Back = maximum backward orbital velocity; Peak For = maximum forward orbital velocity; Uorb = smoothed peak orbital velocity.

Figure B. 17: Bed surface before test (upper) and at end (lower) of test; undisturbed sample BA-4.

Undisturbed natural sample BA-PU

Table B. 1 presents the descriptions of the tests in long wave-current flume for Test BA-PU.

The top layer (upper 10 mm) consisted of a biomat of fluffy mud, benthic fauna, tubes and holes with dry density of about 650 kg/m^3.

Figure B. 19 shows the measured velocity as function of time for Test BA-PU.

Figure B. 20 shows the computed bed-shear stress values as function of time for Test BA-PU.

Figure B. 21 shows the development of surface erosion for Test BA-PU. The bed surface shows many marks of benthic fauna (biomat/film of 10 mm deep) creating additional roughness and local turbulence.

Table B. 7: Critical conditions of undisturbed sample BA-PU in long wave-current flume (October 2021). d.d.= dry density; c=current; w=waves; cw=current and waves; VR= Method van Rijn; S= method of Soulsby.

Sample	**Depth-averaged current velocity (m/s)**	**Wave height (m) and wave period (s)**	**Maximum orbital velocity (ms/)**	**Bed shear stress (N/m^2)**			**Description**
				c	**w (VR)**	**cw (VR; S)**	
BA-PU w.d.=1405 kg/m^3 d.d.= 650 kg/m^3 d.d. top≅600 kg/m^3 $p_{fines<63\ \mu m}$=70% water depth= 0.29-0.32 m bed roughness=0.5-2 mm (C=60-65 m$^{0.5}$/s)	0.25	0.04; 1.9	0.17	0.17	0.19	0.36; 0.62	initiation of erosion at fluffy top layer
	0.35	0.035; 1.8	0.13	0.32	0.14	0.46; 0.63	erosion of biomat/film; chunks of mud -sand are eroded
	0.44	0.04; 1.8	0.14	0.5	0.17	0.67; 0.87	growing erosion of biomat/film; turbid water
	0.44	0.07; 1.1	0.19	0.5	0.32	0.82; 1.2	severe erosion with scour marks
	0.59	0.07; 1.2	0.19	0.89	0.30	1.19; 1.56	initiation of local mass erosion; very turbid water Erosion volum=0.1 liter (1 hour) Erosion rate< 1 g/m^2/s

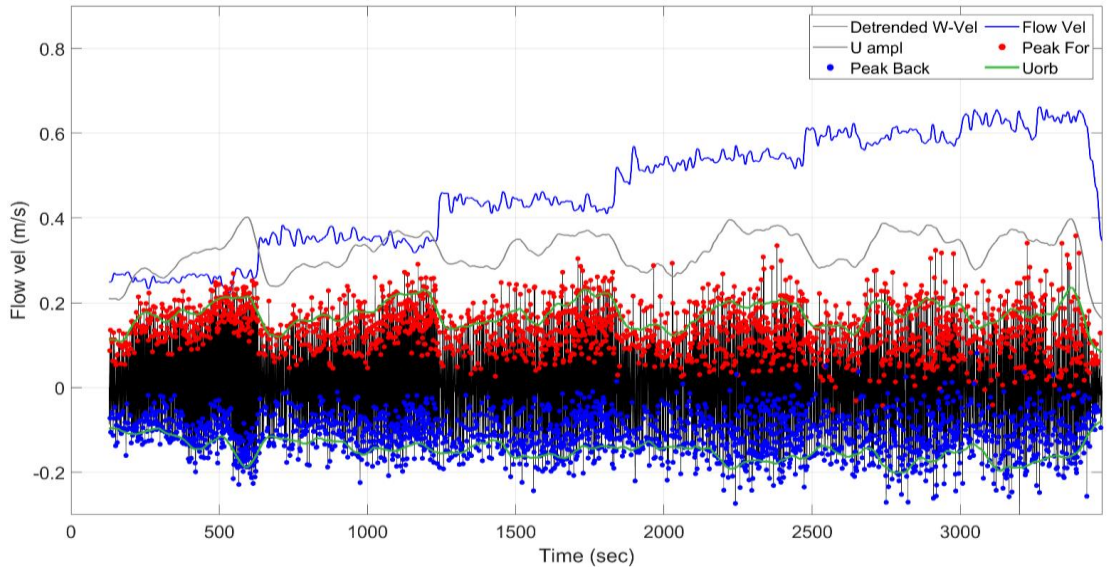

Figure B. 19: Measured velocity signal as function of time; undisturbed sample BA-PU. Detrende W-vel = orbital velocity minus time-averaged velocity; Flow vel = time-averaged flow velocity; U amp = maximum velocity; Peak Back = maximum backward orbital velocity; Peak For = maximum forward orbital velocity; Uorb = smoothed peak orbital velocity.

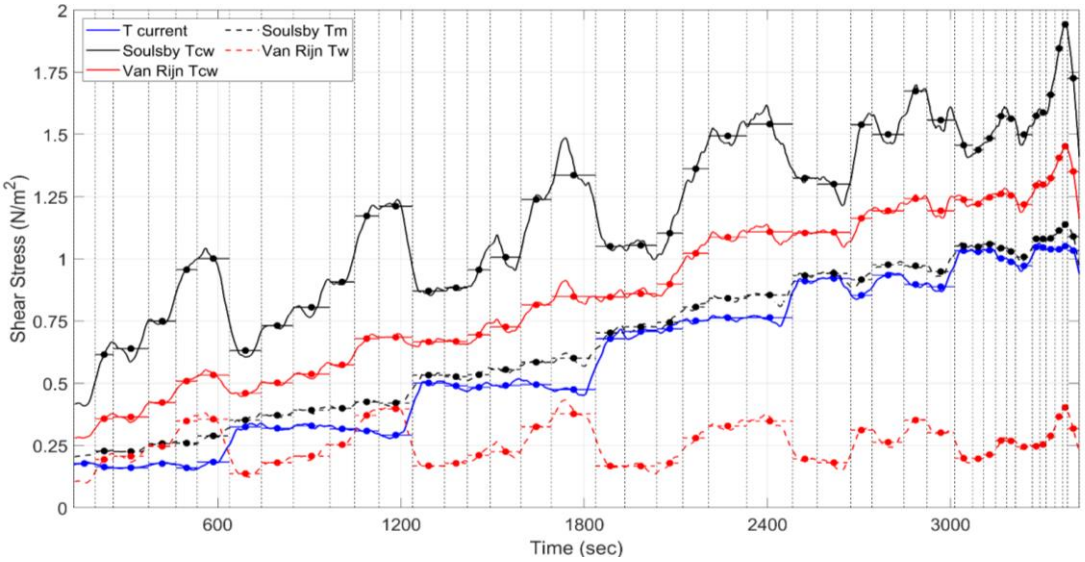

Figure B. 20: Computed bed-shear stress as function of time; undisturbed sample BA-PU. T current = current-related bed-shear stress; Soulsby Tcw = maximum bed-shear stress current+waves according to method of Soulsby; Van Rijn Tcw = time-averaged bed-shear stress current+waves according to method of Soulsby; Van Rijn Tcw = time-averaged bed-shear stress current+waves according to method of Van Rijn; Soulsby Tm = time-averaged bed-shear current+waves according to method of Soulsby; Van Rijn Tw = time-averaged bed-shear stress waves according to method of Van Rijn.

Figure B. 21: Bed surface before test (upper) and at end (lower) of test; undisturbed sample BA-PU.

Appendix C

Short-bed tests in wave-current flume (January-May 2022)

Objective: determine critical bed shear stress for sand and fines particles of different types of mud-sand mixtures due to waves alone (pilot tests).

Test B: short-bed of NPZ-mud and fine sand; mixture with $p_{fines<63um}$=8%; 26 January 2022

Type of bed: artificial mixture of NPZ-mud (dd= 780 kg/m^3; $p_{fines<63um}$=55%) and fine sand (d_{50}=0.13 mm); mud and sand are mixed and placed in the test compartment; wet density of mixture= 1775 kg/m^3; dry density= 1245 kg/m^3; $p_{fines<63\ um}$=8%; smooth surface; consolidation period=20 hrs.

Test conditions (h=water depth=0.25 m) are given in Table C 1.

Bed surface with developing ripples is shown in Figure C. 1.

Table C. 1: Basic data of Test B with mixture of NPZ-mud and fine sand (pfines<63um=8%).

Test	Depth-averaged current u_m (m/s)	Wave height H (m) and period T (s)	Maximum, near-bed velocity U_{max} (m/s)	Sediment dynamics Δ= ripple height λ=ripple length rmv= ripple migration velocity
B-1	0	0.08; 1.5	0.21	weakly mobile bed surface; segregation of sand and mud in top layer into sandy crests and darker muddy troughs (mud washed out); flat sandy ripples Δ< 3 mm
B-2	0	0.12; 1.	0.25	mobile bed surface; flat ripples Δ< 5 mm high, λ=< 30 mm; minor suspension; sand concentrations near bed 50 to 100 mg/l; mud conc≅ 100 mg/l; bed at end: sandy crest; darker fines in troughs (Figure B)

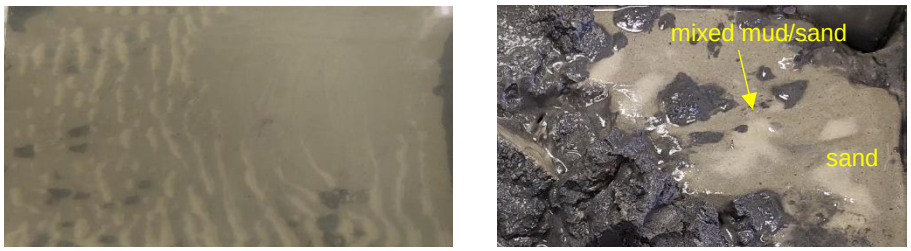

Figure C. 1: Top view bed at end of Test B (light color=sandy crest; grey=silt in ripple troughs; black=deeper mixed mud-sand).

Test C: short-bed of NPZ-mud and fine sand; mixture with $p_{fines<63um}$=17%; 26 January 2022

Type of bed: mixture of NPZ-mud (dd= 780 kg/m^3; $p_{fines<63um}$=55%) and fine sand (d_{50}=0.13 mm);
mud and sand are mixed and placed in the test compartment;
wet density of mixture= 1760 kg/m^3; dry density= 1220 kg/m^3; $p_{fines<63\ um}$=17%;
smooth surface;consolidation period=2 hrs (fluid like mud slurry).

Test conditions (h=water depth=0.25 m) are given in Table C 2.

Bed surface with ripples is in Figure C 2.

Table C. 2: Basic data of Test C with mixture of NPZ-mud and fine sand ($p_{fines<63um}$=17%.).

Test	**Depth-averaged current u_m (m/s)**	**Wave height H (m) and period T (s)**	**Maximum, near-bed velocity U_{max} (m/s)**	**Sediment dynamics Δ= ripple height λ=ripple length rmv= ripple migration velocity**
C-1	0	0.08; 1.5	0.21	top layer of bed is oscillating (10 mm); flat ripples; mud washed out; darker mud/fines in troughs; minor sand suspension < 20 mg/l
C-2	0	0.12; 1.	0.25	top layer of bed is oscillating (10 mm); sand ripples Δ<5 mm; λ< 30 mm; darker mud/fines in troughs; strong suspension 80 mm; sand concentrations up 1000 mg/l; mud concentrations up to 300 mg/l bed at end: sandy spots/crest and muddy troughs

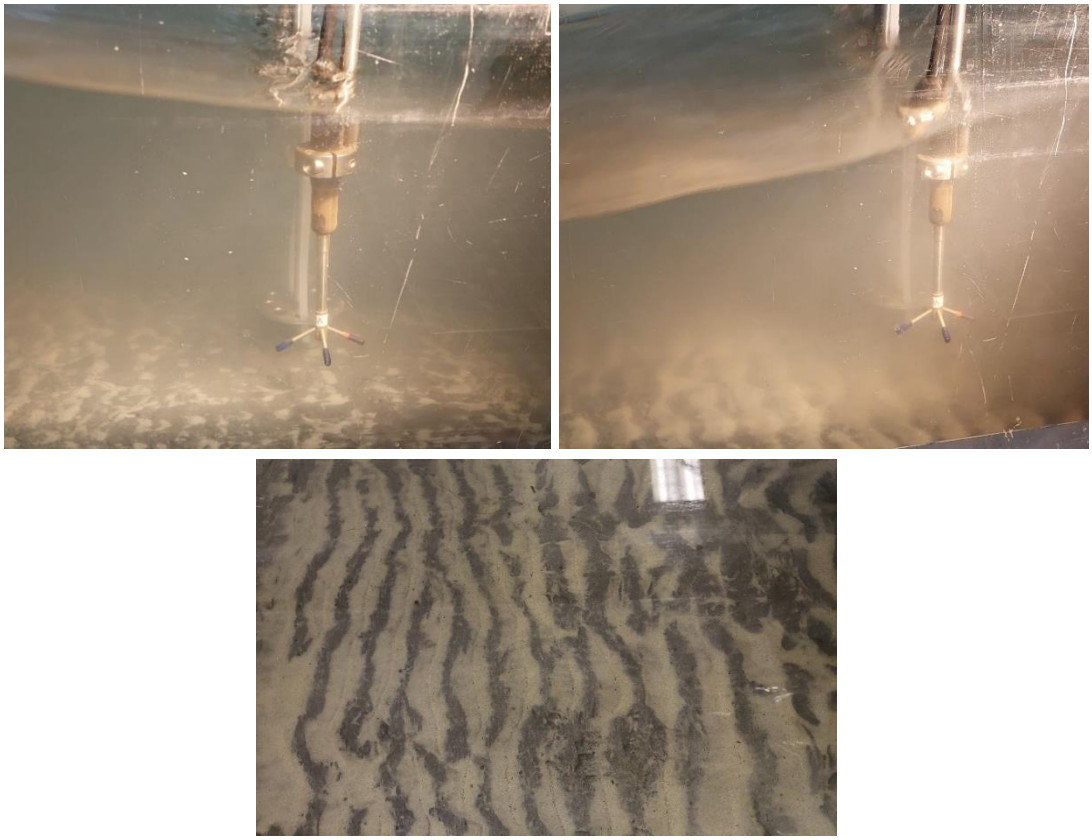

Figure C. 2: Left: Bed at during Test C-1 (H=8 cm); Right: Bed during Test C-2 (H=12 cm). Lower: Top view of bed after Test C-2 (light color=sandy crest; grey=silt in ripple troughs).

Test CC: short-bed of NPZ-mud and fine sand; mixture with $p_{fines<63um}$=17%; 31 January 2022

Type of bed: mixture of NPZ-mud (dd= 780 kg/m^3; $p_{fines<63um}$=55%) and fine sand (d_{50}=0.13 mm); mud and sand are mixed and placed in the test compartment;
wet density of mixture= 1865 kg/m^3; dry density= 1390 kg/m^3; $p_{fines<63\ um}$=17%; smooth surface; consolidation period=4 days.

Test conditions (h=water depth=0.25 m) are given in Table C 3.

Bed surface is shown in Figures C 3.

Table C. 3: Basic data of Test CC with mixture of NPZ-mud and fine sand (pfines<63um=17%.)

Test	**Depth-averaged current u_m (m/s)**	**Wave height H (m) and period T (s)**	**Maximum, near-bed velocity U_{max} (m/s)**	**Sediment dynamics** **Δ= ripple height** **λ=ripple length** **rmv= ripple migration velocity**
CC-1	0	0.08; 1.5	0.21	top layer of bed is stable (not oscillating); weak bed load movement
CC-2	0	0.12; 1.	0.25	top layer of bed is stable (not oscillating); very flat ripples Δ<3 mm; λ< 30 mm; minor suspension; sand concentrations up to 100 mg/l near bed; bed at end: sandy spots/crest and muddy troughs.

Figure C. 3: Bed with flat sand ripples/pots (light) and fines in troughs (grey/darker) during Test CC-2

Test E: short-bed of NPZ-mud and fine sand; mixture with $p_{fines<63um}$=17%; 16 February 2022

Type of bed: mixture of NPZ-mud (dd= 780 kg/m^3; $p_{fines<63um}$=55%) and fine sand (d_{50}=0.13 mm);

mud and sand are mixed and placed in the test compartment;

wet density of mixture (5% extra water added)= 1760-1830 (end) kg/m^3; dry density=1290 kg/m^3; $p_{fines<63\ um}$=17%; smooth surface; consolidation period=2 days.

Test conditions (h=water depth=0.25 m) are given in Table C 4. Bed surface is shown in Figures C 4.

Table C. 4: Basic data of Test E with mixture of NPZ-mud and fine sand (pfines<63um=17%.)

Test	**Depth-averaged current u_m (m/s)**	**Wave height H (m) and period T (s)**	**Maximum, near-bed velocity U_{max} (m/s)**	**Sediment dynamics** **Δ= ripple height** **λ=ripple length** **rmv= ripple migration velocity**
E-1	0	0.08; 1.5	0.21	top layer is oscillating (10 mm); segregation of top; fines are washed out; sandy crests/spots; mobile layer < 0.5 mm; no suspension
E-2	0	0.12; 1.	0.25	top layer is oscillating (10 mm); segregation of top; cracks and craters at top layer from which mud is escaping (minor clouds); mud suspension layer near bed; minor sand spots; sand ripples up to 2 mm; low sand concentrations. bed surface at end: muddy/silty top layer with sand spots/ripples up to 2 mm high and dark mud craters (up to 30 mm diameter; up to 10 mm deep

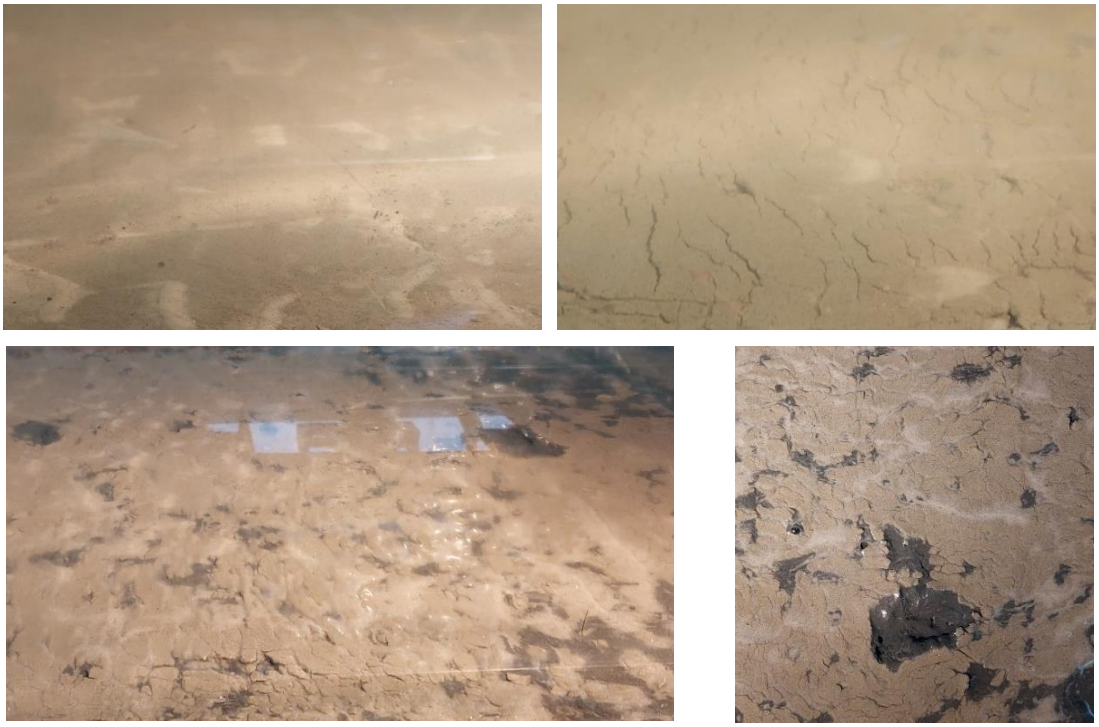

Figure C. 4: Upper left: bed before Test E; Upper right: bed with darker mud cracks/craters during Test E-2 (H=12 cm.)Lower: bed after test E-2 with mud/silt top layer, sand spots, mud craters (30 mm; 10 mm deep)

Test D: short-bed of BB-mud and fine sand; mixture with $p_{fines<63um}$=13%; 31 January 2022

Type of bed: mixture of BB-mud (dd= 1200 kg/m^3; $p_{fines<63um}$= 90%) and fine sand (d_{50}=0.13 mm);
mud and sand are mixed and placed in the test compartment;
wet density of mixture= 1720-1750 kg/m^3; dry density= 1200 kg/m^3; $p_{fines<63\ um}$=13%;
smooth surface; consolidation period=1 day.

Test conditions (h=water depth=0.25 m) are given in Table C 5. Bed surface is shown in Figures C 5.

Table C. 5: Basic data of Test D with mixture of BB-mud and fine sand (pfines<63um= 13%.)

Test	**Depth-averaged current u_m (m/s)**	**Wave height H (m) and period T (s)**	**Maximum, near-bed velocity U_{max} (m/s)**	**Sediment dynamics** **Δ= ripple height** **λ=ripple length** **rmv= ripple migration velocity**
D-1	0	0.06; 2	0.2	no movement
D-2	0	0.08; 1.5	0.21	very mobile top layer; sand ripples Δ=5-10 mm; λ=30-50 mm; minor suspension 60 mm; mud aggregates in troughs;
D-3	0	0.12; 1.	0.25	top layer of bed is stable (not oscillating); very mobile bed; sand ripples Δ=10-15 mm; λ=30-50 mm; major suspension (up to 80 mm high); sand concentrations up to 300mg/l; bed surface at end: sandy ripple crests up to 15 mm high and 50 mm long; mud aggregates/ mud balls in between crests

Figure C. 5: Left Upper: Bed before Test D; Right Upper: Bed during Test D (H=12 cm); Left Lower: Top view after Test D; Right Lower: Side view with sand ripples and mud balls (light color=sandy spots; darker grey=fines and mud balls)

Test F: short-bed of BB-mud and fine sand; mixture with $p_{fines<63um}$=22%; 16 February 2022

Type of bed: mixture of BB-mud (dd= 1220 kg/m^3; $p_{fines<63um}$= 90%) and fine sand (d_{50}=0.13 mm);
mud and sand are mixed and placed in the tests compartment;
wet density of mixture= 1840 kg/m^3; dry density=1350 kg/m^3; $p_{fines<63\ um}$=22%;
smooth surface; consolidation period=1 day.

Test conditions (h=water depth=0.25 m) are given in Table C 6. Bed surface is shown in Figures C 6.

Table C. 6: Basic data of Test F with mixture of BB-mud and fine sand (pfines<63um= 22%.)

Test	**Depth-averaged current u_m (m/s)**	**Wave height H (m) and period T (s)**	**Maximum, near-bed velocity U_{max} (m/s)**	**Sediment dynamics** **Δ= ripple height** **λ=ripple length** **rmv= ripple migration velocity**
F-1	0	0.06; 2	0.2	top layer is oscillating (10 mm); segregation of top; fines are washed out; sandy crests/spots and muddy troughs; sandy flat ripples up to 1 mm; minor suspension; sand conc .< 10 mg/l
F-2	0	0.08; 1.5	0.21	top layer is stable (not oscillating); segregation of top; very mobile; fines are washed out; sandy crests/spots and muddy troughs; sandy flat ripples up to 10 mm; major suspension up to 80 mm
F-3	0	0.12; 1.	0.25	top layer is stable (not oscillating); segregation of top; very mobile; fines are washed out; sandy crests/spots and muddy troughs; sandy flat ripples up to 10 mm; major suspension up to 80 mm; high sand conc; mud conc. up to 300 mg/l Surface at end: sand spots/crest up to 10 mm with silty materials in troughs

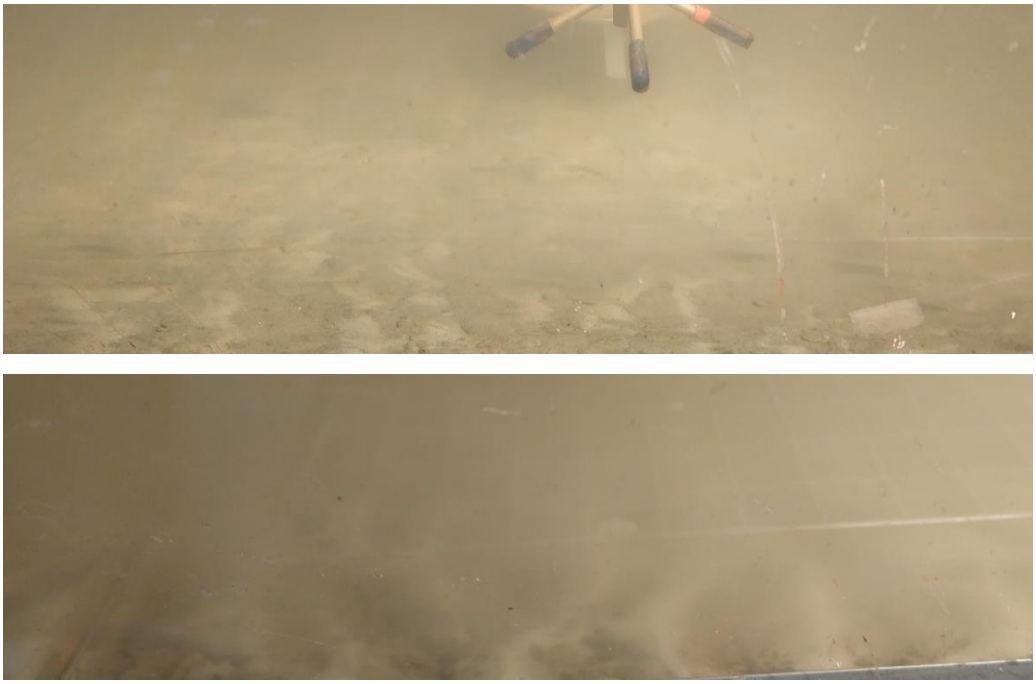

Figure C. 6: Upper: bed before Test F; Lower: bed with sand spots/ripples up to 10 mm during H=0.12 m

Test G1: short-bed of BB-mud with $p_{fines<63um}$= 90%; 23 February 2022

Type of bed: mixture of BB-mud (dd= 1220 kg/m^3; $p_{fines<63um}$= 90 %); diluted with 10% water to make mud slurry;

mud and sand are mixed and placed in the test compartment;

wet density of mud= 1710-1810 kg/m^3; dry density= 1220 kg/m^3; $p_{fines<63\ um}$= 90%;

smooth surface; consolidation period=1 day.

Test conditions (h=water depth=0.25 m) are given in Table 7. Bed surface is shown in Figures 7.

Table C. 7: Basic data of Test G1 with mixture of BB-mud (pfines<63um= 90%.)

Test	**Depth-averaged current u_m (m/s)**	**Wave height H (m) and period T (s)**	**Maximum, near-bed velocity U_{max} (m/s)**	**Sediment dynamics Δ= ripple height λ=ripple length rmv= ripple migration velocity**
G1-1	0	0.06; 2	0.2	forward/backward movement of sediment at surface (segregation of sediments; lighter-colored sand spots); no ripples; no suspension
G1-2	0	0.08; 1.5	0.21	same; no ripples; no suspension
G1-3	0	0.12; 1.	0.25	more spots of lighter-colored sand; no suspension; no ripples; water is clear; lumps of mud/silt break lose after making a small hole in bed surface.
G1-4	0.4	0.08; 1.5	0.45	sand spots are larger and everywhere; top layer of silt is removed; no ripples; no suspension

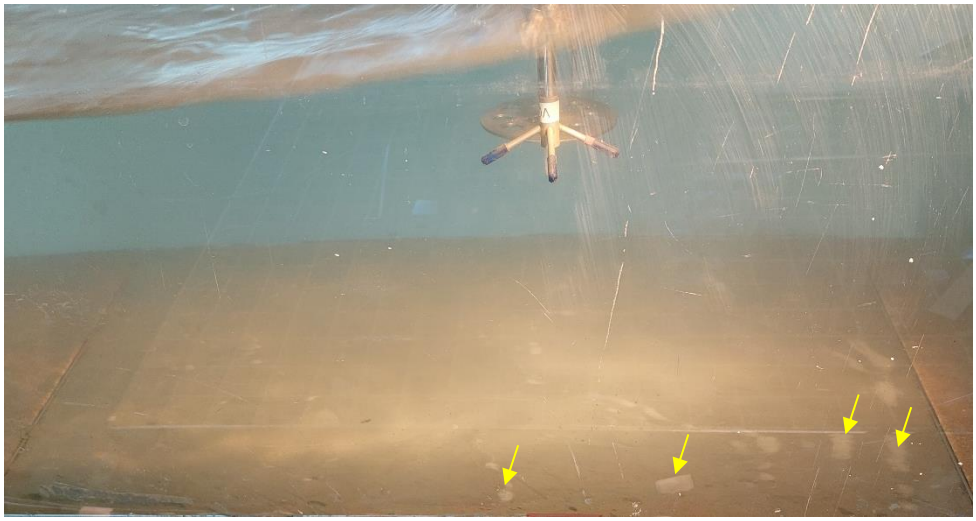

Figure C. 7: Bed surface with sand spots

Test G2: short-bed of BB-mud with $p_{fines<63um}$= 90%; 23 February 2022

Type of bed: mixture of BB-mud (dd= 1030 kg/m^3; $p_{fines<63um}$= 90%); diluted with 20% water to make mud slurry;

mud and sand are mixed and placed in the test compartment;

wet density of mud= 1630-1650 kg/m^3; dry density= 1030 kg/m^3; $p_{fines<63\ um}$=90%;

smooth surface; consolidation period=1 day.

Test conditions (h=water depth=0.25 m) are given in Table C 8. Bed surface is shown in Figure C 8.

Table C. 8: Basic data of Test G2 with mixture of BB-mud (pfines<63um= 90%.)

Test	**Depth-averaged current u_m (m/s)**	**Wave height H (m) and period T (s)**	**Maximum, near-bed velocity U_{max} (m/s)**	**Sediment dynamics Δ= ripple height λ=ripple length rmv= ripple migration velocity**
G2-1	0	0.06; 2	0.2	forward/backward movement of sediment at surface (segregation of sediments; lighter-colored sand spots); no ripples; no suspension
G2-2	0	0.08; 1.5	0.21	same; flat ripples of 1 mm high
G2-3	0	0.12; 1.	0.25	more spots of lighter-colored sand; sheet flow layer of 10 mm high with sediments; suspension up to 30 m; flat ripples 1 mm high at sand spots; concentration at 5 mm a.b≅ 100 mg/l
G2-4	0.25	0.08; 1.5	0.35	same but lower concentrations

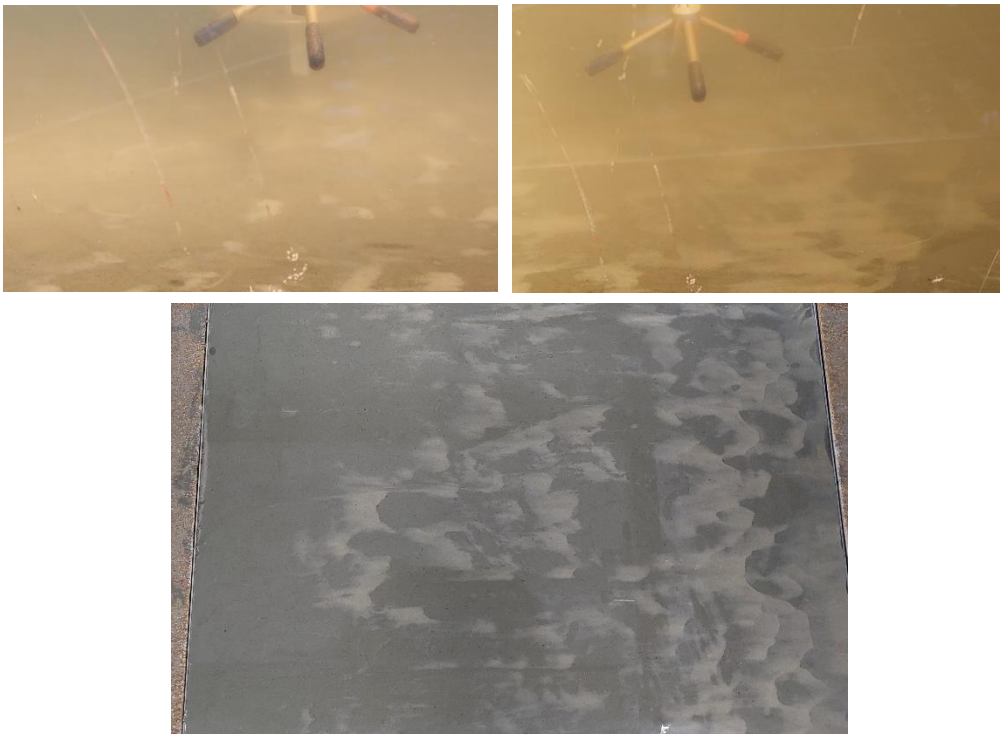

Figure C. 8: Upper: bed surface with sand spots (lighter colour) during test; Lower: plan view of bed surface with sand spots at end of test

Test PT: Pilot tests in small trays

A mud-sand mixture of fine sand (0.13 mm) and new NPZ-mud was placed in a small tray and a layer of water (10 mm) was gently placed on top of the mud-sand layer. The tray was tilted up and own on one side to create oscillatory flow for 5 minutes.

Mud was washed from the top layer and spots of fine sand became visible after 5 minutes. No movement of sand particles was observed, see Table C 9 and Figure C 9.

New NPZ-mud was taken in early April 2022: wet density=1345 kg/m^3; dry denbsity of NPZ-mud=550 kg/m^3.

Table C. 9: Data pilot tests with mixtures of fine sand and NPZ-mud (mud from Noordpolderzijl)

Test **Date**	**Wet/dry density** **(kg/m^3)**	**Type of mixture**	**Sediment dynamics**
PT-1 13 April	1760 1220	40% NPZ-mud (30 μm) 60% fine sand (130 μm)	Oscillatory flow generated in tray: Mud was washed out from top layer creating tiny (lighter) spots of fine sand; no movement of sand
PT-2 13 April	1605 970	25% NPZ-mud (30 μm) 75% fine sand (130 μm)	Oscillatory flow applied in tray: mud was washed out from top layer creating (lighter) spots of fine sand; no movement of sand

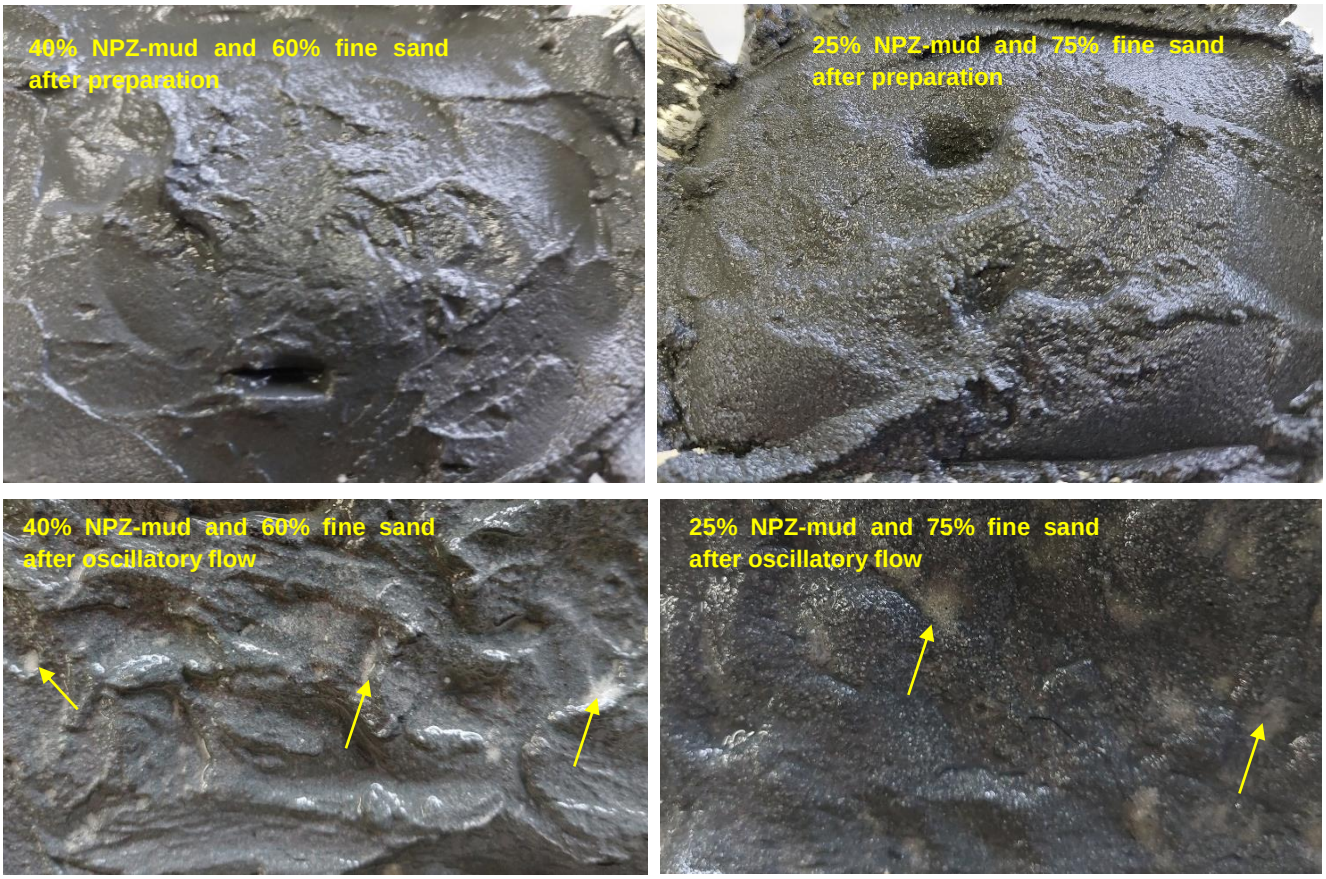

Figure C. 9: Mud-Sand mixture in tray

Upper left: 40% NPZ-mud and 60% sand after preparation

Lower left: 40% NPZ-mud and 60% sand after erosion of mud due to oscillatory flow

Upper right: 25% NPZ-mud and 75% sand and after preparation

Lower left: 25% NPZ-mud and 75% sand after erosion of mud due to oscillatory flow

Appendix D

Long bed tests in wave-current flume January-April 2022

Objective: determine critical bed shear stress for sand and fines particles of remoulded natural and artificial mud-sand mixtures under current and wave conditions.

Test A: long bed of fine sand (no mud); 17 January 2022

Type of bed: fine sand (dry density=1600 kg/m^3; $p_{fines<63um}$=10%; d_{10}=0.05 mm; d_{50}=0.13 mm; d_{90}=0.22 mm)

Test conditions (h=water depth=0.25 m) are given in Table 1.

Bed surface with developing ripples are shown in the figure below.

Data of velocities and concentrations are given in data tables below.

Table Basic data of Test A with fine sand bed (d_{10}=0.05mm; d_{50}=0.13 mm; d_{90}=0.22 mm);

Depth-averaged current u_m (m/s)	**Wave height H (m) and period T (s)**	**Maximum near-bed velocity U_{max} (m/s)**	**Sediment dynamics** **Δ= ripple height** **λ=ripple length** **rmv= ripple migration velocity**
0	0.08; 1.5	0.24	ripples Δ=10-15 mm; λ=40-60 mm; rmv<0.01 mm/s suspension layer=40 mm; $d_{50,\ suspended\ sand}$=0.04 mm
0	0.12; 1	0.27	ripples Δ=7-10 mm; λ=40-60 mm; rmv<0.01 mm/s suspension layer=50 mm; $d_{50,\ suspended\ sand}$=0.05 mm
0.1	0.08; 1.5	0.33	ripples Δ=7-10 mm; λ=40-60 mm; rmv<0.03 mm/s suspension layer=50 mm; $d_{50,\ suspended\ sand}$=0.05 mm
0.1	0.12; 1	0.34	ripples Δ=7-10 mm; λ=40-60 mm; rmv<0.03 mm/s

			suspension layer=60 mm; $d_{50,\ suspended\ sand}$=0.05 mm
0.2	0.08; 1.5	0.37	asymm. ripples Δ=10-15 mm; λ=50-70 mm; rmv<0.1 mm/s suspension layer=70 mm; $d_{50,\ suspended\ sand}$=0.06 mm
0.2	0.12; 1	0.38	asymm. ripples Δ=10-15 mm; λ=60-80 mm; rmv<0.1 mm/s suspension layer=80 mm; $d_{50,\ suspended\ sand}$=0.06 mm
0.35	0.08; 1.5	0.55	asymm. ripples Δ<15 mm; λ=70-90 mm; rmv<0.3 mm/s suspension layer=150 mm
0.75	0.06; 1	1	intense sand transport; long ripples: Δ<7 mm; λ=80-100 mm Erosion mass (60% of sand washed out)=0.6x3x0.4x0.05x1600=58 kg Erosion time= 15 min=900 s Erosion rate=58000/(900x3x0.4) $\cong$ 50 g/m^2/s

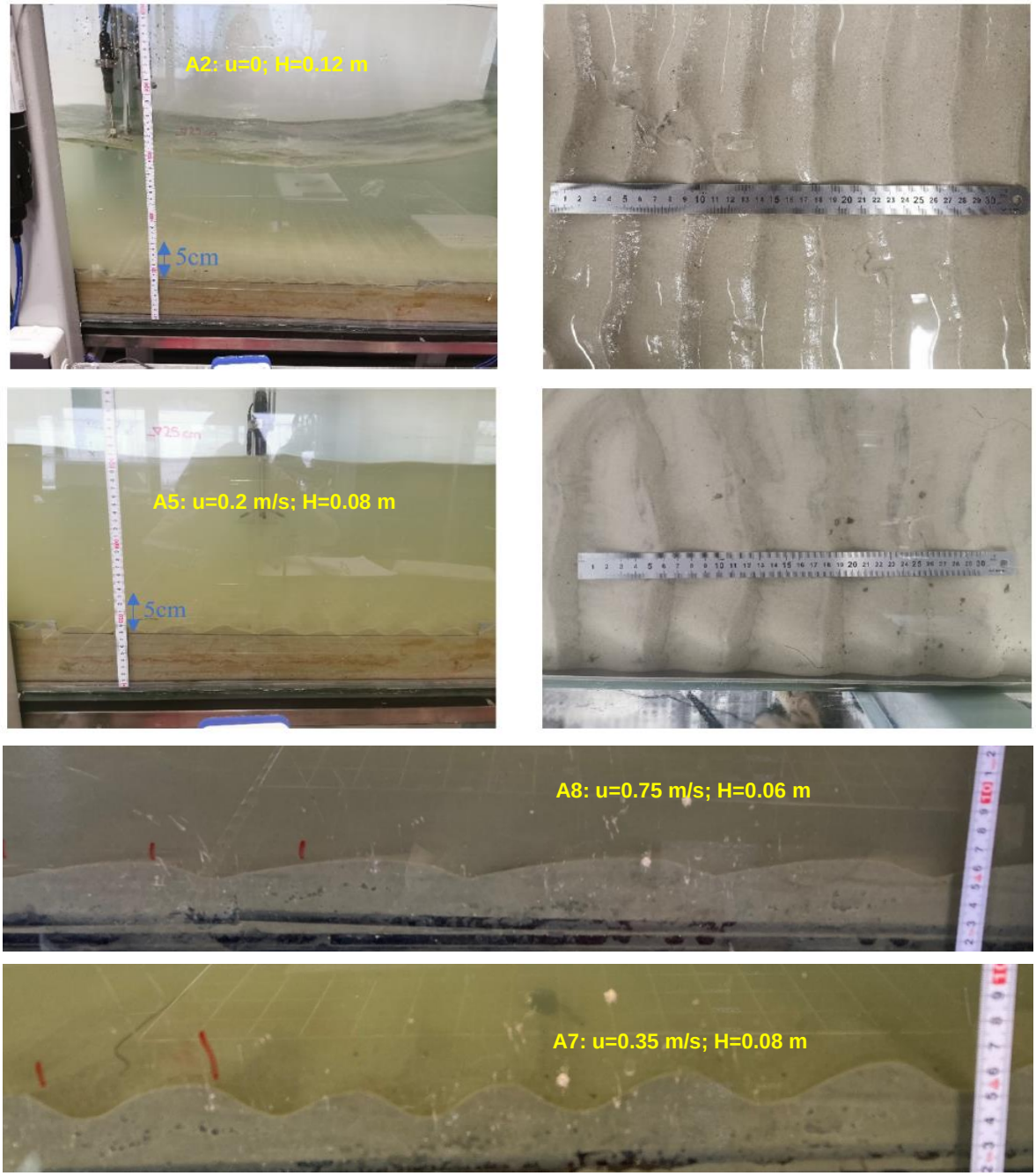

Figure Test A2 (upper); A5 (middle); A7, A8 (lower)

Test A1 Depth-averaged current velocity (m/s)=0; Wave height (m)= 0.08; Wave period (s)=1.4					
Height above bed (m)	**Current velocity (m/s)**			**Concentration (mg/l)**	
	time-averaged	**Minimum**	**Maximum**	**Sand fraction > 63 μm**	**Fine fraction < 63 μm**
0.02	0	-0.22	0.24	2990	
0.03	0	-0.214	0.25	1500	
0.04	0	-0.25	0.28	690	
0.06	0	-0.21	0.26	350	
0.08	0	-0.23	0.21	110	
0.10	0	-0.226	0.27	130	
0.12	0	-0.242	0.284		
0.14	0	-0.253	0.28		

Test A2 Depth-averaged current velocity (m/s)=0; Wave height (m)= 0.12; Wave period (s)=1					
Height above bed (m)	**Current velocity (m/s)**			**Concentration (mg/l)**	
	time-averaged	**Minimum**	**Maximum**	**Sand fraction > 63 μm**	**Fine fraction < 63 μm**
0.02	0	-0.211	0.27	2830	
0.03	0	-0.218	0.264	1200	
0.04	0	-0.218	0.275	610	
0.06	0	-0.232	0.277	250	
0.08	0	-0.251	0.287	50	
0.10	0	-0.245	0.302	20	
0.12	0	-0.256	0.309	10	
0.14	0	-0.286	0.324	5	

Test A3 Depth-averaged current velocity (m/s)=0.1; Wave height (m)= 0.08; Wave period (s)=1.4					
Height above bed (m)	**Current velocity (m/s)**			**Concentration (mg/l)**	
	time-averaged	**Minimum**	**Maximum**	**Sand fraction > 63 μm**	**Fine fraction < 63 μm**
0.015	0.076	-0.114	0.296	1400	
0.025	0.091	-0.102	0.314	670	
0.035	0.11	-0.081	0.336	310	
0.055	0.128	-0.067	0.357	110	
0.075	0.137	-0.059	0.369	40	
0.095	0.147	-0.048	0.386	20	
0.115	0.147	-0.034	0.388	20	
0.135	0.149	-0.067	0.399	10	

Test A4 Depth-averaged current velocity (m/s)=0.1; Wave height (m)= 0.12; Wave period (s)=1					
Height above bed (m)	**Current velocity (m/s)**			**Concentration (mg/l)**	
	time-averaged	**Minimum**	**Maximum**	**Sand fraction > 63 μm**	**Fine fraction < 63 μm**
0.015	0.082	-0.143	0.324	1040	
0.025	0.102	-0.121	0.349	400	
0.035	0.12	-0.11	0.383	220	
0.055	0.133	-0.103	0.403	100	
0.075	0.136	-0.108	0.412	70	
0.095	0.134	-0.121	0.418	80	
0.115	0.138	-0.138	0.431	60	
0.135	0.141	-0.15	0.442	40	

Test A5 Depth-averaged current velocity (m/s)=0.2; Wave height (m)= 0.08; Wave period (s)=1.4					
Height above bed (m)	**Current velocity (m/s)**			**Concentration (mg/l)**	
	time-averaged	**Minimum**	**Maximum**	**Sand fraction > 63 μm**	**Fine fraction < 63 μm**
0.02	0.153	-0.019	0.381	2870	
0.03	0.167	-0.0025	0.403	1630	
0.04	0.192	0.022	0.436	1200	
0.06	0.230	0.059	0.478	700	
0.08	0.254	0.09	0.505	530	
0.1	0.271	0.108	0.531	460	
0.12	0.277	0.128	0.536	270	
0.14	0.283	0.134	0.558	230	
0.16	0.280	0.124	0.570	160	

Test A6 Depth-averaged current velocity (m/s)=0.2; Wave height (m)= 0.11; Wave period (s)=1					
Height above bed (m)	**Current velocity (m/s)**			**Concentration (mg/l)**	
	time-averaged	**Minimum**	**Maximum**	**Sand fraction > 63 μm**	**Fine fraction < 63 μm**
0.02	0.148	-0.033	0.373	3220	
0.03	0.168	-0.006	0.408	1790	
0.04	0.195	0.018	0.437	1150	
0.06	0.241	0.068	0.484	730	
0.08	0.261	0.086	0.505	680	
0.1	0.273	0.102	0.531	480	
0.12	0.274	0.097	0.544	290	
0.14	0.265	0.084	0.556	230	
0.16	0.260	0.067	0.578	170	

Test A7 Depth-averaged current velocity (m/s)=0.35; Wave height (m)= 0.08; Wave period (s)=1.3					
Height above bed (m)	**Current velocity (m/s)**			**Concentration (mg/l)**	
	time-averaged	**Minimum**	**Maximum**	**Sand fraction > 63 μm**	**Fine fraction < 63 μm**
0.01	0.24	0.05	0.4	4480	
0.02	0.23	0.1	0.5	3210	
0.03	0.26	0.1	0.5	2550	
0.05	0.29	0.1	0.55	1780	
0.07	0.32	0.18	0.63	1240	
0.09	0.32	0.2	0.6	1110	
0.11	0.32	0.2	0.65	880	
0.13	0.32	0.2	0.68	740	

Test A8 Depth-averaged current velocity (m/s)=0.75; Wave height (m)= 0.06; Wave period (s)=1					
Height above bed (m)	**Current velocity (m/s)**			**Concentration (mg/l)**	
	time-averaged	**Minimum**	**Maximum**	**Sand fraction > 63 μm**	**Fine fraction < 63 μm**
0.01	0.6	0.4	0.85	9000	
0.02	0.65	0.45	0.9	8390	
0.03	0.66	0.5	0.9	7930	
0.05	0.71	0.5	0.95	7370	
0.07	0.7	0.55	0.98	7000	
0.09	0.72	0.58	1	6900	
0.11	0.72	0.6	1	6780	
0.13	0.73	0.6	1	6700	

Test I: long bed of NPZ-mud and fine sand ($p_{fines<63um}$= 18%; initial wet density=1750 kg/m^3); 6 April 2022

Type of bed: mixture of NPZ-mud (dd=780 kg/m^3; $p_{fines<63um}$=55%) and fine sand (d_{50}=0.13 mm)

mud and sand are mixed and placed in the test compartment;

wet density= 1750 kg/m^3; dry density= 1205 kg/m^3; smooth surface

Test conditions (h=water depth=0.25 m) are given in the table below.

Bed surface with developing ripples are shown in Figures below.

Data of velocities and concentrations are given in data tables below.

Table Basic data of Test I with mixture of NPZ-mud and fine sand ($p_{fines<63um}$=18%)

Depth-averaged current u_m (m/s)	**Wave height H (m) and period T (s)**	**Maximum near-bed velocity U_{max} (m/s)**	**Sediment dynamics** **Δ= ripple height** **λ=ripple length** **rmv= ripple migration velocity**
0.20-0.25	0	0.15	initiation of sand particles moving over darker muddy spots
0	0.05; 2.5	0.19	initiation of moving sand particles
0	0.06; 2	0.20	mud washed from top layer; suspension layer=20 mm; initiation flat ripples Δ=1 mm (light spots)
0	0.08; 1.5	0.21	mud washed from top layer; suspension layer=30 mm; very flat ripples Δ=1-2 mm, λ= 40-60 mm; sand concentrations < 10 mg/l
0	0.12; 1	0.25	suspension layer=50 mm; flat ripples Δ=3-5 mm, λ= 40-60 mm; sand as ripples moving over darker mud in troughs; mud entrainment from troughs; sand concentrations < 10 mg/l; water slowly more turbid
0.2	0.08; 1.5	0.4	sand ripples are flattened and more asymmetric Δ=3 mm; λ=40-60 mm; rmv=0.1-

			0.2 mm/s; sand concentrations near bed < 100 to 200 mg/l; water turbid
0.2	0.115; 1.1	0.4	sand ripples are flattened and asymmetric Δ=2-3 mm; λ=40-60 mm rmv=0.1-0.2 mm/s; water very turbid
0.35	0.08; 1.5	0.55	sand ripples are flattened and asymmetric Δ=1-2 mm; λ=40-60 mm rmv=0.2-0.4 mm/s; water very turbid
0.75	0.06; 2	1.0	intense sand transport in lowest 50 to 100 mm; irregular bed surface with large scour marks (Δ=20-30 mm; λ=50-200 mm); black, muddy water in flume Erosion mass=3x0.4x0.025x1205=35 kg Erosion time=50 min=3000 s Erosion rate=35000/(3000x3x0.4)=10 kg/m^2/s

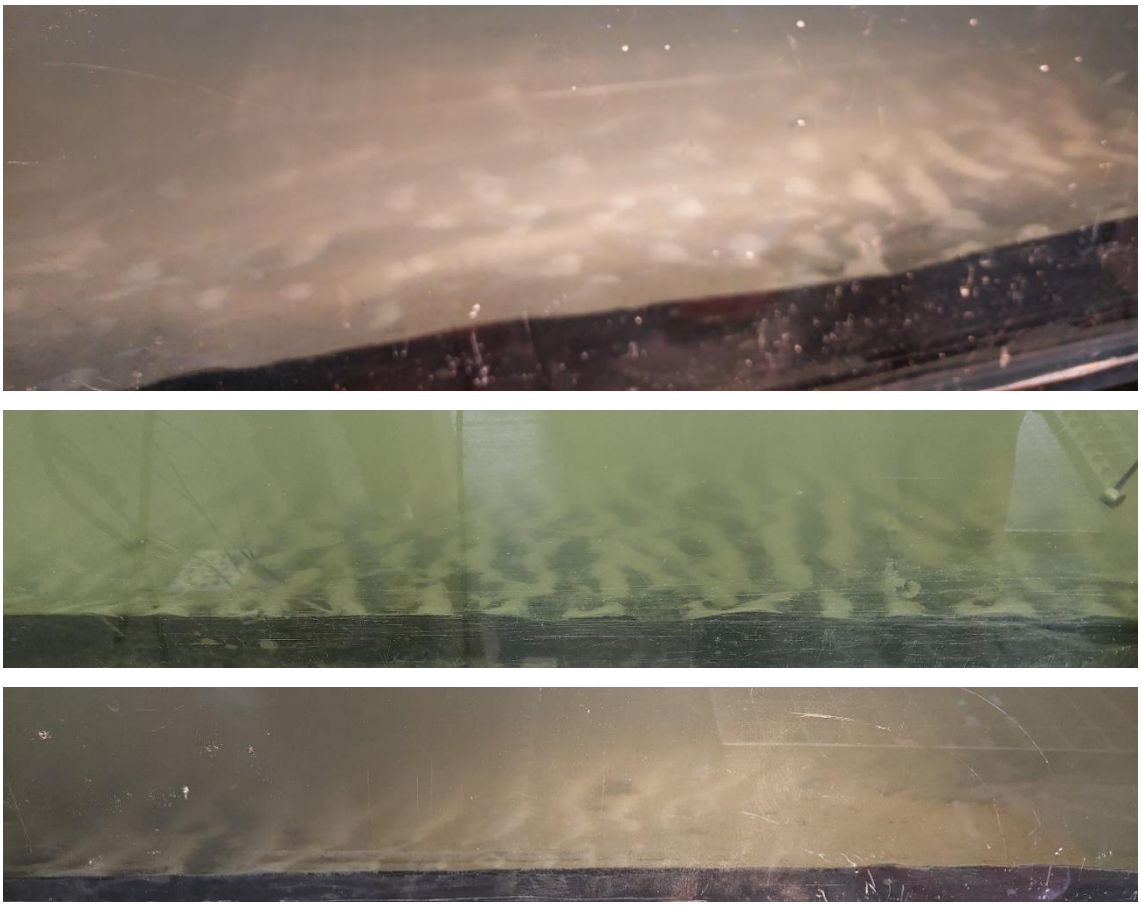

Figure Generation of ripples with waves alone H= 0.08 m (upper); H= 0.12 m (middle, Lower); sand visible as light spots; darker mud in troughs

Figure Plan view of bed surface after tests (left) and side view (right); u_m=0.75 ms/, H=0.06 m

Test I2 Depth-averaged current velocity (m/s)=0; Wave height (m)= 0.12; Wave period (s)=1					
Height above bed (m)	**Current velocity (m/s)**			**Concentration (mg/l)**	
	time-averaged	**Minimum**	**Maximum**	**Sand fraction > 63 μm**	**Fine fraction < 63 μm**
0.01	0	-0.21	0.29	400	150
0.02	0	-0.22	0.30	300	140
0.03	0	-0.22	0.30	260	130
0.05	0	-0.23	0.30	130	90
0.07	0	-0.25	0.30	100	70
0.09	0	-0.28	0.30	80	70
0.11	0	-0.28	0.30	20	70
0.13	0				

Test I3 Depth-averaged current velocity (m/s)=0.2; Wave height (m)= 0.08; Wave period (s)=1.5					
Height above bed (m)	**Current velocity (m/s)**			**Concentration (mg/l)**	
	time-averaged	**Minimum**	**Maximum**	**Sand fraction > 63 μm**	**Fine fraction < 63 μm**
0.01	0.16	-0.05	0.4	70	110
0.02	0.18	-0.05	0.4	20	90
0.03	0.20	-0.05	0.44	10	80
0.05	0.20	0	0.45	1	70

Test I4 Depth-averaged current velocity (m/s)=0.2; Wave height (m)= 0.12; Wave period (s)=1.1					
Height above bed (m)	**Current velocity (m/s)**			**Concentration (mg/l)**	
	time-averaged	**Minimum**	**Maximum**	**Sand fraction > 63 μm**	**Fine fraction < 63 μm**
0.01	0.16	-0.05	0.4	20	70
0.02	0.18	-0.05	0.42	10	70
0.03	0.2	-0.05	0.42	5	70
0.05	0.2	0	0.45	3	70

Test I5 Depth-averaged current velocity (m/s)=0.35; Wave height (m)= 0.08; Wave period (s)=1.1					
Height above bed (m)	**Current velocity (m/s)**			**Concentration (mg/l)**	
	time-averaged	**Minimum**	**Maximum**	**Sand fraction > 63 μm**	**Fine fraction < 63 μm**
0.01	0.31	0.1	0.56	50	90
0.02	0.33	0.12	0.60	40	80
0.03	0.34	0.15	0.60	30	10

Test I6 Depth-averaged current velocity (m/s)=0.75; Wave height (m)= 0.06; Wave period (s)=1					
Height above bed (m)	**Current velocity (m/s)**			**Concentration (mg/l)**	
	time-averaged	**Minimum**	**Maximum**	**Sand fraction > 63 μm**	**Fine fraction < 63 μm**
0.01	0.7	0.5	0.95	960	260
0.02	0.72	0.55	0.95	1240	330
0.03	0.73	0.58	0.98	1570	460
0.05	0.75	0.6	1	1900	540
0.07	0.76	0.6	1.05	2010	560
0.09	0.76	0.6	1.05	2230	710
0.11	0.75	0.6	1.07	2420	750
0.13	0.74	0.6	1.1	2210	740

Test J: long bed of NPZ-mud and fine sand ($p_{fines<63um}$=13%; initial wet density=1785 kg/m^3); 13 April 2022

Type of bed: mixture of NPZ-mud (dd=550 kg/m^3; $p_{fines<63um}$=85%) and fine sand (d_{50}=0.13 mm)
mud and sand are mixed and placed in the test compartment;
wet density of mixture= 1785 kg/m^3; dry density= 1260 kg/m^3; smooth surface

Test conditions (h=water depth=0.25 m) are given in the Table below.
Bed surface with developing ripples and sand transport are shown in Figures below.
Data of velocities and concentrations are given in data tables below.

Table Basic data of Test J with mixture of NPZ-mud and fine sand ($p_{fines<63um}$=13%.)

Depth-averaged current u_m (m/s)	**Wave height H (m) and period T (s)**	**Maximum, near-bed velocity U_{max} (m/s)**	**Sediment dynamics** **Δ= ripple height** **λ=ripple length** **rmv= ripple migration velocity**
0.20-0.25	0	0.15	initiation of sand particles moving over darker muddy spots
0	0.05; 2.5	0.17	initiation of moving sand particles
0	0.06; 2	0.2	loose mud particles moving in parallel streaks; suspension layer=20 mm; initiation flat ripples Δ=1-2 mm (light spots)
0	0.08; 1.5	0.22	mud washed out; suspension layer=30 mm; very flat ripples Δ=1-2 mm, λ= 40-60 mm; sand concentrations < 10 mg/l
0	0.12; 1	0.25	suspension layer=50 mm; regular flat ripples Δ=5-7 mm, λ= 40-60 mm; sand as ripples moving over darker mud in troughs; mud entrainment from troughs; sand concentrations < 10 mg/l; water slowly more turbid (300 to 500 mg/l)
0.2	0.08; 1.5	0.4	suspension layer =50-70 mm; sand ripples are flattened and more asymmetric Δ=5 mm; λ=50-70 mm; sand concentrations near bed < 100 to 200 mg/l; water turbid
0.2	0.115; 1.1	0.4	suspension layer =70-100 mm; sand ripples are flattened and asymmetric Δ=5 mm; λ=50-70 mm; water very turbid

0.35	0.08; 1.5	0.55	sand ripples are flattened and asymmetric Δ=3-5 mm; λ=50-70 mm rmv=0.3-0.4 mm/s; black muddy spots in trough regions; water very turbid
0.75	0.06; 2	1.0	intense sand transport in lowest 50 to 100 mm; irregular bed surface with large scour marks (Δ=20-30 mm; λ=50-200 mm); black, muddy water in flume Erosion mass=3x0.4x0.025x1260=40 kg Erosion time=40 min=2400 s Erosion rate=40000/(2400x3x0.4)$\cong$15 kg/m^2/s

Figure Bed before the tests; plan view (upper) and side view (lower)

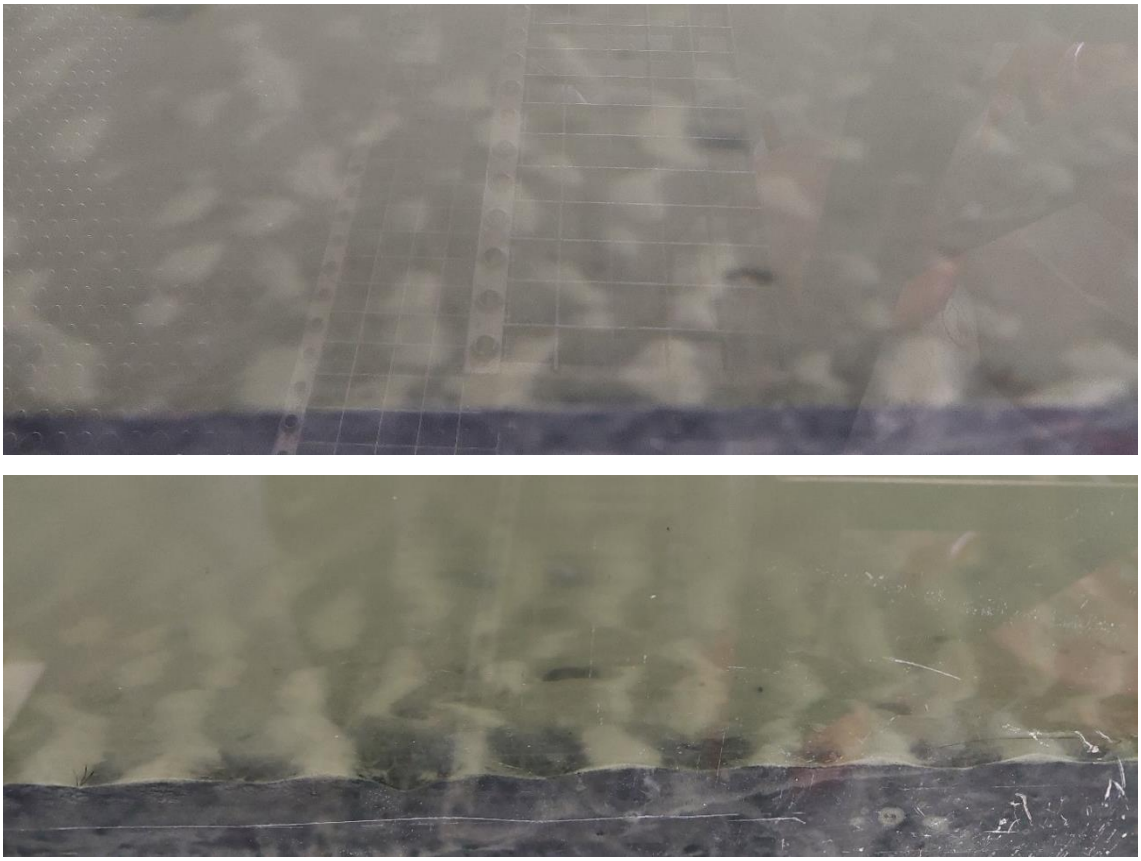

Figure Bed with ripples (side view) during waves alone H=0.08 m (upper) and H= 0.12 m (lower)

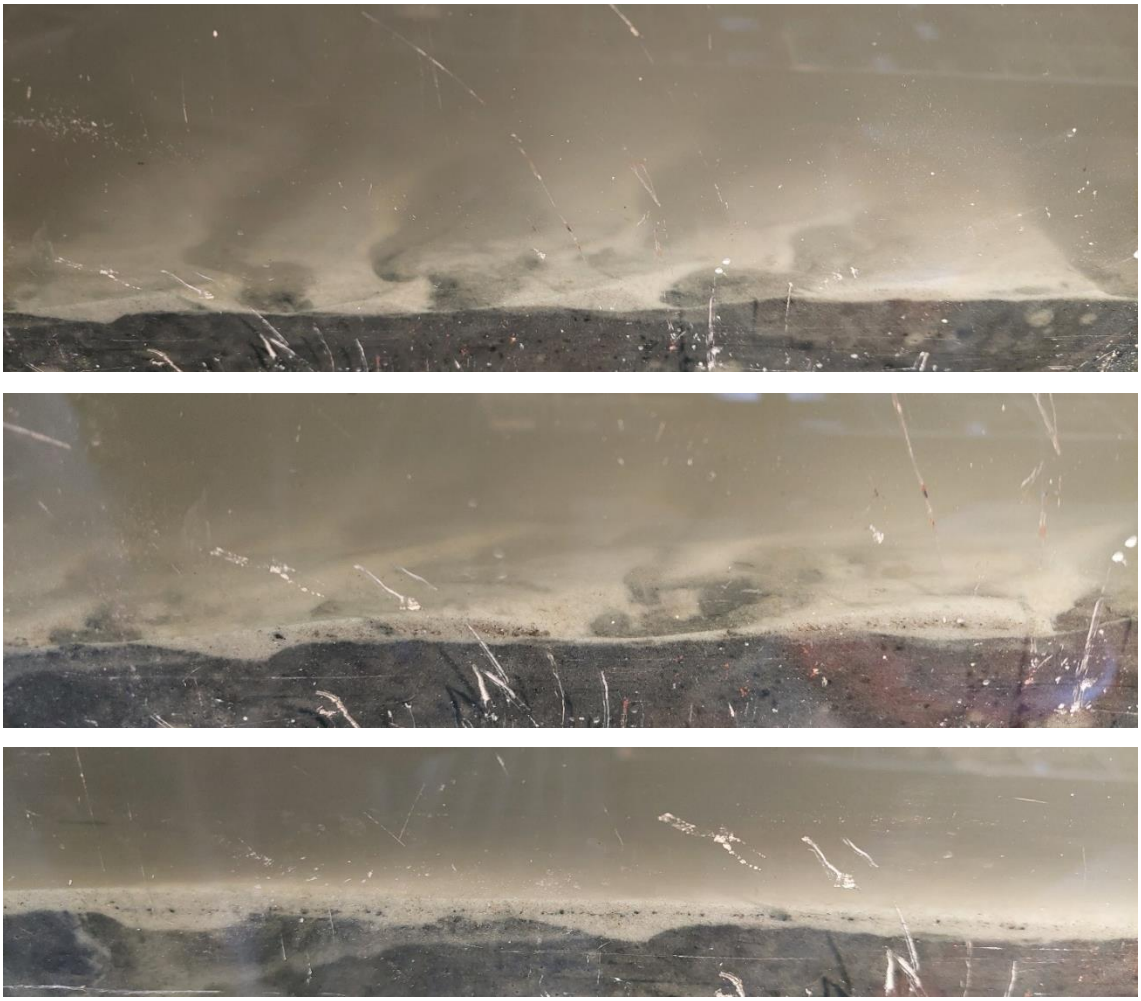

Figure Bed with ripples and sand transport (side view) during combined current+waves

u_m=0.2 m/s H=0.11 m (upper)

u_m=0.35 m/s H=0.08 m (middle)

u_m=0.75 cm/s H=0.06 m (lower)

Figure Bed at end of tests; plan view (left) and side view (right); u_m=75 m/s, H=0.06 m

Test J1 Depth-averaged current velocity (m/s)=0; Wave height (m)= 0.08; Wave period (s)=1.3					
Height above bed (m)	**Current velocity (m/s)**			**Concentration (mg/l)**	
	time-averaged	**Minimum**	**Maximum**	**Sand fraction > 63 μm**	**Fine fraction < 63 μm**
0.01	0	-0.16	0.25	<10	50
0.02	0	-0.16	0.25	<10	50
0.03	0	-0.15	0.25	<10	40

Test J2 Depth-averaged current velocity (m/s)=0; Wave height (m)= 0.12; Wave period (s)=1.					
Height above bed (m)	**Current velocity (m/s)**			**Concentration (mg/l)**	
	time-averaged	**Minimum**	**Maximum**	**Sand fraction > 63 μm**	**Fine fraction < 63 μm**
0.01	0	-0.2	0.2	410	160
0.02	0	-0.21	0.21	360	150
0.03	0	-0.21	0.21	330	180
0.05	0	-0.2	0.23	190	130
0.07	0	-0.21	0.22	170	180
0.09	0	-0.22	0.25	20	130
0.11	0	-0.23	0.25	0	110

Test J3 Depth-averaged current velocity (m/s)=0.2; Wave height (m)= 0.08; Wave period (s)=1.3					
Height above bed (m)	**Current velocity (m/s)**			**Concentration (mg/l)**	
	time-averaged	**Minimum**	**Maximum**	**Sand fraction > 63 μm**	**Fine fraction < 63 μm**
0.01	0.12	-0.05	0.37	160	110
0.02	0.12	-0.05	0.38	70	110
0.03	0.15	-0.05	0.42	30	110
0.05	0.19	-0.03	0.44	20	100
0.07	0.19	-0.03	0.43	10	100
0.09	0.19	-0.02	0.44	10	100

Test J4 Depth-averaged current velocity (m/s)=0.2; Wave height (m)= 0.12; Wave period (s)=1					
Height above bed (m)	**Current velocity (m/s)**			**Concentration (mg/l)**	
	time-averaged	**Minimum**	**Maximum**	**Sand fraction > 63 μm**	**Fine fraction < 63 μm**
0.01	0.15	-0.05	0.4	40	100
0.02	0.17	-0.04	0.42	20	90
0.03	0.18	-0.04	0.43	20	90
0.05	0.18	-0.04	0.45	10	90
0.07	0.19	-0.03	0.46	10	90
0.09	0.18	-0.04	0.48	5	90

Test J5 Depth-averaged current velocity (m/s)=0.35; Wave height (m)= 0.08; Wave period (s)=1.2					
Height above bed (m)	**Current velocity (m/s)**			**Concentration (mg/l)**	
	time-averaged	**Minimum**	**Maximum**	**Sand fraction > 63 μm**	**Fine fraction < 63 μm**
0.01	0.28	-0.11	0.53	460	160
0.02	0.28	-0.1	0.54	310	160
0.03	0.29	-0.15	0.55	250	150
0.05	0.3	-0.15	0.56	190	150
0.07	0.33	-0.15	0.58	150	150
0.09	0.32	-0.15	0.58	130	150
0.11	0.3	-0.15	0.60	110	150
0.13	0.27	-0.15	0.61	90	150

Test J6 Depth-averaged current velocity (m/s)=0.75; Wave height (m)= 0.06, Wave period (s)=1					
Height above bed (m)	**Current velocity (m/s)**			**Concentration (mg/l)**	
	time-averaged	**Minimum**	**Maximum**	**Sand fraction > 63 μm**	**Fine fraction < 63 μm**
0.01	0.67	0.52	0.93	3340	250
0.02	0.67	0.52	0.93	3360	340
0.03	0.7	0.54	0.95	3780	360
0.05	0.73	0.54	0.97	4200	580
0.07	0.71	0.57	0.98	4380	530
0.09	0.71	0.55	0.99	4270	590
0.11	0.71	0.56	0.99	4210	460
0.13	0.72	0.56	1.0	4010	550

Test H: long bed of BB-TP ($p_{fines<63um}$= 90%; initial wet density=1750 kg/m^3); 24 March 2022

Type of bed: silty mud from BB (TP1,2,3); (dd= 1205 kg/m^3; $p_{fines<63um}$= 90%)
sediment of base container is mixed and placed in test compartment of flume;
wet density of mixture= 1750 kg/m^3; dry density= 1205 kg/m^3; smooth surface;
consolidation=1 day

Test conditions (h=water depth=0.25 m) are given in the table below.
Bed surface with developing ripples are shown in the Figures below.
Data of velocities and concentrations are given in data tables below.

Table Basic data of Test H with silty mud of BB ($p_{fines<63um}$=90%)

Depth-averaged current u_m (m/s)	**Wave height H (m) and period T (s)**	**Maximum, near-bed velocity U_{max} (m/s)**	**Sediment dynamics** **Δ= ripple height** **λ=ripple length** **rmv= ripple migration velocity**
0.2		0.15	initiation of silt particles; 5% of bed is moving
0.25		0.2	10% of bed is moving
0.35		0.25	50% of bed is moving
0.45		0.35	100% of bed is moving
0.55		0.4	initiation of small ripples
0	0.04; 2.5	0.18	some particles moving
0	0.05; 2.2	0.19	5%-10% of surface moving
0	0.06; 2	0.20	50% of surface moving
0.15	0.03; 2.5	0.25	5%-10% of bed is moving
0.15	0.05; 2.2	0.32	50% of bed moving
0.15	0.06; 2	0.35	100% of bed moving
0.2	0.06; 2	0.20	suspension layer=50 mm; isolated ripples Δ=1-3 mm, λ= 10-50 mm; separation of darker mica particles (up to 0.3 mm size) and other silt particles; sorting of mica and silt around small ripple features

0.2	0.08;1.5	0.22	suspension layer =30 mm; isolated flat ripple-type features Δ=1-3 mm, λ= 30-50 mm; concentrations up to 90 mm above bed surface
0.2	0.12; 1	0.25	suspension layer =90 mm; isolated flat ripple-type features Δ=1-2 mm, λ= 30-50 mm; no more sorting of mica and silt; concentrations up to 90 mm above bed surface
0.35	0.08; 1.5	0.55	ripple features are smoothed < 2 mm; sand concentrations are lower; sand concentrations measured up to 90 mm above bed; silt concentrations measured up to 150 mm above bed
0.75	0.06; 2	1.0	ripples smoothed out < 2 mm; flat bed conditions; sand concentrations measured up to 150 mm above bed; silt concentrations measured up to 150 mm above bed; silt concentrations also measured near water inlet (no sand concentrations upstream near water inlet); minor erosion marks

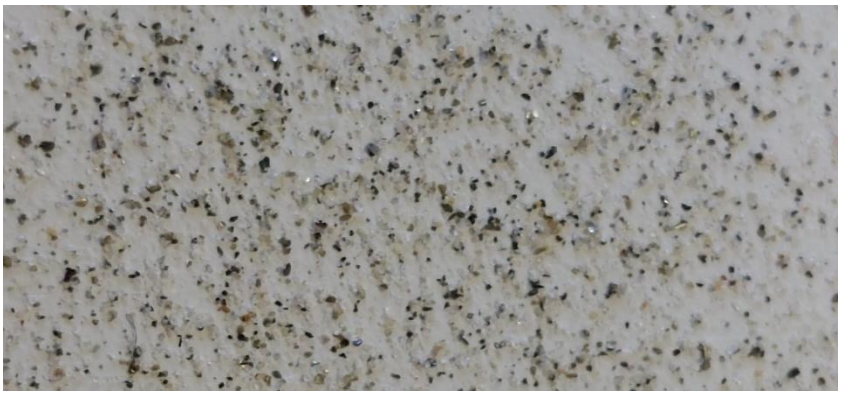

Figure Particles of silty BB-mud (very platy black/dark mica particles)

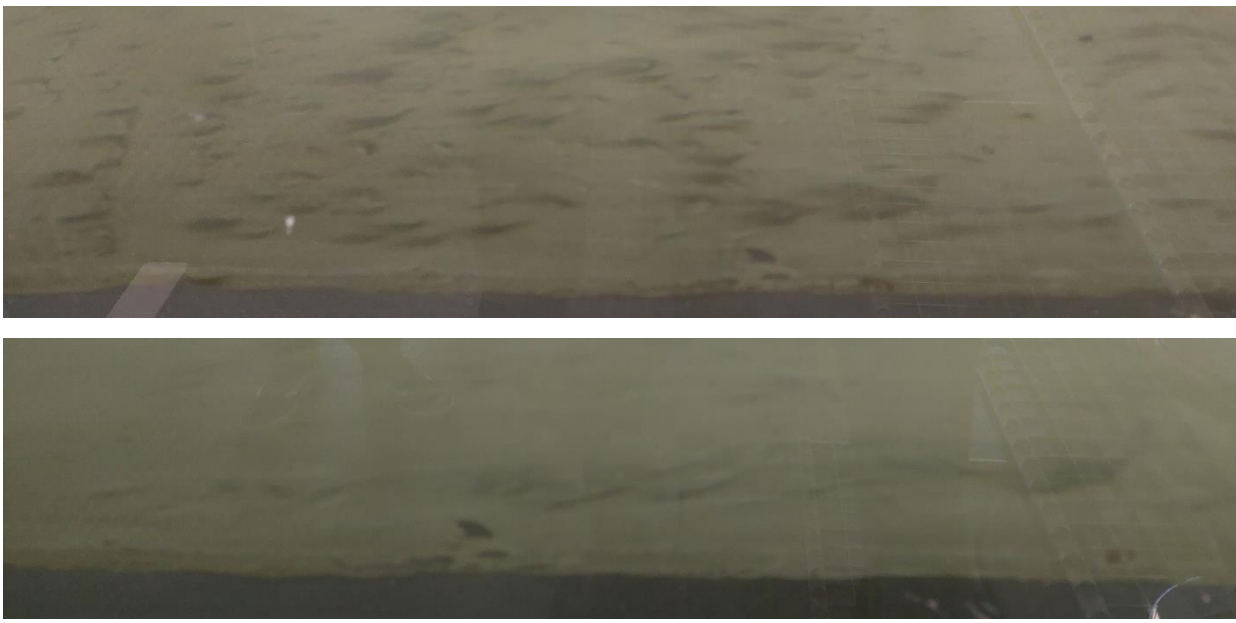

Figure Bed surface during conditions with waves alone H=0.06 m(upper) and H=0.05 m (lower)

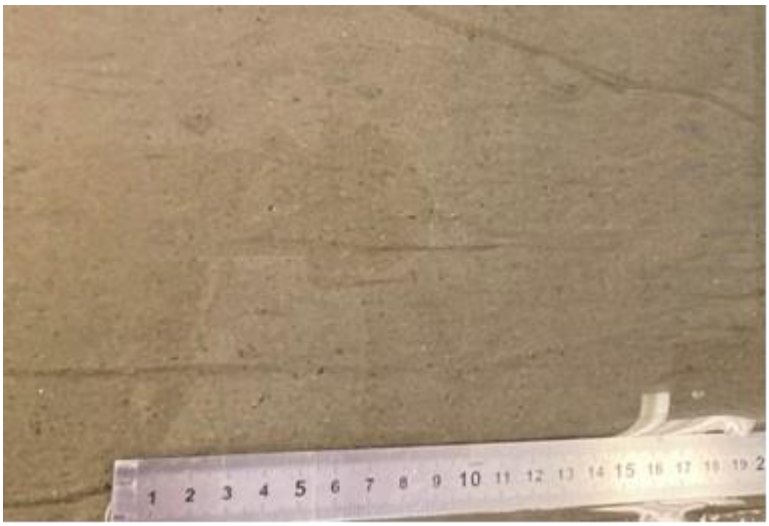

Figure Bed surface at end of tests

Test H1 Depth-averaged current velocity (m/s)=0; Wave height (m)= 0.06; Wave period (s)=1.9					
Height above bed (m)	**Current velocity (m/s)**			**Concentration (mg/l)**	
	time-averaged	**Minimum**	**Maximum**	**Sand fraction > 63 μm**	**Fine fraction < 63 μm**
0.01	0	-0.12	0.23	0	10
0.02	0	-0.12	0.24	0	10
0.03	0	-0.12	0.24	0	10
0.05	0	-0.13	0.24	0	10

Test H2; Depth-averaged current velocity (m/s)=0; Wave height (m)= 0.08; Wave period (s)=1.5					
Height above bed (m)	**Current velocity (m/s)**			**Concentration (mg/l)**	
	time-averaged	**Minimum**	**Maximum**	**Sand fraction > 63 μm**	**Fine fraction < 63 μm**
0.01	0	-0.15	0.3	0	60
0.02	0	-0.15	0.32	0	50
0.03	0	-0.16	0.32	0	50
0.05	0	-0.17	0.32	0	50
0.07	0	-0.17	0.33	0	30
0.09	0	-0.18	0.34	0	20

Test H3 Depth-averaged current velocity (m/s)=0; Wave height (m)= 0.12; Wave period (s)=1					
Height above bed (m)	**Current velocity (m/s)**			**Concentration (mg/l)**	
	time-averaged	**Minimum**	**Maximum**	**Sand fraction > 63 μm**	**Fine fraction < 63 μm**
0.01	0	-0.2	0.24	5	80
0.02	0	-0.2	0.24	3	60
0.03	0	-0.2	0.25	2	60
0.05	0	-0.22	0.26	1	60
0.07	0	-0.25	0.28	0	40
0.09	0	-0.25	0.29		30

Test H4 Depth-averaged current velocity (m/s)=0.35; Wave height (m)= 0.08; Wave period (s)=1					
Height above bed (m)	**Current velocity (m/s)**			**Concentration (mg/l)**	
	time-averaged	**Minimum**	**Maximum**	**Sand fraction > 63 μm**	**Fine fraction < 63 μm**
0.01	0.3	0.12	0.56	10	40
0.02	0.33	0.13	0.60	5	40
0.03	0.36	0.16	0.63	3	40
0.05	0.37	0.17	0.65	0	30
0.07	0.38	0.18	0.66	0	40
0.09	0.38	0.18	0.67	0	20

Test H5 Depth-averaged current velocity (m/s)=0.75; Wave height (m)= 0.06; Wave period (s)=1.					
Height above bed (m)	**Current velocity (m/s)**			**Concentration (mg/l)**	
	time-averaged	**Minimum**	**Maximum**	**Sand fraction > 63 μm**	**Fine fraction < 63 μm**
0.01	0.65	0.5	0.95	40	100
0.02	0.72	0.6	1.0	30	150
0.03	0.75	0.6	1.05	25	120
0.05	0.78	0.64	1.05	20	90
0.07	0.78	0.65	1.07	20	110
0.09	0.78	0.62	1.08	20	140
0.11	0.79	0.63	1.09	10	150
0.13	0.79	0.6	1.1	10	140

Test K: long bed of NPZ-mud and fine sand ($p_{fines<63um}$= 30%; initial wet density=1715 kg/m^3); 29 April 2022

Type of bed: mixture of NPZ-mud (dd=780 kg/m^3; $p_{fines<63um}$=55%) and fine sand (d_{50}=0.13 mm)
mud and sand are mixed and placed in the test compartment;
wet density= 1715 kg/m^3; dry density= 1150 kg/m^3;
Consolidation time=2 days;
(soft/buttery smooth mud surface with light-coloured isolated sand spots;
roughness < 0.5 mm)

Test conditions (h=water depth=0.25 m) are given in the table below.

Bed surface with developing ripples are shown in the Figures below.

Data of velocities and concentrations is given in data tables below.

Table Basic data of Test K with mixture of NPZ-mud and fine sand ($p_{fines<63um}$=30%.)

Depth-averaged current u_m (m/s)	**Wave height H (m) and period T (s)**	**Maximum, near-bed velocity U_{max} (m/s)**	**Sediment dynamics** **Δ= ripple height** **λ=ripple length** **rmv= ripple migration velocity**
0.25	0	0.15	initiation of sand particles moving over darker muddy spots
0	0.06; 2.3	0.18	brown film of mud particles./flocs moving over surfaces; no sand movement
0	0.08; 1.5	0.25	suspension layer=20-30 mm; very flat ripples Δ<1 mm, λ= 40-80 mm; sand concentrations < 10 mg/l; clear water
0	0.12; 1	0.25	suspension layer=30-50 mm; isolated flat ripples Δ<3 mm, λ= 40-80 mm; sand as ripples moving over darker mud spots; no mud entrainment; low sand concentrations < 10 mg/l; clear water
0.2	0.12; 1	0.45	suspension layer =50-70 mm; sand ripples are flattened and more asymmetric Δ<3 mm; λ=50-70 mm; ripple migration=0.1 mm/s; concentrations near bed < 100 mg/l; water turbid
0.35	0.08; 1.4	0.55	sand ripples are growing (larger area per ripple) and asymmetric Δ<7 mm; λ=50-80 mm; rmv=0.35 mm/s; water turbid
0.75	0.06; 1	0.95	intense sand transport in lowest 50 to 100 mm; ripples are washed out; smooth bed <3 mm; irregular bed surface with scour marks (Δ=10 mm; λ=100-200 mm); black, muddy water in flume Erosion mass=3x0.4x0.005x1150=7 kg=7000 g Erosion time=20 min Erosion rate=7000/(20x60x3x0.4)=5 kg/m^2/s

Figure Bed before the tests; plan view (left) and side view (right)

Figure Low, isolated bed ripples (side view) during waves alone H=0.08 m and H= 0.12 m

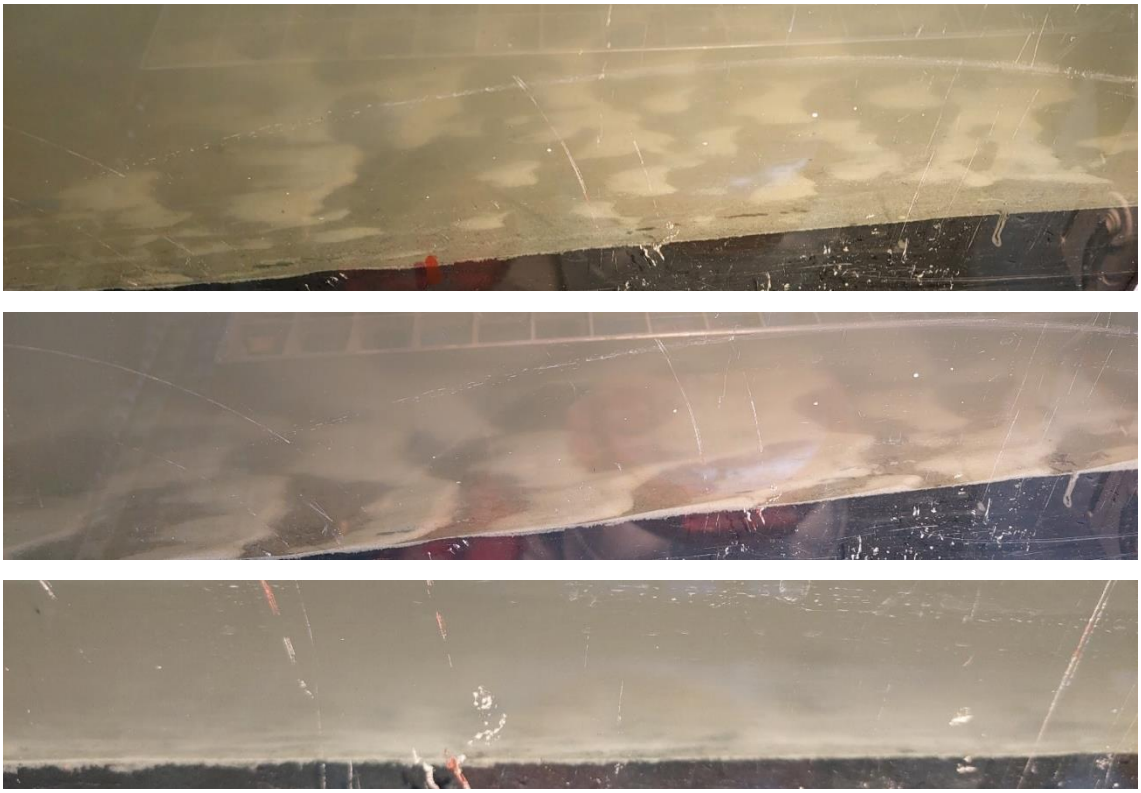

Figure Bed with ripples and sand transport (side view) during combined current+waves

u_c=0.2 m/s H=0.12 m (upper); u_c=0.35 m/s H=0.08 m (middle); u_c=0.75 cm/s H=0.06 m (lower)

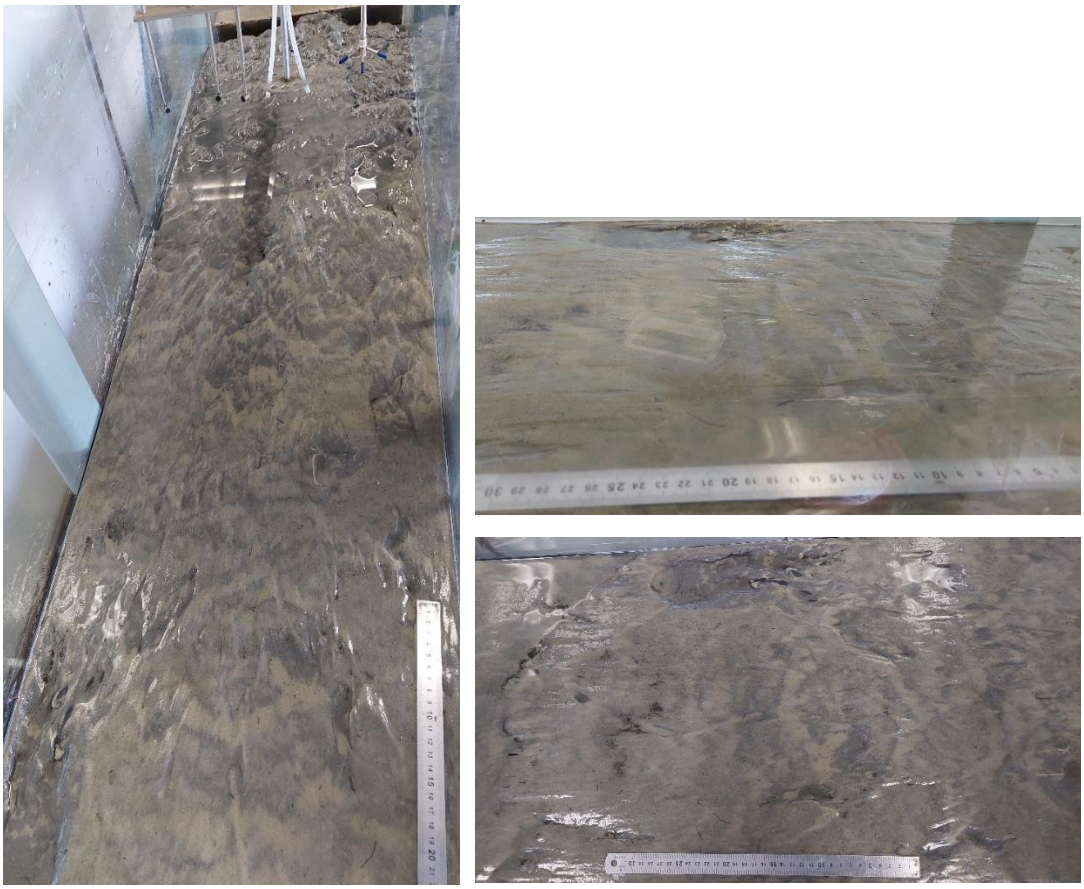

Figure Bed at end of tests; plan view (left) and side view (right); u_c=75 m/s, H=0.06 m

Test K1 Depth-averaged current velocity (m/s)=0; Wave height (m)= 0.08; Wave period (s)=1.4					
Height above bed (m)	**Current velocity (m/s)**			**Concentration (mg/l)**	
	time-averaged	**Minimum**	**Maximum**	**Sand fraction > 63 μm**	**Fine fraction < 63 μm**
0.01	0	-0.16	0.25	20	50
0.02	0	-0.15	0.27	10	20
0.03	0	-0.16	0.28	0	20

Test K2 Depth-averaged current velocity (m/s)=0; Wave height (m)= 0.12; Wave period (s)=1					
Height above bed (m)	**Current velocity (m/s)**			**Concentration (mg/l)**	
	time-averaged	**Minimum**	**Maximum**	**Sand fraction > 63 μm**	**Fine fraction < 63 μm**
0.01	0	-0.18	0.25	30	70
0.02	0	-0.2	0.25	20	50
0.03	0	-0.22	0.25	20	40
0.05	0	-0.25	0.25	15	40
0.07	0	-0.25	0.25	15	40
0.09	0	-0.25	0.25	10	30
0.11	0	-0.25	0.25	10	30

Test K4 Depth-averaged current velocity (m/s)=0.2; Wave height (m)= 0.12; Wave period (s)=1					
Height above bed (m)	**Current velocity (m/s)**			**Concentration (mg/l)**	
	time-averaged	**Minimum**	**Maximum**	**Sand fraction > 63 μm**	**Fine fraction < 63 μm**
0.01	0.13	-0.05	0.35	40	40
0.02	0.16	-0.03	0.37	15	40
0.03	0.18	-0.03	0.4	10	40
0.05	0.19	-0.02	0.43	5	40
0.07	0.18	-0.02	0.44	3	40
0.09	0.19	0	0.45	1	40

Test K5 Depth-averaged current velocity (m/s)=0.35; Wave height (m)= 0.08; Wave period (s)=1.4					
Height above bed (m)	**Current velocity (m/s)**			**Concentration (mg/l)**	
	time-averaged	**Minimum**	**Maximum**	**Sand fraction > 63 μm**	**Fine fraction < 63 μm**
0.01	0.3	0.12	0.53	230	70
0.02	0.3	0.15	0.55	170	60
0.03	0.31	0.15	0.57	130	60
0.05	0.33	0.18	0.60	110	60
0.07	0.34	0.18	0.61	90	60
0.09	0.34	0.18	0.63	80	60
0.11	0.35	0.18	0.65	70	55
0.13	0.34	0.2	0.65	60	50

Test K6 Depth-averaged current velocity (m/s)=0.75; Wave height (m)= 0.06; Wave period (s)=1					
Height above bed (m)	**Current velocity (m/s)**			**Concentration (mg/l)**	
	time-averaged	**Minimum**	**Maximum**	**Sand fraction > 63 μm**	**Fine fraction < 63 μm**
0.01	0.64	0.48	0.90	2240	120
0.02	0.70	0.52	0.95	1770	180
0.03	0.74	0.60	1.0	1490	210
0.05	0.76	0.62	1.03	1310	240
0.07	0.76	0.60	1.05	1200	140
0.09	0.78	0.63	1.07	1180	190
0.11	0.77	0.64	1.05	1000	150
0.13	0.76	0.62	1.10	930	150